SLOPE STABILITY ANALYSIS AND EVALUATION OF ROAD CUT SLOPE IN CASE OF GORO TO ABAGADA ROAD, ADAMA

By

Fentahun Ayalneh Mekonnen

A Thesis Submitted to Department of Civil Engineering

School of Civil Engineering and Architecture

Office of Graduate Studies

Adama Science and Technology University

August 2020

Adama, Ethiopia

SLOPE STABILITY ANALYSIS AND EVALUATION OF ROAD CUT SLOPE IN CASE OF GORO TO ABAGADA ROAD, ADAMA

By

Fentahun Ayalneh Mekonnen

Advisor: Endalu Tadele Chala, PhD

A Thesis Submitted to Department of Civil Engineering

School of Civil Engineering and Architecture

Office of Graduate Studies

Adama Science and Technology University

August 2020

Adama, Ethiopia

APPROVAL PAGE

We, the undersigned, members of the Board of Examiners of the final open defense by Fentahun Ayalneh Mekonnen have read and evaluate his thesis entitled "*Slope Stability Analysis and Evaluation of Road Cut Slope: In Case of Goro to Abagada Road; Adama*." and examined the candidate. This is, therefore, to certify that the thesis has been accepted in partial fulfillment of the requirement of the Degree of Masters in Civil Engineering (Geotechnical Engineering).

Name	Signature	Date
Fentahun Ayalneh *Name of student*	______________	27-07-2020
Endalu Tadele, PhD *Advisor*		27-07-2020
Yadeta Chamdessa, PhD *Chairperson*	______________	______________
Argaw Asha, PhD *Internal Examiner*		10-08-2020
Siraj Mulugeta, PhD *External Examiner*		28-07-2020
______________ *Head of Department*	______________	______________
______________ *School Dean*	______________	______________
______________ *Post Graduate Dean*	______________	______________

DECLARATION

I hereby declare that this MSc thesis is my original work and has not been presented for a degree in any other university, and all sources of material used for this thesis have been duly acknowledged.

Name: Fentahun ayalneh

Signature: ______________

This MSc thesis has been submitted for examination with my approval as a thesis advisor.

Name: Endalu Tadele, PhD

Signature: __________________

Date of submission: ___________________________

ACKNOWLEDGEMENT

First, I would like to thank God for helping me in every aspect of my life. Then, I would like to express my sincere and deepest thank to my advisor Dr. Endalu Tadele for his unlimited support, close guidance, and consultation throughout my work. Besides, I would like to extend my gratitude and appreciation to M. Sc. Zerihun Lemesa, and Dr. Yadeta Chamdessa for their advice and valuable comments during my work.

I am grateful for Adama since and technology university for sponsoring me to study M.Sc. Program. My heartfelt thanks also extend to Anuar Said general contractor, AASTU, and ASTU laboratory stuff especially M.Sc. Teshome and B.Sc. Yosef for their support during my laboratory work.

Finally, I would like to express my appreciation for my family for their encouragement and unlimited support.

LIST OF ACRONYMS AND ABBREVIATIONS

ASTM	American Society for Testing and Materials
2D	Two Dimensional
c	cohesion
CSS	Critical Slope Section
D	Disturbance factor
E	Modulus of Elasticity
FEM	Finite Element Method
FS	Factor of Safety
GSI	Geological Strength Index
HB	Hoeks Brown
JRC	Joint Roughness Coefficient
JCS	Joint Compressive Strength
LEM	Limit Equilibrium Method
MC	Mohr-Coulomb
mb	rock mass coefficient
mi	intact rock coefficient
R	Rebound number
RSC	Rock Slope Cut
SRF	Strength Reduction Factor
SSC	Soil Slope Cut
SSF	Soil Slope Fill
UCS	Unconfined compressive strength
v	poisons ratio
$\emptyset$	The angle of internal friction
ψ	angle of dilatancy
$\emptyset_b$	basic friction angle

ABSTRACT

Slope failures are among the common geo-environmental natural hazards in the hilly and mountainous terrain of the world causing damages to human life and destruction of infrastructures. In Ethiopia, the demand for the construction of infrastructures especially highway and railways are increased to connect the developmental centers. However, the failure of roadside slopes formed due to the difficulty of geographical locations is the major difficulty for this development. As a result, a comprehensive site-specific investigation about destabilizing agents and suitable selection of slope profile is needed during design. Hence, this study was emphasized on the stability analysis and performance evaluation of slope profiles (single slope, multi-slope, and benched slope). The analysis was conducted for static and dynamic loading conditions using limit equilibrium (slide software) and finite element method (Plaxis software). The analysis results in selected critical sections show that the slope is marginally stable with FS varying from 1.2 to 1.5 in static condition and unstable with FS below 1 in dynamic condition. From the comparison of analysis methods, the finite element method provides more valuable information about the failure surface of a slope than limit equilibrium analysis. Performance evaluation of geometric profiles shows that geometric modification provides better and economical slope stability. Benching provides significant stability for cut slope (i.e. the use of 2m and 3m bench improves the factor of safety by 7.5% and 12% from single slope profile). The method is more effective in steep slopes. Similarly, the use of a multi slope profile improves the stability of slope in stratified soil with varied strength. The performance is more significant when it is used in combination with benches. The study also recommends drainage control and slope reinforcement as a remedial measure for cut slope.

Keywords*; Slope failure, Slope profile, Bench slope, Multi slope.*

TABLE OF CONTENT

CONTENTS PAGE

ACKNOWLEDGEMENT i
LIST OF ACRONYMS AND ABBREVIATIONS ii
ABSTRACT iii
TABLE OF CONTENT iv
LIST OF TABLES vii
LIST OF FIGURE ix
CHAPTER 1: INTRODUCTION 1
1.1 Background 1
1.2 Statement of the problem 2
1.3 Objectives of the study 3
1.3.1 General objectives 3
1.3.2 Specific objectives 3
1.4 Scope of the study 3
1.5 Significance of the study 4
1.6 Organization of the thesis 4
CHAPTER 2: LITERATURE REVIEW 6
2.1 General 6
2.2 Factors Affecting Slope Stability 6
2.2.1 Geometry of the slope 7
2.2.2 Rock and soil properties of the slope 7
2.2.3 Rock discontinuities 8
2.2.4 Rainfall and groundwater condition 8
2.2.5 Dynamic forces 9
2.2.6 Excavation and human activity 10
2.2.7 Shear strength parameter of the slope material 10
2.3 Types of Slope Failure 12
2.4 Shear strength criteria of soil and rock 13
2.4.1 Mohr-Coulomb Failure Criterion for Soil 13
2.4.2 Shear strength of rocks 14
2.4.3 Shear Strength Criterion for discontinuities 14
2.4.4 Shear strength criterion for rock mass 16

2.5 Slope stability analysis approaches 18
2.5.1 Conventional methods of analysis 18
2.5.2 Numerical methods 21
2.5.3 Seismic Slope Stability Analysis 23
2.5.4 Factor of safety 26
2.6 Slope stability assessments 26
2.6.1 Local slope stability studies 26
2.6.2 Other related works 27
2.7 Slope stabilization methods 29
2.8 Software applications 30
2.8.1 Plaxis software 30
2.8.2 SLIDE software 31
CHAPTER 3: METHODOLOGY AND DISCRIPTION OF THE AREA 32
3.1 Description of the study area 32
3.1.1 Geology of the study area 33
3.1.2 Geomaterial of the slope 34
3.1.3 Rainfall, Temperature and ground water table 34
3.1.4 Seismicity of the area 35
3.2 Methodology 36
CHAPTER 4: FIELD AND LABORATORY INVESTIGATION 39
4.1 Introduction 39
4.2 Filed Investigation 39
4.2.1 Determination of uniaxial compressive strength in the field 41
4.3 Laboratory test 42
4.3.1 Determination of rock density 42
4.3.2 Index properties of soil 43
4.3.3 Soil classification 45
4.3.4 Compaction test 45
4.3.5 Direct shear test 46
4.4 Correlation and Data processing 47
4.4.1 Determination of rock mass properties 47
CHAPTER 5: NUMERICAL MODELING AND VALIDATION 50
5.1 Introduction 50
5.2 Formulation of finite element method 50

5.3 Modeling with plaxis 2D ... 51
5.3.1 Geometric modeling ... 51
5.3.2 Material modeling ... 53
5.3.3 Boundary conditions ... 53
5.3.4 Mesh generation ... 54
5.3.5 Calculations with plaxis ... 55
5.4 Modeling with slide ... 58
5.5 Performance evaluation of the slope profiles ... 59
5.6 Numerical validation ... 60
CHAPTER 6: RESULT AND DISCUSSION ... 63
6.1 Introduction ... 63
6.2 Discussion on the analysis results of the critical slope section ... 63
6.2.1 Deformation analysis result ... 63
6.2.2 Results of Safety analysis ... 65
6.2.3 Stability condition of the slope ... 67
6.2.4 Remedial measures ... 68
6.2.5 Comparison of LEM and FEM ... 69
6.3 Parametric study on performance of Geometric profiles ... 71
6.3.1 Effect of slope height and slope angle ... 71
6.3.2 Performance of bench on the slope stability ... 72
6.3.3 Performance of multi slope profile on slope stability ... 75
6.4 Comparison of slope profiles ... 77
CHAPTER 7: CONCLUSION AND RECOMMENDATION ... 79
7.1 Conclusion ... 79
7.2 Recommendations ... 81
REFERENCES ... 83
APPENDIX ... 90
Appendix A Rock density in the laboratory ... 90
Appendix B Determination of Schmidt Hammer Rebound value in the field ... 90
Appendix C Geological strength index (GSI) and disturbance factor(D) ... 92
Appendix E Intact rock coefficient ... 93
Appendix F Determination of rock shear strength and deformation properties using rock data software. ... 93
Appendix G Index and strength properties of soil in the laboratory ... 95
Appendix H Numerical validation ... 101

LIST OF TABLES

TABLES PAGE

Table 2.1: Factors affecting slope stability 7
Table 2.2: Common types of soil and rock slope failures........ 12
Table 2.3: Advantages and limitations of conventional analysis methods 19
Table 2.4: Methods of LE slope stability analysis........ 21
Table 2.5. Advantages and limitations of numerical modeling methods........ 22
Table 3.1: Peak ground acceleration for the study area 36
Table 4.1: Sample result of Schmidt rebound hammer test 42
Table 4.2: Rock unit weight........ 42
Table 4.3: Specific gravity and optimum moisture content........ 43
Table 4.4: Atterberg limit and plastic index 45
Table 4.5: Summary of unified soil classification 45
Table 4.6: MDD and OMC from compaction test 46
Table 4.7: Summary of shear strength parameters of soils from direct shear test........ 47
Table 4.8: Summary of equivalent rock mass parameters 49
Table 5.1: Soil and rock parameters used in numerical modeling........ 53
Table 5.2: Loading conditions and its calculation phase in plaxis software........ 57
Table 5.3: FS from Cheng et al., (2007) and this study 61
Table 5.4: Calculation of resisting and driving forces for each slice........ 62
Table 6.1: FS from Plaxis software for CSS-1 and CSS-2 66
Table 6.2: FS from Slide software for CSS-1 and CSS-2........ 67
Table 6.3: FS for different multi slope profiles 76
Table A.1: Determination of rock unit weight from buoyancy test 90
Table A.2: Schmidt hammer test for UCS 91
Table A.3: Summary of UCS from curves........ 91
Table A.4: Geological strength index and Disturbance factor........ 93
Table A.5: Deformation modulus and poisons ratio of the rock mass........ 94
Table A.6: Mohr coulomb equivalent shear strength parameters from Hoke's-brown generalized criterion for rock mass structure. 95

Table A.7: Grain size distribution test 95
Table A.8: Sample Atterberg limit and water content test of soil 96
Table A.9: Summary of Atterberg limit and plasticity index 97
Table A.10: Specific gravity test for soil sample SSC... 97
Table A.11: Summery of specific gravity test 98
Table A.12: Records of reading and shear stress calculation 98
Table A.13: Normal stress vs shear stress curve... 99
Table A.14: Records of reading and shear stress calculation 99
Table A.15: Summery of stiffness parameters of soil…………………………………………..100
Table A.16: Material properties slope section used for the validation….……. ……………....101
Table A.17: FS result of different researchers and this evaluation……..…………………………102
Table A.18: Material properties used for validation……………………………………………103
Table A.19: FS of analysis result and previous works……………………………………………103

LIST OF FIGURE

FIGURES PAGE

Figure 2.1: Cumulative distribution of earthquake damage in Ethiopia 10
Figure 2.2: Some types of Slope failure.. 13
Figure 2.3: Mohr-Coulomb failure criterion 13
Figure 2.4: The shear strength changes between intact rock, discontinuities and rock mass 14
Figure 2.5: Shear test and its Mohr coulomb shear strength envelope 15
Figure 2.6: Non-linear Hoek–Brown and equivalent linear Mohr-Coulomb failure criteria........ 18
Figure 2.7: The method of slice and forces acting on a typical slice 20
Figure 2.8: Assumptions regarding side forces in different LE methods 20
Figure 2.9: Forces acting on pseudo-static slope stability analysis 24
Figure 2.10: Relationship of permanent slope displacement with yield acceleration.................. 25
Figure 3.1: Project location and slope section of the project 32
Figure 3.2: The geological composition of the cut slope 33
Figure 3.3: Mean monthly rainfall distribution of study area 34
Figure 4.1: Failure manifestations in the road cut slope 40
Figure 4.2: Schmidt hammer rebound strength test: 41
Figure 4.3: Particle size distribution curve 44
Figure 4.4: Sample liquid limit graph for SSC-22 44
Figure 4.5: Shear stress vs shear displacement curve, and Shear stress vs normal stress curve.. 46
Figure 4.6: Equivalent rock mass properties as calculated from MC and HB criterion 48
Figure 5.1: Geometry of cut slope 52
Figure 5.2: Sensitivity analysis for the selection of model boundary.. 52
Figure 5.3: Boundary conditions for Plaxis 2D modeling 54
Figure 5.4: Sensitivity analysis for mesh size... 55
Figure 5.5: Meshing/ discretization of the model 55
Figure 5.6: Deformation of slope section 1 for phase 2 in plaxis 2D 57
Figure 5.7: Deformation of slope section 1 for phase 3 in plaxis 2D 57
Figure 5.8: FS evaluation using slide software 58
Figure 5.9: Typical cross-section of the road cut slope in the Goro to Abagada road project 59
Figure 5.10: FS from different researchers and this study on Zhang (1988) slope section. 60

Figure 5.11: Slip surface for hand calculation on slope section 1 61
Figure 5.12: Comparison of CSS-1 with hand calculation 62
Figure 6.1: Total horizontal displacement for static condition with and without surcharge 63
Figure 6.2: Sample result of deformation (load-displacement curve) 64
Figure 6.3: Deformation of slope section 1 from pseudo-static and surcharge loading 64
Figure 6.4: FS for slope section-1 from Plaxis 2D using strength reduction method.................. 66
Figure 6.5: FS evaluation using slide software (slope section-1) 67
Figure 6.6: Total displacements at each node of finite element 70
Figure 6.7: Relative shear stress of slope section 1 70
Figure 6.8: FS and slip surface using LEM (Slide). 70
Figure 6.9: Effect of slope angle on the FS of the slope... 71
Figure 6.10: Effect of slope height on the FS and deformation of slope 72
Figure 6.11: Effect of bench, and bench width on the FS from plaxis 2D 73
Figure 6.12: Effect of bench on different slope angle 74
Figure 6.13: The effect of bench height on FS with constant and varied slope within bench...... 74
Figure 6.14: Idealized slope section and its plaxis 2D model.. 75
Figure 6.15: FS and its change from single slope in % 76
Figure 6.16: FS of critical slope section 1 for different slope profiles 77
Figure 6.17: Summary of slope profiles on different point of view 78
Figure A.1: GSI values characterizing blocky rock masses……………………………………92
Figure A.2: Determination of rock mass strength using rock data software 94
Figure A.3: Particle size distribution curve 96
Figure A.4: Liquid limit determination... 97
Figure A.5: Shear stress vs shear displacement curve and Normal stress vs shear stress curve ..99
Figure A.6: Shear stress vs shear displacement curve and Normal stress vs shear stress curve..100
Figure A.7: Geometry of slope used for validation…………...…………………………………101
Figure A.8: Modeling of slope section used for validation……………………………….......102
Figure A.9: Slope section used for validation……………………………………………………103
Figure A.10: Plaxis and slide modeling for validation…………………………………….....103

CHAPTER 1: INTRODUCTION

1.1 Background

A slope is an inclined ground surface formed naturally or by excavation for different human activities. Its stability is an important consideration in the open-pit mining operations or/and civil engineering infrastructural projects because of the tremendous loss of properties and infrastructure caused annually in many places of the word (Shioi and Sutoh, 1999; Zhang, 2001). In civil engineering projects including transportation systems such as highways and railways, dams for power production and water supply, and industrial and urban development slope stability is a series concern.

Instability of slopes can occur due to the combination of internal and external factors which causes an immediate or near immediate slope failure either by reducing the shear strength of slope material or by increasing the shear stress on the slope (Searom, 2017). Rainfall, increase in groundwater table, change in stress conditions, changing geometry, rock discontinuity characteristics, deep weathering, surcharge, and dynamic force like earthquakes are among the common factors responsible for slope instability. The mechanism of slope failure varies and takes place as speed or slow rate, and it depends on the type of material, slope geometry, and types of triggering factors.

As both natural and human activities are responsible for the failure of slopes, it is difficult to prevent the problem entirely. However, the level of damage can be significantly reduced by assessing the stability condition and adopting different preventive measures on it. There are various remedial measures used to reduce the impact of slope failures and these can be grouped into four general classes (i.e. geometric modification, drainage control, slope reinforcement, and retaining structure) (Popescu, 2001). It must be noted that, to design safe and economical slopes, assess the stability of existing slopes, and adopt suitable remedial measures on it, understanding the cause of failure, mode of failure, and methods of stability analysis approaches are necessary.

Now a day slope stability studies have been attracted researcher's attention as their understanding of the impact of slope failure in human life and infrastructural development increases. Numerous slope stability studies were carried around the world and better understandings are established about causes of failure, mechanisms of failure, methods of analysis, and possible remedial measures. Likewise, studies were carried out in Ethiopia at different locations in the last decades. However, the damages due to slope failure are increasing from year to year and still the major difficulty for the development of infrastructural constructions. A review of previous slope stability assessments (Woldearegay, 2013; Eleyas et al., 2016 and Samuel, 2017) indicates that slope failures are the main constraint for road and railway construction in Ethiopia.

The stability of road cut slopes is always considered to be crucial as the slightest failure can be destructive in terms of monetary losses and harm to human lives. Hence, the cut slopes need to be carefully analyzed for this failure mechanism, before excavation, during excavation and post-excavation. Slope stability analysis is an assessment of the stability condition of new or existing slopes for various destabilizing agents as a function of the factor of safety. There are many ways to compute the factor of safety of man-made and natural slopes including kinematic method, the probabilistic method, limit equilibrium methods, finite element method, finite difference method, discrete element method, etc. This stability evaluation can be performed in 2-Dimensional or 3-Dimensional approaches. It has also been noted that each method has computational advantages and limitations. In recent years, the finite element method has been widely used for quick initial stage slope stability analysis, but limit equilibrium methods are still common in practice.

1.2 Statement of the problem

The demand for construction of highway and railways are growing rapidly in Ethiopia to connect the development centers and ports of neighboring countries. However, due to the difficulty of geographical locations, the construction of infrastructures especially highways and railways needs cutting of slopes and construction of embankments. This leads to slope instability problems whereby any external destabilizing agents like rainfall and earthquake occur. The failure of these roadside slopes is currently an issue in Ethiopia causing considerable damage to the construction. According to previous case studies, failure of these slopes is due to inappropriate design of embankments, cut slopes, and support structures by considering all expected destabilizing agents. Lack of awareness about advanced computational methods in the construction industry can be taken as one reason for this problem. On the other hand, a familiarity about the performance and its suitable condition of different geometric profiles on slope stability will contribute an important role in the design of safe and economical slopes. Hence, studies are needed to understand the performance of different geometric profiles on slope stability.

The newly constructed highway road cut slope (case study) is in the rift valley area (Earthquake-prone zone) which is suspectable for seismic loading. The slope under construction extends up to 40m height and a considerable sign of slope failures such as tension cracks, debris flows, and erosion are observed on it. Moreover, from field survey and informal interviews of the construction engineer's proper investigation of slope material and design of cut slope was not made before construction. Hence, this study is conducted to evaluate the stability of the cut slope for static and dynamic loading.

1.3 Objectives of the study

1.3.1 General objectives

The general objective of this study is stability analysis and performance evaluation of slope profiles on cut slopes using LEM and FEM.

1.3.2 Specific objectives

The specific objective of this study includes: -

1. Identifying the geo-mechanical parameters governing the failure of cut slope.
2. Evaluating the stability condition of the road cut slope for different destabilizing agents using a numerical model.
3. Comparing the stability analysis methods; LEM and FEM.
4. To evaluate the effect of Geometric profiles (single slope, multi-slope, and bench slope) on the stability of slopes.

1.4 Scope of the study

The scope of this study is limited to the slope stability analysis and performance evaluation of geometric effects on the newly constructed road cut slope in Adama. The analysis was carried using both LEM (slide software) and FEM (Plaxis software) on critical cut sections for static and dynamic (pseudo-static) loading. Suitable data for the numerical evaluation was obtained from field investigation, laboratory tests, and correlations using the literature. The performance evaluation was made on slope profiles (single slope, multi slope, and bench slope) and geometric parameters (slope height and slope angle) in selected slope sections using plaxis software. The modeling results are evaluated interims of deformation and factor of safety. All analysis was carried on dry condition by using the phreatic water level below the model. Validation of numerical models was made using previous case studies on the literature.

1.5 Significance of the study

The results of the study will have a valuable significance on the increasing highway and railway construction involving cut and embankment slopes. The performance and its suitable condition of different slope profiles presented in this study will assist the selection and economical design of cut slopes with similar geologic conditions. This study presents the stability condition of the cut slope and the causes of instability in the study area so that appropriate measures can be taken. Similarly, the study includes a comparison of analysis methods (i.e. LEM vs FEM). Hence it is expected to support the selection of suitable stability analysis methods in design and stability assessment of existing slopes.

1.6 Organization of the thesis

This work is reported in seven chapters. Chapter 1 provides a general introduction of slope stability, statement of the problem, and the research objectives including its scope and significance.

Chapter 2 presents a literature review about slope failure and its stability analysis. Various types and causes of failure, shear strength criteria, and different stability analysis approaches are discussed. Further slope stability studies, stabilization methods, and software applications also included in this chapter.

Chapter 3 presents a brief description of the study area and the methodology followed to attain the objectives of the study.

Chapter 4 Presents the collection and processing of data used for numerical modeling from field investigation, laboratory works, and secondary sources.

Chapter 5 presents the numerical modeling procedures of critical slope sections in both FEM (plaxis software) and LEM (slide software). Modeling of geometric profiles for performance evaluation and validation of numerical models using previous works also included in this chapter.

Chapter 6 Presents the result and discussions of numerical analysis. Discussions on the stability conditions of slope and comparisons of analysis methods are presented. Discussions also included the performance of geometric profiles, comparison, and suitable conditions for them. Finally, Chapter 6 provides a general conclusion and recommendations of the study.

CHAPTER 2: LITERATURE REVIEW

2.1 General

Slope failure is an ongoing problem all over the world causing damages to infrastructures, human life, and natural resources. The primary concern of slope stability studies is to contribute to the safe and economic design of new slope and stability assessment of existing slopes. The engineering solutions to slope stability problems require a good understanding of cause and mechanisms of slope failure, analytical methods, investigative tools, and stabilization measures. Hence, in this section review was made on causes and mechanisms of failure, shear strength criteria, analysis methods, previous stability assessments, stabilization methods, and software applications.

2.2 Factors Affecting Slope Stability

Slope failure occurs when the downward movements of material due to gravity and shear stresses exceed the shear strength. Therefore, factors that tend to increase the shear stresses or decrease the shear strength increase the chances of failure of a slope. Different processes can lead to a reduction in shear strengths. Increased pore pressure, cracking, swelling, decomposition of clayey rock fills, creep under sustained loads, leaching, weathering, and cyclic loading are common factors that decrease the shear strength. In contrast to this, the shear stress in slopes may increase due to additional loads at the top of the slope, increase in water pressure, increase in soil weight due to increased water content, excavation at the bottom of the slope, and seismic effects (Searom, 2017). In addition to these reasons factors contributing to the failure of slope include slope geometry, state of stress, and erosion. The factors affecting slope failure have been shown in Table 2.1 and important factors have been described in this chapter.

Table 2.1: Factors affecting slope stability (Prasad, 2017; Raghuvanshi, 2017 & Searom, 2017)

S. No	Name of the parameters	Descriptions
1	Geometry of the slope	Height of slope, angle of slope, and slope profiles
2	Rock discontinuities	Fault, Joint, bedding plane properties
3	Rock and Soil properties	Index and strength properties (density, grain size, Atterberg limit, UCS, tensile strength, and shear strength parameters).
4	Rainfall and groundwater	Rainfall, drainage pattern, permeability, and groundwater conditions.
5	Dynamic forces	Blasting and Seismic activity
6	Excavation	Cutting, drilling and other human activities

2.2.1 Geometry of the slope

The basic geometrical slope design parameters such as slope angle, slope height, slope profile, dip, and dip direction play a key role in slope stability. Due to the increase in shear stress and a decrease in normal stress on the potential rupture plane steep slopes have a greater risk of instability (Prasad, 2017). The overall angle increases the possible extent of the development of any failure to the rear of the crests increases and it should be considered so that the ground deformation at the mine peripheral area can be avoided. Similarly, the possibility of slope failure or landslide occurrence will increase with increasing slope relative relief or height. Moreover, the inappropriate selection and design of slope profile (i.e. single slope, multi slope, or benched slope) lead to slope instability problems.

2.2.2 Rock and soil properties of the slope

The rock materials forming a slope determine the rock mass strength. Low rock mass strength is characterized by circular; raveling and rockfall instability. Slopes having alluvium or weathered rocks at the surface have low shearing strength and the strength gets further reduced if water seepage takes place through them. Generally, the composition, texture, fabric, cementing, and other properties of slope material (soil and rock) influence shear strength, permeability, and susceptibility to chemical and physical weathering of slope material (Varnes, 1978). As a result, the type and characteristics of slope material govern the mechanism and probability of slope failure. For example, loose unconsolidated materials, have higher infiltration rates which lead to an increase of pore water pressure and a decrease of shear strength than consolidated slope materials (Searom, 2017). On the other hand, the strength parameters of the rock considerably change by mechanical and chemical weathering. According to Endalu and Rao (2018), weathering degrades the mechanical properties of rocks and causes rock slope failures. especially, cohesion and tensile strength are more sensitive to weathering.

2.2.3 Rock discontinuities

Structural discontinuities and their inter-relationship with the slope geometry affect the stability condition of rock slopes (Searom, 2017). Spacing, orientation, persistence, surface characteristics, separation of discontinuity surface, and nature as well as the thickness of material filled in discontinuities are the main characteristics of discontinuities that control the stability of rock slopes. The relationship of structural discontinuities within a slope like parallelism of dip direction and slope as well as the relationship between dip of discontinuity and inclination of slope controls the stability condition of rock slopes. For example, the planner mode of rock slope failure occurs when the dip of the potential failure plane is less than the dip of the slope face and greater than friction angle along the failure plane (Gadaawin, 2019).

2.2.4 Rainfall and groundwater condition

Rainfall and groundwater cause slope failure by, a) altering the cohesion and frictional parameters and b) reducing the normal effective stress. Groundwater causes increased up thrust and driving water forces and has an adverse effect on the stability of the slopes. Physical and chemical effects of pore water pressure in joints filling material can thus alter the cohesion and friction of the discontinuity surface. This will reduce the shearing resistance along the potential failure plane by reducing the effective normal stress acting on it. Physical and chemical effects of the water pressure in the pores of the rock cause a decrease in the compressive strength, particularly where confining stress has been reduced. An increase in the groundwater table along the potential failure surface reduces the shear strength and lubricates the surface facilitating the sliding process (Raghuvanshi, 2017). The water within rock discontinuity develops water forces in discontinuities leading to rock mass sliding. Whereas groundwater increases in soil slope result development of pore water pressure which reduces the shear strength in the soil mass (Ermias et al., 2017).

Many soil and rock slope failures in Ethiopia are associated with rainfall. Numerous case studies in different places (Samuel, 2017; Christofer et al., 2017; Fathiyah et al., 2017; Chung & Yong, 2019) show that rainfall infiltration reduces FS of slope significantly. Rainfall increases the saturation of earth material which intern increases the pore water pressure. According to studies ((Fathiyah & Early, 2017) and (Chung & Yong, 2019), the intensity and duration of rainfall also play a major role in the mechanism and amount of slide. Small landslides like soil slips and debris flow occur during heavy rainfall of a short period as it affects only the near-surface material. Whereas Bedrock and deeper slides in unconsolidated materials will be triggered by the cumulative effects of a series of storms. Heavy rainfall increases the water pressure on materials laying on the bed slope temporarily, which is enough to decrease strength and leading to debris slips and flows. Many roadside slope failures like debris/earth slides, debris/earth flows, and rockslides in Ethiopia have occurred during the time of continued and heavy rainfalls (Woldearegay, 2013).

2.2.5 Dynamic forces

Earthquake-induced ground shaking is the cause of slope failures in marginally to moderately stable slopes before the earthquake. According to Kramer (1996), seismically-triggered slope failures may occur due to an increase in driving movement or the reduction of shear strength. During earthquake shocks, particularly in a shorter duration of larger acceleration the horizontal dynamic component of the force increases which increases driving forces. On the other hand, an earthquake can decrease the shear strength in loosely deposited and fully saturated sand by increasing the water compression stress through cyclic loading, possibly leading to liquefaction. Several case studies (Lian et al., 2015; Eleyas et al., 2016; Chung & Yong, 2019) demonstrates the effect of earthquake on slope stability. The effect is more pronounced when the saturation of soil increases.

Ethiopia is in the East African Rift Valley region, which has a history of generating large earthquakes. This can cause damages on infrastructures of active seismic zones (i.e. Afar Triangle, Main Ethiopian Rift (MER), and Southern Most Rift (SMR)) (Eleyas et al., 2016). For example, the 1961 Karakore earthquake (M=6.1) destroyed the town of Majete and produces cracks, fissures, rockslides, and subsidence of up to 1m deep on the Addis Ababa –Asmara highway. According to Samuel (2012), the cumulative distribution of earthquake damage in Ethiopia is increasing due to the rapid growth of infrastructural construction as shown in Figure 2.1.

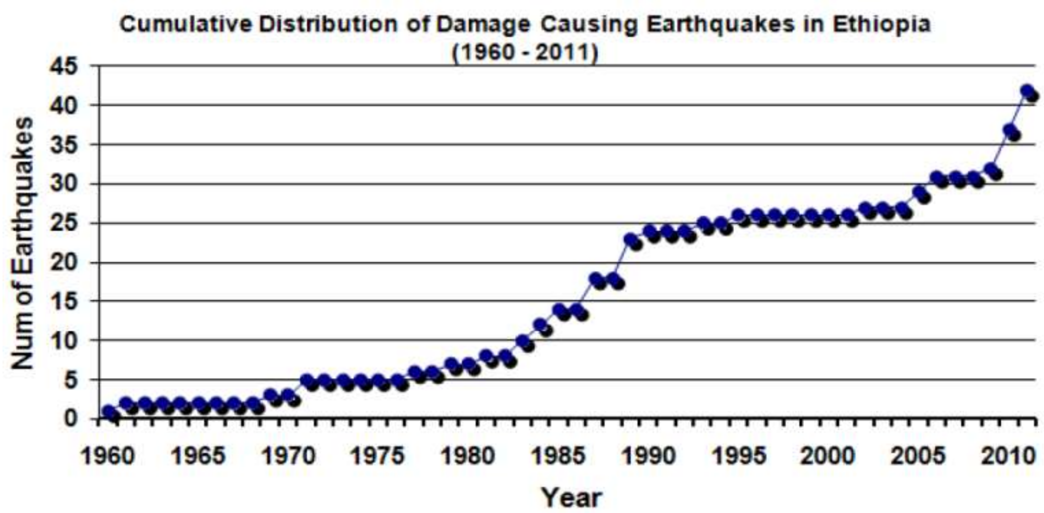

Figure 2.1: Cumulative distribution of earthquake damage in Ethiopia (Samuel et al., 2012)

2.2.6 Excavation and human activity

Several man-made activities result in the instability condition of slopes. Some of the activities include excavation for construction of infrastructures, deforestation, leakages of water in irrigational activities, mining in search of natural minerals, traffics in roads, loading and dumping on top of the slope (Searom, 2017). For example, cutting of hill slopes in an unplanned manner for road construction is the major manmade activity disturbing the stability of natural slopes (Ermias et al., 2017). The type of land cover at the surface of the earth like grass, asphalt, trees, bare ground, water, etc. and the modification of the natural environment affects the stability condition of slopes. Barren lands are more prone to instability compared with slopes of thick vegetation cover. The root system of the vegetation improves the shear strength of the slope mass in shallow depth through mechanical reinforcement, anchoring, and compaction but it has no longer an effect on the stability of slides deeper than the penetration depth of the root.

2.2.7 Shear strength parameter of the slope material

Shear strength parameters of the slope material (i.e. cohesion and angle of internal friction) are the key factors that define resisting force acting normal to the failure plane (Raghuvanshi, 2017). Hence any reduction of these shear strength parameters will significantly affect the stability of slopes. For example, shear strength parameters of rock change when the strength of intact rock and conditions of discontinuities like roughness, aperture, and filling changes (Gadaawin, 2019). As discussed in the strength creations both discontinuity and rock mass shear strength parameters are responsible for rock slope failures.

2.2.7.1 Cohesion

It is the characteristic property of a rock or soil that measures how well it resists being deformed or broken by forces such as gravity. In soils/rocks true cohesion is caused by electrostatic forces in stiff overconsolidated clays, cementing by Fe2O3, CaCO3, NaCl, etc. and root cohesion. However, the apparent cohesion is caused by negative capillary pressure and pore pressure response during undrained loading. Slopes having rocks/soils with less cohesion tend to be less stable. The factors that strengthen cohesive force include, a) Friction b) Stickiness of particles can hold the soil grains together. c) Cementation of grains by calcite or silica deposition can solidify earth materials into strong rocks. d) Man-made reinforcements can prevent some movement of material. The factors that weaken cohesive strength include, a) High water content can weaken cohesion because abundant water both lubricates (overcoming friction) and adds weight to a mass. b) Alternating expansion by wetting and contraction by drying of water reduces the strength of cohesion, just like alternating expansion by freezing and contraction by thawing. c) Undercutting in slopes. d) Vibrations from earthquakes, sonic booms, blasting that create vibrations which overcome cohesion and cause mass movement.

2.2.7.2 Internal Friction Angle

Internal friction angle is measured between the normal force and resultant force, that is attained when failure just occurs in response to shearing stress. It is a measure of the ability of a unit of rock or soil to withstand shear stress. This is affected by particle roundness and particle size. Lower roundness or larger median particle size results in a larger friction angle.

2.3 Types of Slope Failure

Slope failures can take place in various types of movements, depending on the cause of failure, geometry, materials involved, and rate of movement (Searom, 2017). Table 2.1 summarizes the common type of soil and rock slope failures.

Table 2.2: Common types of soil and rock slope failures (Searom, 2017, Raghuvanshi, 2017)

Type of Failure	Conditions of failure
Slides	It can be a translational or rotational movement that occurs in the surface of rupture when there is a distinct zone of weakness that separates the slide material from the more stable underlying material. It is a common type of failure in deeply weathered residual soils, colluvial soils, and alluvial deposits.
Falls	Sudden movement on steep slopes formed due to undercutting, differential weathering and stream wearing down.
Earth flow	It occurs on liquefiable soils especially when dynamic force occurs in saturated materials
Debris flow	It is a rapid mass movement in a combination of loose soil, rock & organic matter caused by intense surface-water flow, due to heavy precipitation or rapid snowmelt that erodes and mobilizes slack/loose soil on steep slopes.
Topples	It is the forward rotation of a unit or block of rock, in the events of gravity and forces exerted by neighboring units.
Planar failure	Rock slope failure occurs under gravity when rock blocks rest on an inclined failure like a joint that daylight into free space. It is controlled by the relationship of slope & strike angle, dip direction & discontinuity friction angle.
Wedge failure	occurs when two discontinuities striking obliquely into the rock slope face and slide of wedges take place along the line of intersection of two such a plane.

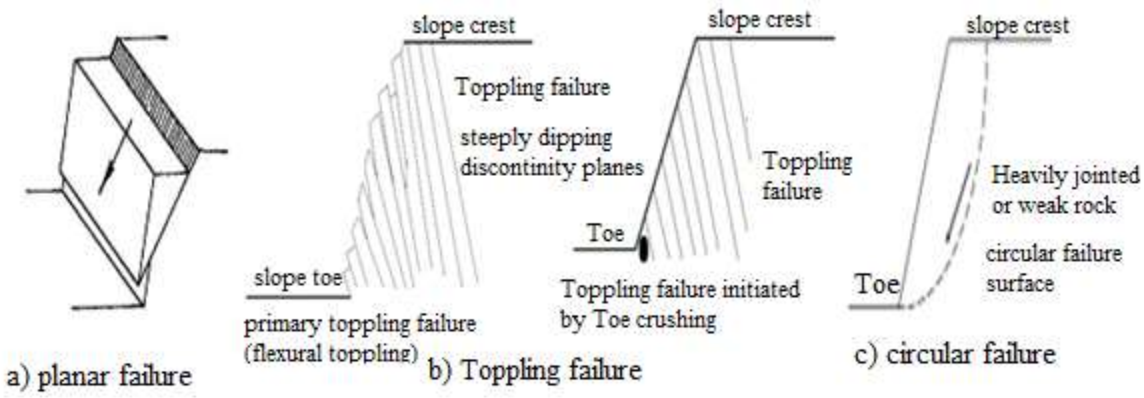

Figure 2.2: Some types of Slope failure (Endalu, 2017)

2.4 Shear strength criteria of soil and rock

2.4.1 Mohr-Coulomb Failure Criterion for Soil

Mohr-coulomb provides a failure criterion of soil material using a critical combination of normal and shear stress (Das, 2010). The Mohr-Coulomb criterion relates the shear strength of the material on the failure plane to the cohesion, normal stress, and angle of internal friction of the material (Eqn.2.1). As shown in Figure 2.3 any combination of normal and shear stress along with the MC failure envelop (B) leads slope failure, any combination of normal and shear stress below the MC envelope (A) is safe and no combination of normal and shear stress can be existing above the failure envelope (C).

$$\tau_f = c' + \sigma_n tan\emptyset' \quad (2.1)$$

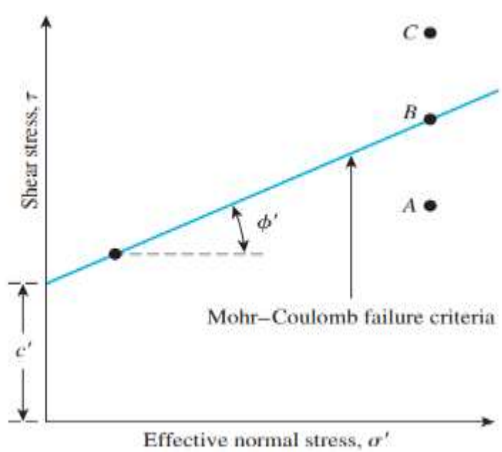

Figure 2.3: Mohr-Coulomb failure criterion (Das, 2010)

2.4.2 Shear strength of rocks

Based on the scale effects and geological conditions rock slope failures can be formed either along discontinuity surfaces or through the rock mass (Wyllie & Mah, 2004). Therefore, the selection of an appropriate rock shear strength criteria for slope stability depends on the relative scale between the sliding surface and structural geology as shown in Figure 2.4. If the dimensions of the overall slope are much greater than the discontinuity length, the failure will occur through the jointed rock mass, and the rock mass strength is used for slope stability analysis. On the other hand, slope failures occur along the discontinuities of a single joint if the joint length is nearly equal to the height of slope, and discontinuity rock strength is used for stability analysis.

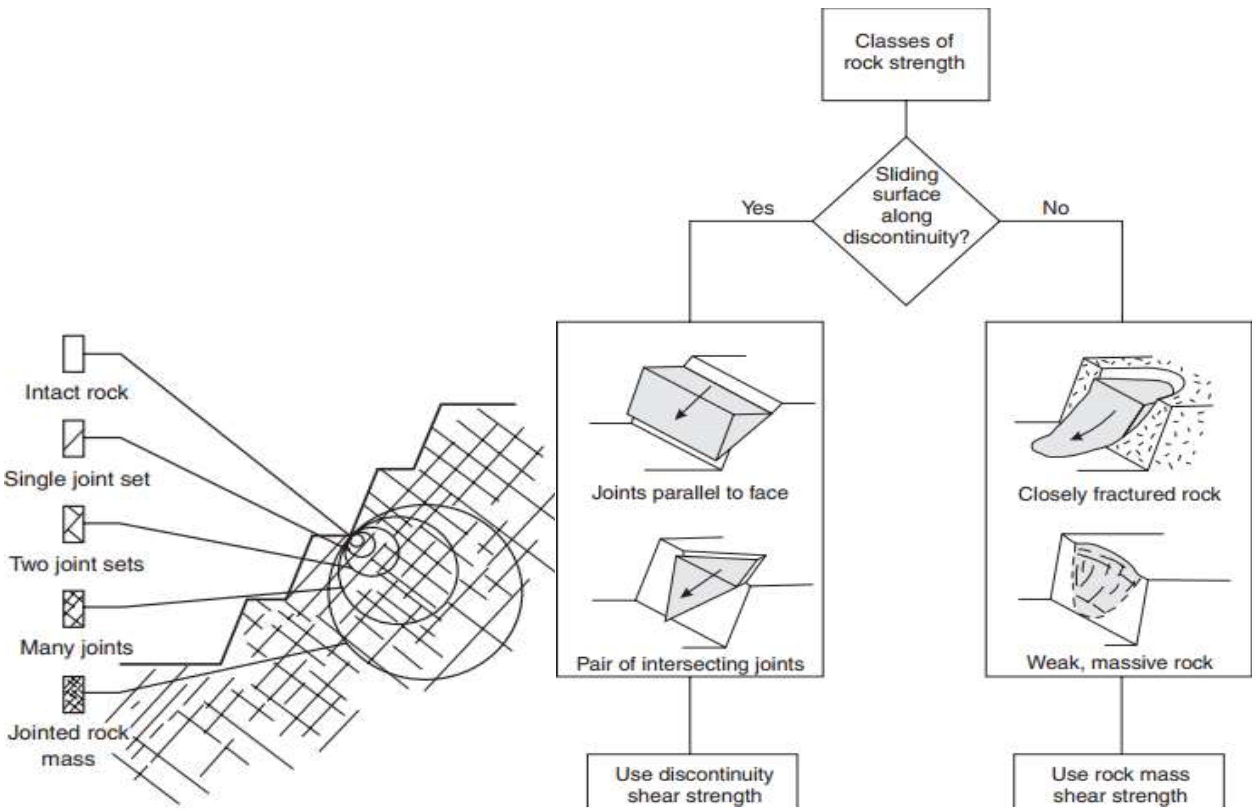

Figure 2.4: The shear strength changes between intact rock, discontinuities and rock mass with increasing sample size (Wyllie & Mah, 2004)

2.4.3 Shear Strength Criterion for discontinuities

By taking rocks as Mohr-Coulomb material, the shear strength of the sliding (discontinuity) surface can be expressed in terms of cohesion (c) and friction angle (φ) (Mohr-Coulomb, 1773).

The shear strength parameters can be determined from shear test (Figure 2.5) or correlations with discontinuity characteristics.

.Barton, (1973) also proposed an empirical low of basic friction angle to determine the shear strength of discontinuities. The shear strength of discontinuity surfaces in rock slope depends on the combined effects of the surface roughness, the rock strength at the surface, the applied normal stress, and the amount of shear displacement as shown in Eqn. 2.4 (Wyllie & Mah, 2004)

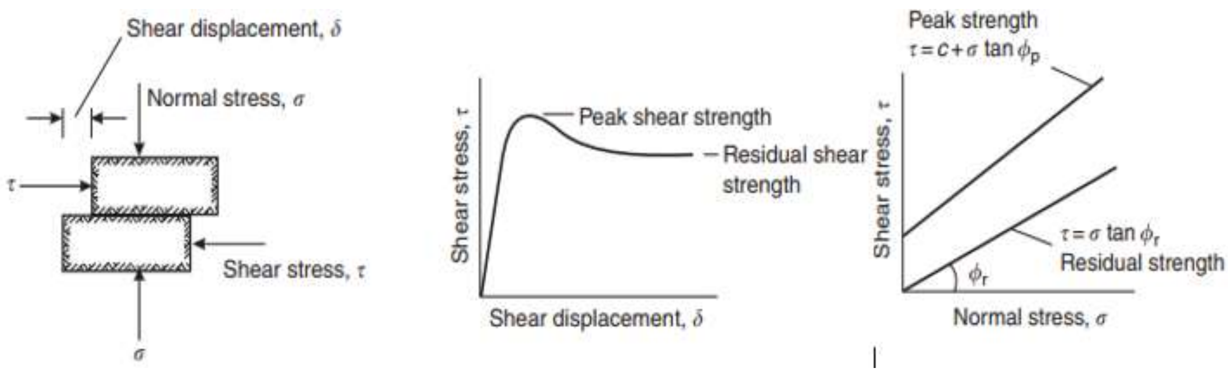

Figure 2.5: Shear test and its Mohr coulomb shear strength envelope (Wyllie & Mah, 2004)

$\tau = \sigma_n \tan\phi_r + c$	Mohr – Coulomb, 1773	(2.2)
$\tau = \sigma_n \tan(\phi_r + i)$	Patton, 1963	(2.3)
$\tau = \sigma_n \tan\{\emptyset_b + JRC * \log_{10}(\frac{JCS}{\sigma_n})$	Barton, 1973	(2.4)

Joint wall compressive strength (JCS) is the strength of a layer of rock adjacent to joint and it controls the strength and deformation properties of the rock mass (Barton, 1973). It is taken as a uniaxial compressive strength (UCS) of un-weathered rock and about 25% of the UCS on the weathered rock (Barton and Choubey, 1977). The joint roughness coefficient (JRC) is the coefficient of joint surface roughness having a value ranging from 0 to 20 (smoothest to roughest) as described by Barton and Choubey (1977). Basic friction angle ($\emptyset_b$) is an angle with flat, planar, and un-weathered rock surface in which its value ranges from 25º-35º (Barton 1973). For variably weathered joints, basic friction angle can be correlated with residual friction angle (ϕr) using Schmidt rebound number of wet weathered (r) and dry weathered surfaces (Eqn. 2.5) as stated by Barton and Choubey (1977)

$$\emptyset_r = (\emptyset_b - 20) + 20(r/R) \tag{2.5}$$

2.4.4 Shear strength criterion for rock mass

The shear strength of rock mass can be determined from the generalized Hoek-Brown strength criterion which expresses the shear strength in terms of the major and minor principal stresses.

2.4.4.1 Hoek-Brown Strength criterion for rock Mass

The Hoek-Brown failure criterion for rock mass has been updated several times since 1983. To describe the properties of the rock mass, correlations between the criterion and rock mass rating parameters were introduced. Endalu, 2018 summarized the Hoek-Brown strength criteria for rock mass and presented as follows: In the original, updated, and modified version, the RMR-system was used, but for the generalized Hoek-Brown criterion the Geological Strength Index (GSI) was suggested by Hoek et al. (1995). The original Hoek-Brown failure criterion in 1980 was developed for both intact rock and rock mass. Hoek and Brown (1980) found that the peak triaxial strength of a wide range of rock materials could reasonably be represented by the Eq. (2.6).

$$\left(\frac{\sigma_1 - \sigma_3}{\sigma_c}\right)^2 = \left(\frac{m\sigma_3}{\sigma_c}\right) + s \tag{2.6}$$

This results in a linear graph (y=mx+s) with slope m and intercepts s. Where m and s are constants which depend on the properties of the rock and on the extent to which it has been broken before being subjected to the stresses. The unconfined compressive strength of rock mass is expressed as Eq. (2.7).

$$\sigma_{cm} = \sigma_3 * s^{1/2} \tag{2.7}$$

In the 2002 edition of Hoek-Brown failure criterion, the generalized expression is used (see Eq. 2.8), but with the following modifications of the (m_b), (s) and (a) values as follows:

$$\sigma'_1 = \sigma'_3 + \sigma_{ci}\left(m_b \frac{\sigma_3}{\sigma_{ci}} + s\right)^a \tag{2.8}$$

$$a = \frac{1}{2} + \frac{1}{6}\left(e^{\frac{-GSI}{15}} - e^{\frac{-20}{3}}\right) \tag{2.9}$$

$$s = e^{\left(\frac{GSI-100}{9-3D}\right)} \tag{2.10}$$

$$m_b = m_i e^{\left(\frac{GSI-100}{28-14D}\right)} \tag{2.11}$$

where σ_{ci} is the uniaxial compressive strength of intact rock, m_b is a value depend upon the characteristics of rock mass determined from equation 2.11 and m_i is for intact rock determined from a triaxial test or the tabulated data proposed by Hoek, Kaiser, and Bawden (1995) for different types of rock, s, and α are constants depending upon the GSI value of rock mass. Geological strength index (GSI)- an estimate of the reduction in rock mass strength for different geological conditions. Its value is obtained by considering the weathering condition of discontinuity surface, rock mass structure, and interlocking of rock blocks proposed by (Wyllie & Mah, 2004). D is a disturbance factor depends upon the degree of disturbance for rock mass subjected to blasting and mechanical excavation (it varies from 0 for undisturbed to 1 for very disturbed rock masses).

2.4.4.2 Equivalent linear Mohr-Coulomb failure criteria for rock mass

Mohr-Coulomb also provides an equivalent failure criterion which gives a straight-line plot between $\tau - \sigma'_n$ plane in rock mass compared to the curved hoeks brown failure envelope (Figure 2.6). Equation 2.12 and 2.13 is used to determine the Hokes brown equivalent Mohr-Coulomb parameters for practical applications.

$$sin\emptyset' = \frac{6am_b(s+m_b\sigma'_{3n})^{a-1}}{2(1+a)(2+a)+6am_b(s+m_b\sigma'_{3n})^{a-1}} \tag{2.12}$$

$$c' = \frac{\sigma_{ci}[(1+2a)s+(1-a)m_b\sigma'_{3n}](s+m_b\sigma'_{3n})^{a-1}}{(1+a)(2+a)\sqrt{1+\frac{6am_b(s+m_b\sigma'_{3n})^{a-1}}{(1+a)(2+a)}}} \tag{2.13}$$

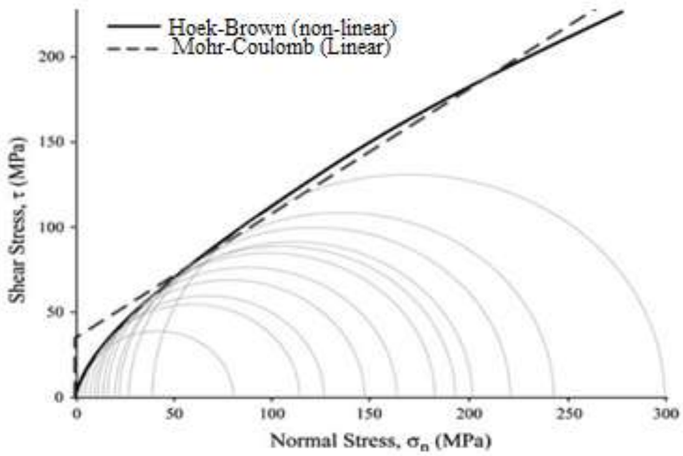

Figure 2.6: Non-linear Hoek–Brown and equivalent linear Mohr-Coulomb failure criteria

2.5 Slope stability analysis approaches

Analysis of slope stability is the common task in geotechnical engineering as the need for a better understanding of the failure mechanism of both man-made and natural slopes increase. Stability analysis techniques are broadly classified as a conventional method (i.e. kinematic, empirical, deterministic/limit equilibrium, probability methods) and numerical method (continuum, discontinuum, and hybrid modeling) (Raghuvanshi, 2017).

2.5.1 Conventional methods of analysis

Kinematic methods of stability analysis deal with the stability condition of slope based on the geometric condition that is required for the movement of the rock block over the discontinuity plane, without considering any forces responsible for the sliding (Hoek & Bray, 1981). The stereographic projections are used to determine the possible mode of rock slope failure (planer, wedge, toppling) by considering the strike angle, dip angle, and dip direction of slope and discontinuity surface in the kinematic analysis (Gadaawin, 2019). A probabilistic approach of stability analysis determines the probability of soil and rock slope failure by considering uncertainty in the input parameter used for stability analyses (Raghuvanshi, 2017). The method reduces the uncertainty and variation of the input parameter as it takes a range of values of the parameters defined by its probability density function. Whereas the deterministic method of stability analysis is a quantitative method that describes the stability condition of the slope in terms of factor of safety by considering the shear strength of the slope materials.

Each method available in conventional methods of analysis has certain advantages and limitations as shown in Table 2.3 (Raghuvanshi, 2017). Hence the selection of these methods must depend on their governing parameters. Accordingly, LEM is selected for this study, and further description was made on the next paragraphs.

Table 2.3: Advantages and limitations of conventional analysis methods (Raghuvanshi, 2017)

Method	Advantage	Limitations
Kinematic method	Simple in its application. Essential for a preliminary assessment	Only suggest the potential failure (don't provide quantitative stability condition
Empirical method	Able to investigate the large area in less time	Not suitable for complex geometric and geologic conditions.
LEM	Simple to apply and gives quantitative stability conditions.	Assumptions made on it may lead to nonrealistic results.
Probabilistic methods	Recognizes uncertainties on leading parameters for a realistic result.	Requires a collection of detailed and well distribute data over the slope

2.5.1.1 Limit equilibrium method

The limit equilibrium method is the oldest method of conventional stability analysis. The stability of slopes using limit equilibrium utilizes the Mohr-Coulomb expression to determine the shear strength (τf) along the sliding surface (Aryal, 2006). A state of limit equilibrium is obtained by expressing the mobilized shear stress (τ) as a fraction of the shear strength (τf). The available shear strength depends on the type of soil and the effective normal stress, whereas the mobilized shear stress depends on the external and internal forces acting on the soil mass. Hence, limit equilibrium analysis defines FS as a ratio of shear strength (τf) to mobilized shear stress (τ) (Das, 2010).

Shear strength available $(\tau f) = c' + \sigma' \tan\emptyset'$ (2.11)

Mobilized shear stress $(\tau) = \frac{\tau f}{FS} = \frac{c' + \sigma' \tan\emptyset'}{FS}$ (2.12)

The slope stability analysis in LEM generally involves an iterative process until the critical slip surface is found out, where the critical slip surface is defined as the slip surface with the lowest

FS. Slope stability analysis in limit equilibrium can be performed by mass procedure and method of slices. The mass procedure is used when the soil that forms the slope is assumed to be homogeneous which considers the mass of the soil above the surface of sliding is as a unit (Das, 2010). In the method of slices, the soil above the surface of sliding is divided into several vertical parallel slices as shown in Figure 2.7 and the stability of each slice is calculated separately. This is a versatile technique as the non-homogeneity of the soils, pore water pressure, and the variation of the normal stress along the potential failure surface can be taken into consideration.

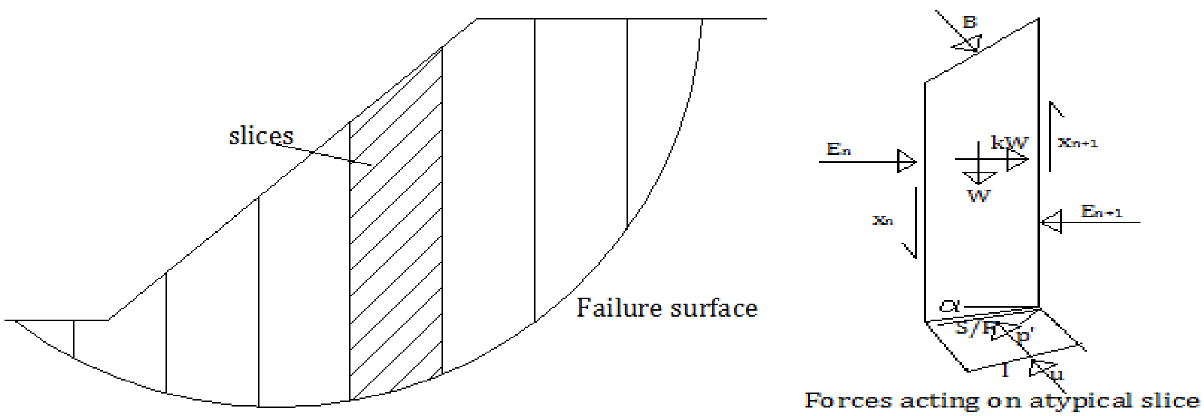

Figure 2.7: The method of slice and forces acting on a typical slice (Burman et al., 2015)

As shown in figure 2.7 the forces acting on a typical slice include the weight of slice (W), seismic force applied to the center of a slice (*kW*), mobilized shear force at the base of a slice (*S*/*F*), effective normal forces on base (*P*'), water pressure force on base (*U*), resultant top boundary force (*B*), vertical side force (*X)* and horizontal slide force (*E*). There are different methods of LE analysis proposed by scholars and their basic difference is the way they are determining or assumed the interslice normal and shear forces as described in Figure 2.8 and Table 2.4

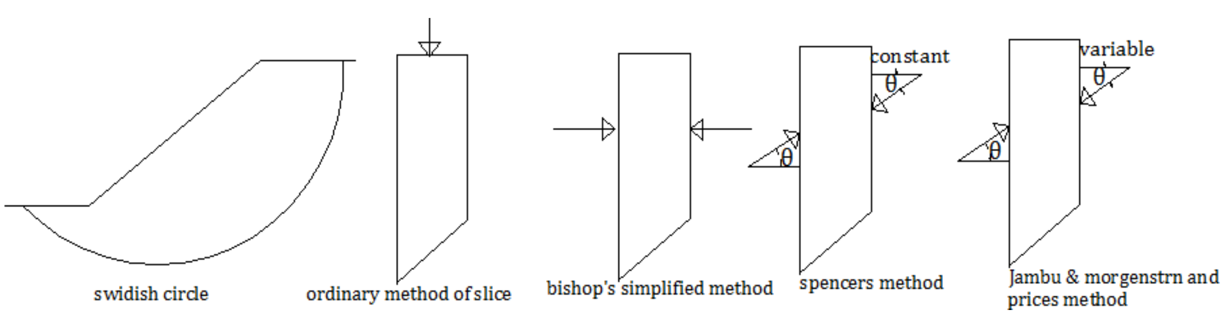

Figure 2.8: Assumptions regarding side forces in different LE methods (Burman et al., 2015)

Table 2.4: Methods of LE slope stability analysis (Das, 2010; Burman et al., 2015)

Method of analysis	Description
Swedish Circle	Simplest stability analysis of mass procedure which assumes slide occurs along a circular arc.
The ordinary method of a slice (Fellenius, 1927)	Used only for circular slip surface, satisfies moment equilibrium, and does not satisfy horizontal & vertical force equilibrium.
Bishops modified method (1955)	Used only for circular slip surface, satisfies moment and vertical force equilibrium, but doesn’t satisfy horizontal force equilibrium.
Janbu’s generalized procedure of slice (1968)	Used for any type of slip surface, satisfies all conditions of equilibrium, and permits side force locations to be varied.
Spencer’s method (1967)	Used for any type of slip surface and satisfies all conditions of equilibrium. Assumes the inclination of side forces is the same for all slices.
Morgenstern and price’s method (1965)	Used for any type of slip surface, satisfies all conditions of equilibrium and permits side force orientation to be varied.
Generalized Limit Equilibrium (GLE) (Ferdlund et al., 1981)	Used for circular and non-circular failure surfaces. Satisfies both force and moment equilibrium. Encompasses most of the assumptions used by various LEM.

Generally, LEM has various limitations compared to advanced computational (numerical) methods. The use of trial predetermined failure mechanism, its incapability to analysis 3D problems, inability to define the stress, strain and deformation behavior, its assumption of considering soil mass movement as a rigid block along the failure surface and local mobilization of shear stresses along the failure surface uniformly are some of the limitations in limit equilibrium method (Burman et al., 2015).

2.5.2 Numerical methods

Numerous slopes in physical problems experience variability in geometric, material, and loading conditions and conventional methods cannot address all these conditions (Raghuvanshi, 2017). These limitations of the conventional method can be solved by using continuum, discontinuum, or hybrid numerical modeling. The continuum modeling approach is used to simulate slopes as a mass by ignoring the discontinuity of the slope material. The method is suitable for soils and heavily disintegrated rock mass considering them continuous all over the slope. Finite element and finite difference are commonly used continuum slope stability analysis methods. In the discontinuum numerical method, the discontinuities of slope materials are considered. The method is suitable for the analysis of slopes whose failure mechanism is controlled by pre-existing discontinuities (rock slopes with discontinuities). The hybrid method is used to model slopes with the combined effect of both continuum and discontinuum methods (i.e. slope stability along with its structure and discontinuities).

Even if numerical methods have many advantages over conventional methods still some advantages and difficulties are existing between them as shown in Table 2.5. It has been seen that the slope under study is composed of soils and highly weathered or disintegrated rock mass. Hence continuum (FEM) is suitable for analysis and the next paragraphs describe the finite element method.

Table 2.5.Advantages and limitations of numerical modeling methods (Raghuvanshi, 2017)

Analysis method	Advantages	Limitations
Continuum method	Suitable for soils and weak rock mass w/o discontinuity.	Not reliable in slopes whose failure mechanism is governed by discontinuity
Discontinuum method	Suitable for slopes with various joints and discontinuity	Non-availability of discontinuity data at a block-level
Hybrid modeling	Able to simulate complex slope and discontinuity geometry	Requires high memory and computational capacity

2.5.2.1 Finite Element Method

FEM is a new and powerful computational method in engineering which able to simulate the physical behaviors of a problem using advanced computational tools without the need to simplifying it (Kramer, 1996). The ability to analyze any geometry of slope in two and three-dimension, ability to analyze both linear and nonlinear problems, ability to give FOS without having assumptions about the shape and position of the sliding plane, the ability to employ various soil material models and its ability to consider the stress-strain relationship of the material makes the FEM preferable analysis over conventional limit equilibrium method (Burman et al., 2015). Furthermore, FEM gives information about the deformations at working stress levels and can monitor progressive failure including overall shear failure.

Stress increase and strength reduction method are commonly used methods for slope stability analysis using the finite element method (Chen, 2018). In the Stress increase method, the gravity force is increased gradually until the slope fails. FS is determined as a ratio of gravitational acceleration at the failure of the actual gravitational acceleration. In strength reduction method the soil strength parameters are reduced until the slope becomes unstable and FS is determined as a ratio of initial strength parameter to the critical strength parameter. The strength of structural objects like plates and anchors are not influenced by strength reduction. In this method, FS of a slope is defined as the factor by which the original shear strength parameters must be divided to bring the slope to the point of failure (Eqn. 2.13) (Burman et al., 2015).

$$\mathrm{c'f} = \frac{\mathrm{c'}}{\mathrm{SRF}} \quad \text{and} \quad \emptyset'\mathrm{f} = \tan^{-1}\left(\frac{\tan\emptyset'}{\mathrm{SRF}}\right) \tag{2.13}$$

Where $\emptyset'$ *and* $\mathrm{c'}$ are original shear strength parameters, $\mathrm{c'f}$ and $\emptyset'\mathrm{f}$ is reduced shear strength parameters and SRF is a strength reduction factor its value at the failure is equal to the factor of safety of slope. The strength reduction method uses a constant stiffness modulus from the previous step during computations (Chen, 2018). The method has the same behavior as the Mohr-Coulomb model where a constant stiffness modulus is used. Non-convergence within a user-specified number of iterations in finite element analysis, the appearance of plastic zone from the foot to the top of the slope and the infinite movement of the sliding mass (mutate of strain and displacement) on the sliding surface is regarded as the sign for the overall slope instability (Chen, 2018). At this point, no stress distribution can be achieved to satisfy both the Mohr-Coulomb criterion and global equilibrium results in an increase in the displacements.

2.5.3 Seismic Slope Stability Analysis

According to Kramer (1996), seismic slope stability evaluation can be carried using inertial slope stability analysis or weakening slope stability analysis. The former is preferred for slope materials that retain their shear strength during the earthquake. The latter is suitable for materials that will experience a significant reduction in shear strength during the earthquake. Pseudo static, Newmark method and deformation analysis are the commonly used types of inertial slope stability analyses (Eleyas et al., 2016).

2.5.3.1 Pseudo static Analysis

Pseudo static analysis is the method of applying lateral and vertical earthquake force as a scalar multiple of static force through the centroid of the sliding mass as shown in Figure 2.9 (Kramer, 1996). The method ignores the cyclic nature of the earthquake and treats it as an additional static force applied laterally.

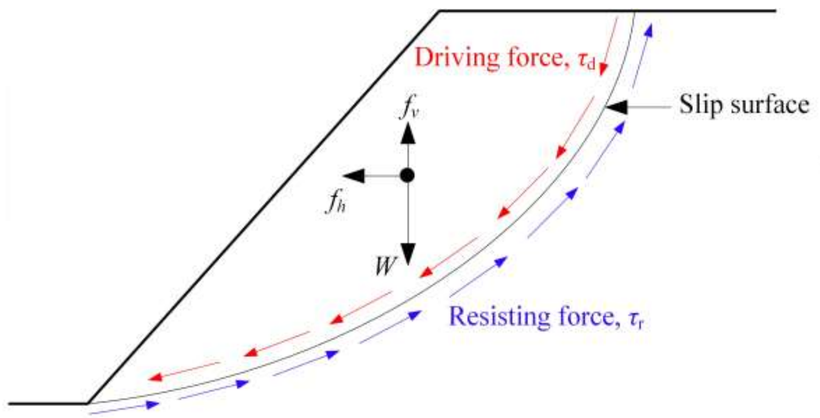

Figure 2.9: Forces acting on pseudo-static slope stability analysis (Yingbin, 2015)

$$FS= \frac{\text{resisting force}}{\text{driving force}} = \frac{cl+[(W-f_v)\cos\beta-f_h\sin\beta]\tan\emptyset}{(W-f_v)\sin\beta-f_h\cos\beta} \quad (2.14)$$

$$f_h=\frac{\alpha_h W}{g} = k_h W \quad \text{and} \quad f_v=\frac{\alpha_v W}{g} = k_v W \quad (2.15)$$

where c and $\emptyset$ are Mohr-coulomb strength parameters l is the length of the failure plane, β is the angle of failure plane from the horizontal, f_h and f_v horizontal and vertical pseudo-static forces, k_h and k_v dimensionless horizontal and vertical pseudo-static coefficients, α_h and α_v horizontal and vertical pseudo-static accelerations and W the weight of failure mass.

The effect of vertical seismic force is usually neglected in the pseudo-static analysis because it reduces or increases both the driving force and the resisting force (Eleyas et al., 2016). The accuracy of the method is quite crude as it represents the complex, transient effects of dynamic shaking in a single constant pseudo-static acceleration. Spatially it gives inaccurate results for soils that build up large pore pressures or show more than 15% degradation of strength due to earthquake shaking. The method provides an index of the factor of safety but no information on the vibration-induced deformations. Apart from its limitation, the method is a relatively simple and straight forward approach.

2.5.3.2 Newmark Method

Newmark's (1965) method proposed to estimate the deformation of slope for those cases where the pseudo-static factor of safety is less than 1.0 (failure condition). The method assumes a rigid slope deformation and will occur for those portions of the earthquake forces that cause the pseudo-static factor of safety to below 1. The longer that the slope is subjected to the pseudo-static factor of safety below 1 the greater the slope deformation. This indicates that deformation depends on the amount of acceleration that exceeds the yield acceleration (the minimum pseudo-static acceleration required to produce instability of the block). The permanent displacement of slope increases as the ratio of yield acceleration to maximum earthquake acceleration (α_y/α_{max}) decreases as shown in Figure 2.10 (Kramer, 1996).

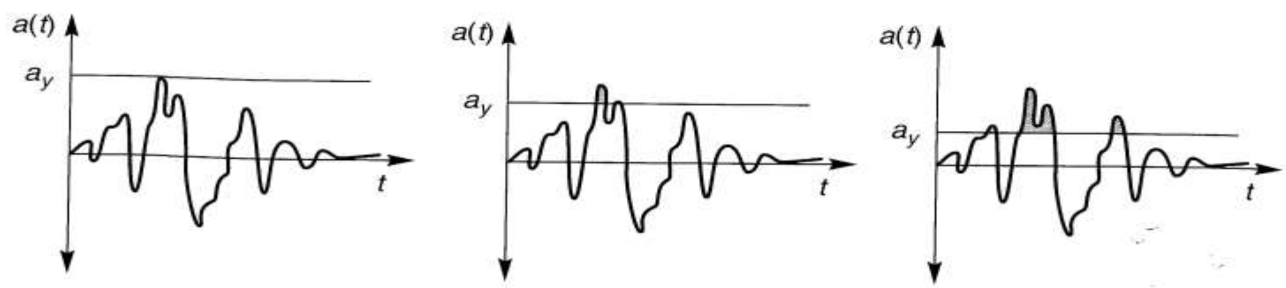

Figure 2.10: Relationship of permanent slope displacement with yield acceleration and maximum acceleration (Kramer, 1996)

2.5.3.3 Deformation analysis

Stress-deformation analysis of seismic slope stability is a FEM, where seismically induced permanent strains in each element of a mesh are integrated to obtain the permanent deformation of the slope (Kramer, 1996). Permanent strains within an individual element can be estimated using strain potential, stiffness reduction, or nonlinear analysis. The analysis of slopes in the dynamic stress deformation method is performed by applying a time-dependent dynamic loading at the base of the slope.

2.5.4 Factor of safety

Geotechnical engineers are usually carried the relative stability of a slope using a factor of safety (FS) (Eleyas et al., 2017). Which is generally the ratio between the resisting forces/moments and the motivating force/moments. In many LEM FS is obtained using a grid search on a predefined failure surface where an automatic selection of minimum FS is made in FEM. According to Kramer (1996) slopes with a factor of safety greater than 1 are theoretically stable but this is not always true in a practical case. The reason behind this is that the value is affected by various factors including uncertainties in representing the actual failure mechanisms in the slope stability analysis, uncertainties in the determination of input parameters, uncertainties on the possibility and duration of exposure to various types of loading, and the consequences of slope failure. Hence many standards mention the typical minimum factor of safety used in slope design 1.3 for short-term conditions and about 1.5 for long-term loading conditions.

2.6 Slope stability assessments

Slope failures are causing large infrastructural damages constructed on mountainous terrains around the world. Hence numerous slope stability studies were carried to get a better understanding of causes of failure, mechanisms of failure, analysis methods, and possible remedial measures. Some of the related works on the proposed study were summarized in the following paragraphs.

2.6.1 Local slope stability studies

Samuel (2017) study the effect of rainfall (i.e. intensity and duration) on the failure of Gohatsion to dejen road (abay gorge) using LEM. Accordingly, failures in the area occur due to loss of suction by rainfall infiltration. Similarly, Bisrat et al (2017) conduct a study to know the groundwater level fluctuation in the region by using both steady and transit states of flow analysis. The result indicates a high groundwater level fluctuation and complex flow direction causes failure in the region. In addition to this many individual researchers (Jemal, 2005; Henok et al., 2014; Shiferaw et al., 2014; Tesfaye, 2017) and institutions (TCDSCo, 2003; JICA and GSE, 2012) investigates on the area to solve successive slope failures in the road. However, the problem is still not solved in the area.

Eleyas et al (2016) study the cause and mitigation measures of slope instability problems in the case of Ethiopian railways. Accordingly, the hilly terrains in the highlands of Ethiopia remain highly fragile in terms of slope stability whereby any external factors could trigger slope failure. The study states that rainfall, earthquake, and expansive soil are the major causes of slope failures in Ethiopian railways. Eleyas et al (2016) conduct probabilistic slope stability evaluation on Awash – Kombolcha – Hara Gebaya railway project using LEM for static and earthquake loading conditions. The study gives a critical factor of safety 2.199 and 2.585 in short- term and long-term conditions and the value is reduced by 44.5% and 35.9% respectively, due to the introduction of the seismic load. In 2017 the author also investigates the stability of the railway embankment by using three different stochastic approaches (First Order Reliability Method, Point Estimate Method, and Monte Carlo Simulation). The result indicates a failure probability of 3.2% in the first-order reliability method, 4.14% in Monte Carlo Simulation, and 1.5% in the Point-estimate method.

Kedir et al (2018) conduct stability analysis on the Wozeka-Gidole road cut slope using both LEM & FEM. The analysis result from different scenarios indicates that the cut slope is unstable. Furthermore, a comparison of modeling results in 2D LEM shows a variation of FS up to 13% depending on the analysis method.

Gadaawin (2019) study the slope stability in the road from Gutane Migiru to Finca'a sugar factory. The study identifies wedge and planar failure as the main modes of rock failures from kinematic analyses. The factor of safety and probability of failure was calculated using Rocplane and Swedge software for planar and wedge mode of rock failure respectively. Similarly, the stability analysis of soil slopes was carried using slide software. The deterministic and probabilistic stability analysis shows that both critical rock and soil slopes were unstable under dynamic saturated conditions as compared to slopes in the dry conditions. Furthermore, the study identifies rainfall, groundwater, and unfavorable orientation of rock discontinuities as a causative factor for critical slope failures.

2.6.2 Other related works

Several researchers (Christofer et al., 2017; Fathiyah et al., 2017; Chung & Yong, 2019; Chien, 2019) studies the effect of rainfall on the stability of slopes. In general, most of the researchers argue on the significant reduction of FS when the slope is located on extreme rainfall area. Chung & Yong (2019) investigates that the reduction in FS is due to significant loose of suction in unsaturated soil through rainfall infiltration. Fathiyah & Early (2017) also investigates the effect of rainfall pattern on slope stability with different slope angle. From the result, critical FS for gentle and steep slope is reached under the application of advanced and delayed rainfall patterns respectively. Further FS reduction in gentle slope is found to be higher than the FS reduction in steep slope in any rainfall pattern.

Ahemed et al (2016) study the stability of rock slope under static and dynamic loading conditions using Mohr coulomb rock mass properties. Accordingly, the critical FS is reduced from 1.75 (static condition) to 0.48 (dynamic condition) when a horizontal coefficient of acceleration 0.16 is applied. Similarly, several case studies (Eleyas et al., 2016; Chien, 2019; Lian et al., 2016) confirm that the earthquake force produces instability in stable and marginally stable slopes. Chien (2019) also illustrates that the effect of earthquakes is more pronounced in saturated slope (i.e. when it occurs after successive rainfall).

S Alfat et al (2019) and Navya & Hymavathi (2017) investigate the effect of slope geometry on slope stability. The study indicates that FS increases with decreasing slope angle in a single slope profile and further improvement of FS were observed by applying benches. Similarly, Anand et al (2019) and Halder et al (2017) confirm that an increase in slope height and slope angle results in a significant reduction of FS.

Burman et al (2015) conduct a comparative study on LE and FEM in solving slope stability problems. The result shows the value of FS from both methods agrees very well in homogeneous soils. On the other hand, Aryal (2006) investigates that FEM may give 5-14 % lower FS than LEM due to better computations stress redistributions in different geometric and loading conditions. Generally, comparative studies (Chen et al., 2017; Burman et al., 2015; Albataineh, 2006) show that FEM provides various advantages over LEM in simulating slopes with complicated boundary conditions.

Despite numerous researches were conducted in slope stability analysis at different locations in Ethiopia damages due to slope failures were growing from year to year. Hence, slope stability analysis was carried out in this study to evaluate the stability of the road cut slope and the performance of the slope profiles.

2.7 Slope stabilization methods

Slope stabilization improves the factor of safety either by reducing driving force or increasing resistive force (Popescu, 2001). There are various remedial measures for slope instability problems. Modification of slope geometry, drainage, retaining structures, and internal slope reinforcement are the common ones.

Drainage is used for controlling surface and subsurface water conditions which is the main cause of slope failures in Ethiopia. Surface water control (ditches, trenches, vegetation cover) are used to prevent rainfall infiltration and surface runoff away from tension cracks and other discontinues. Subsurface drainage (horizontal/vertical drains and drainage tunnels) are used to drain groundwater from the slope. Control of the amount of water in soil and rock slope increases the shear strength of the slope material by reducing the excess pore water pressure in soil and hydrostatic pressure in rocks (Gadaawin, 2019).

Modification of slope geometry such as removal of driving material, the addition of material to area maintaining stability and change of slope profile provides good slope stabilization technique (Popescu, 2001). Selection of slope profiles such as single sloped, multi-sloped, or benched slope depends on the materials involved, the amount of cut or fills, and hydraulic conditions (S Alfat et al., 2019). The use of a single slope profile is reasonable in dense slope materials with enough resistance to failure and low height of cut. In the case of slopes with multiple soil strata having different shear strength, the use of multi-sloped profiles gives the advantage of providing both steep and gentler slope. On the other hand, when the location of the slope is on high rainfall area and control of surface runoff is needed the use of benched slope profiles provides the best option (ERA, 2013).

The reinforcement of slope increases the stability of steep slopes by providing tensile reinforcement, erosion protection, and strength improvement. Internal slope reinforcements such as rock bolts, micro piles, soil nailing, anchors, grouting, stone columns, freezing, electro-osmotic anchors, vegetation planting, and geotextile are used to improve cut or embankment slopes

(Popescu, 2001). On the other hand, retaining structures such as gravity-retaining walls, crib-block walls, gabion walls, passive piles, piers/caissons, cast-in-situ reinforced concrete walls, and reinforced earth-retaining structures are used for slope stabilization

2.8 Software applications

2.8.1 Plaxis software

Plaxis is finite element-based software used for deformation and stability analysis in geotechnical engineering. The software can model soil and rock layers, structures, construction stages, loads, and boundary conditions. It allows an automatic unstructured finite element mesh generation. Plaxis 2D uses quadratic 6-node and 4th order 15-node triangular elements to model soil elements. The software has many features such as modeling of spatial beam elements like walls, tunnel lining and shells using plates, modeling of soil structure instruction using interface materials, analysis of slope and excavation supports using anchors, soil reinforcement using geogrids and analysis of circular and non-circular tunnels (Plaxis, 2013).

Plaxis 2D has four features (i.e. input, calculation, output, and curves). Plaxis input is used for modeling of geometry, material, and boundary condition with a generation of mesh and initial condition (pore water pressure and initial stress condition). Plaxis calculation is used for the analysis of different structures, loading conditions, construction stages, and porewater conditions. It allows the use of various types of calculations such as plastic calculations, consolidation analysis, safety analysis, fully coupled flow deformation analysis, and dynamic calculations using different load stepping procedures. Plaxis output and curves are used to view and display analysis results (Plaxis, 2013).

Plaxis describes the mechanical behavior of soils and rocks as a stress-strain relationship using constitutive models. Different soil models are incorporated in the software such as the HB model, the MC model, soft soil model, hardening soil model, soft soil creep model, and jointed rock model. The feature also enables the use of self-programmed or user-defined constitutive models. Considering the slope material Mohr Coulomb's model was selected for this analysis.

2.8.2 SLIDE software

SLIDE software is a 2D-LE based computer program used to evaluate the safety factor of soil and rock slopes with circular, non-circular, and composite failure surfaces. The software is easy to uses and able to model the slopes with different loading conditions (i.e. surcharge, pseudo-static earthquake), groundwater condition, and support conditions. It analyzes the stability of slopes by vertical slice using different limit equilibrium analysis methods (i.e. Bishop, Janbu's, Spencer, GLE, Fellenius) discussed in section 2.5. The software also has various features including searching for critical surface, modeling of multiple, anisotropic, and non-linear Mohr-Coulomb materials, defining and analyzing groundwater problems, and viewing detailed analysis results (Slide, 2002).

CHAPTER 3: METHODOLOGY AND DESCRIPTION OF THE AREA

3.1 Description of the study area

The study area is located in Adama city in a newly constructed ring road project. Adama is a busy transportation center as it is situated along the road that connects Addis Ababa and Mojo with Dire Dawa the centers of import-export. The road under construction titled as Adama city ring road project lot 2 is 40m wide and constructed by Anwar Said General Contractor under the employer of Adama city administration in Oromia National regional state. It will help to facilitate the traffic conjunction in the town occurs due to heavy vehicles from the ports of Djibouti to mojo dry port. The construction of the road especially from Goro to Abagada creates a large amount of cut slope as shown in Figure 3.1. The height of the cut extends up to 40m and the cut is made using a 3m bench every 10m.

Figure 3.1: Project location and slope section of the project

3.1.1 Geology of the study area

The study area is in Wonji Fault Belt, the main structural system in central Rift Valley which is dominated by escarpments of bordering. Abera (2007), describes the region in various landscapes such as (1) high plateau volcanic lands, (2) Plains and low plateau with hills, moderately dissected side slopes and plains residual landforms, (3) high to mountainous relief hill of volcanic lands, and (4) plains occupied by alluvial and lacustrine deposits and undulating side slopes of residual landforms. The physiographic conditions are mainly the result of volcano-tectonic activities that occurred in the past and also partly the result of the deposition of sediments, which are considered largely of fluvial and lacustrine origin (Dagnachew, 2011). The dominant rocks in the region include basalt tuffs, agglomerates of Paleocene and Miocene age, ignimbrites of Miocene to Pleistocene age, rhyolites, trachyte, and pumice as described in Abera (2007). Similarly, (Dagnachew, 2011) mentions andosols, fluvisols, and lithosols as the major types of soils found in the region.

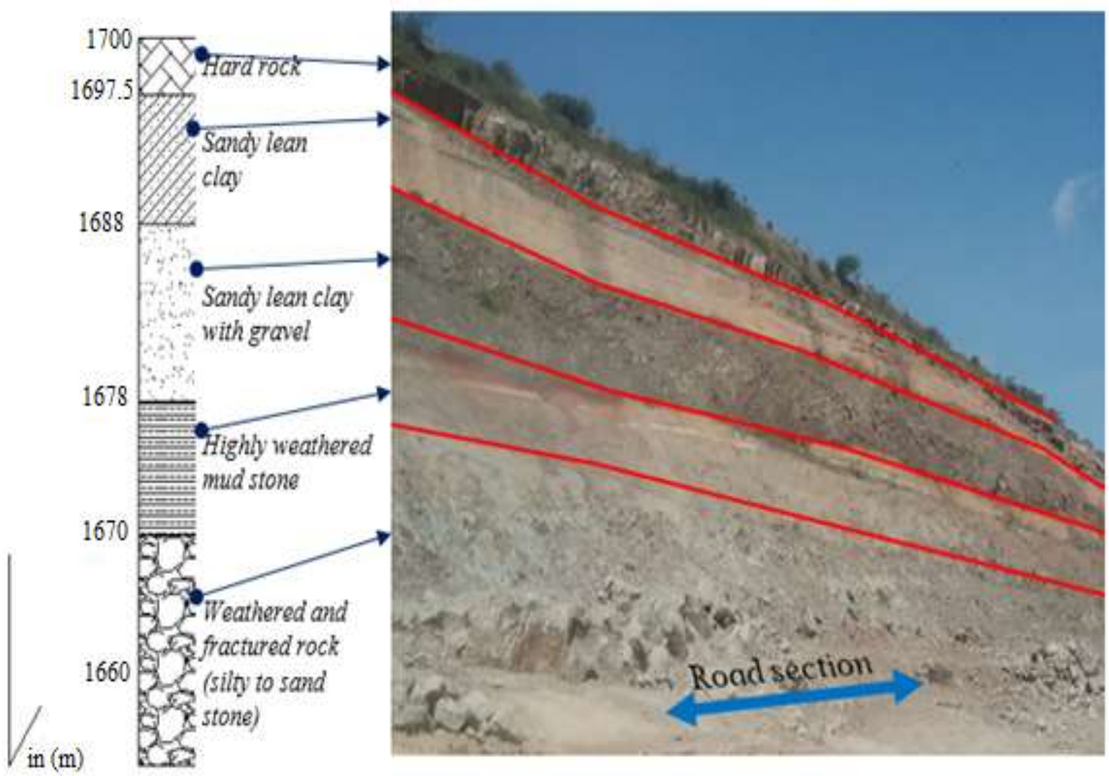

Figure 3.2: The geological composition of the cut slope

3.1.2 Geomaterial of the slope

The road is constructed on one side of Adama town by excavating the ridges made of volcanic rocks. Therefore, the slope formed from the excavation is comprising various types of soils and rocks as shown in Figure 3.2. Reddish to brownish color residual soils formed by a physical and chemical process from parent rock materials are the major type of soil found in the cut slope. Lose unconsolidated material composed of heterogeneous types soils ranging from silt to rock fragments of various sizes are another type of soils found in the cut slope section. Moreover, the bottom two layers of the slope section comprised rocks with different degrees of weathering.

3.1.3 Rainfall, Temperature and groundwater table

The records of national meteorological service agency from Adama observatory substation show that the mean annual rainfall for the past twenty years is 881.9mm at an altitude of 1622m above mean sea level, latitude of 39°17' and longitude of 8°33'. High rainfall occurs in July and August covering around 50% of the annual rainfall. The rest months are obtained rainfall almost equal to or below the evaporation rate of the city.

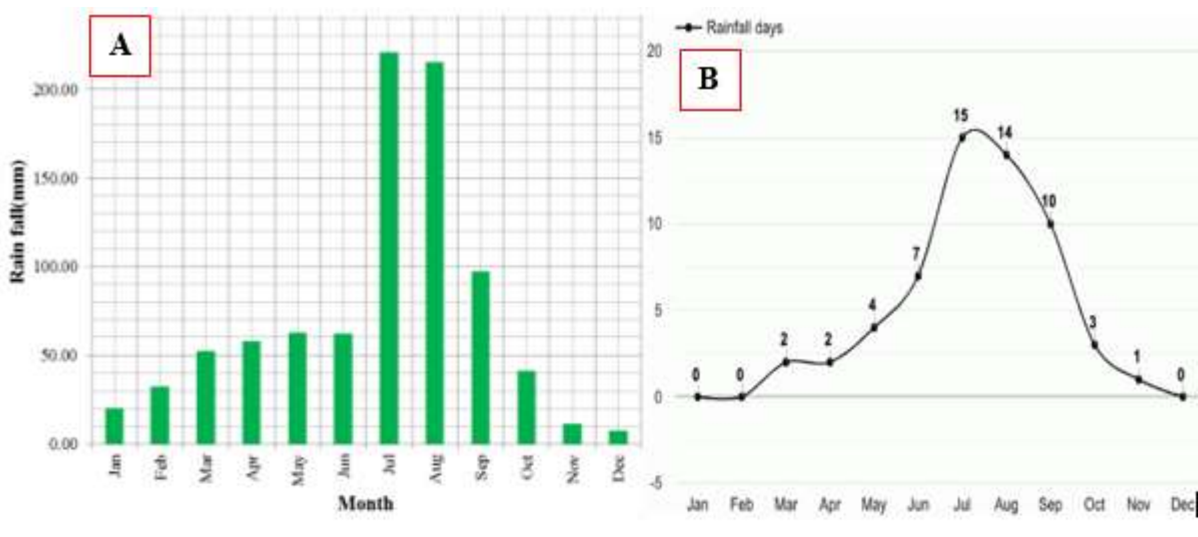

Figure 3.3: A, Mean monthly rainfall distribution of study area B, average rainfall days in the study area

The area is positioned, with an altitude ranging from 1500-1700meters a.m.s.l., which has a mean minimum, mean maximum and mean average monthly temperatures of 14.3, 28.1, and

21.2°C respectively. The highest temperature occurs during March, April, May, and June whereas November, December, and January have low temperatures. The Mean monthly average temperature ranges from 19.33°c to 23.54°c which shows almost the same variation throughout the year. It has been seen that the amount of rainfall in the area is small and rains only in July and August. In the other months, it is less than or equal to the evaporation rate of the area. According to Abera (2007), the groundwater recharge from rainfall is negligible in the area and many of the rainfall are changed in to run off. Hence deep slope failure due to commutative infiltration will not be a problem in the area. However, rainfall may cause erosion and shallow slides in the road cut slope. From previous case studies (Tamiru et al.,1997; Abera, 2007 and Sifu, 2013) groundwater table on the study area is located at a depth of 80 to 100m from the ground surface.

3.1.4 Seismicity of the area

Ethiopian Building Code of Standard (EBCS- 2015) divides the country into six major earthquake zones which range from the no-risk zone (zone 0) to zones of major damages (zone 4 and 5). The study area is in the rift valley region and from the seismic hazard map in figure 3.4. The project site falls in a high-risk earthquake zone with Modified Mercalli (MM) intensity of VI to IX. The area experiences an earthquake of magnitude 5 in 1993 resulting collapse of several adobe buildings (Samuel et al., 2012). Therefore, the design of civil engineering structures to be made in the area should be based on the assumption of a realistic earthquake with a magnitude of M = 7 which is correlated with a suitable acceleration coefficient (Dagnachew, 2011).

For seismic stability analysis, the bedrock acceleration coefficient was adopted from Ethiopia building code of standard. The older EBCS (1995) was developed based on 100 years return period which reduces the peak ground acceleration by half as compared to the commonly used 475 years return-period. However, the new EBCS (2015) uses 475 years return period (i.e. 10% exceedance within 50 years). It is also noted that the tabular listing and the hazard map give different peak ground acceleration. The value of peak ground acceleration for the study area for each case is summarized in Table 3.1

Table 3.1: Peak ground acceleration for the study area

Source	EBCS 1995	EBCS 2015		
		From map 3.4A	From map 3.4B	From table
Zone	3	4	4	4
a	0.07	0.08	0.1-0.115	0.15

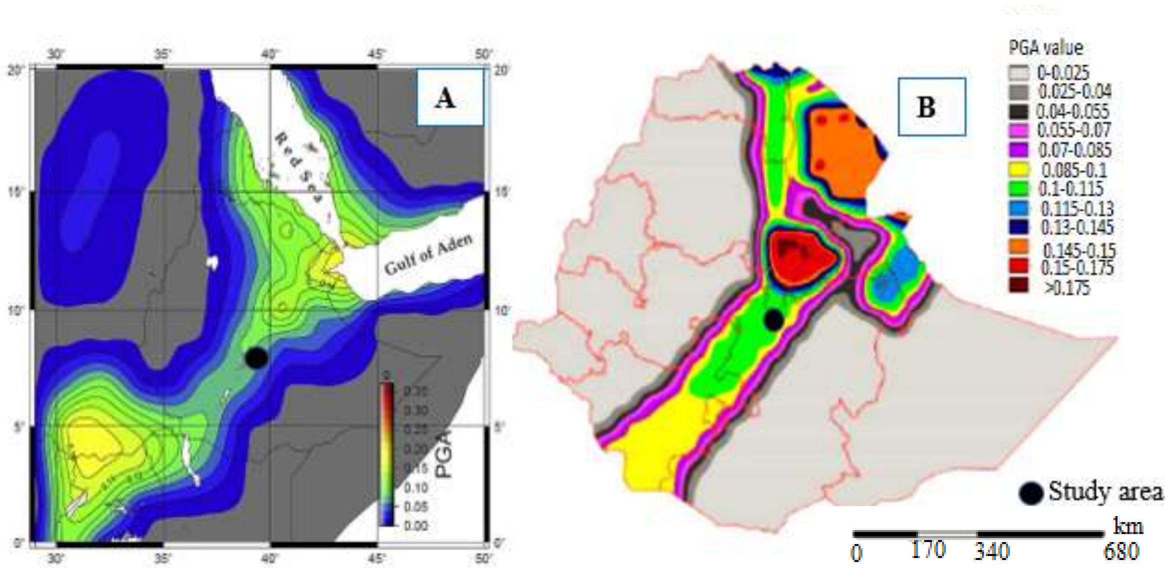

Figure 3.4 Seismic hazard map: (A) along the Horn of Africa, and (B) of Ethiopia, in terms of PGA (ES EN 1998:2015, Zetseat, 2018)

3.2 Methodology

This section emphasizes the research methodology followed to achieve the general and specific objectives of the study. First, a systematic literature review was made on existing literature and theories to get a better understanding of the cause and mechanism of slope failure, methods of stability assessments, and possible remedies as described in chapter 2. Then various data needed for the stability analysis of the cut slope were collected from different sources such as from organizations, through literature review, field investigation, and laboratory work.

Secondary data such as geological data, earthquake data, groundwater table of the site, and stiffness parameters of the soil, and rocks are obtained from literature and correlations. Rock data software is used for rock strength and stiffness determination. The zone and acceleration coefficient of earthquake for the study area was adopted from the seismic risk map of Ethiopia and Ethiopian building codes of standard (EBCS-2015). On the other hand, data such as rainfall data, topographic maps, and some investigation reports were collected from organizations. Rainfall data was taken from the metrological agency of Adama substation and site condition, the cross-section of cut, horizontal and vertical profiles of the road section including some investigation reports were obtained from Anwar Said General Contractor.

A successive field investigation was made to obtain reliable data used to characterize the cut slope. In this investigation, information on geological structures of the site, discontinuity, and strength characteristics rock section and geometry of the critical slope section were identified. Before the filed survey, information was gathered from a thorough literature review of different standards (Hoek & Bray, 1981; IS, 1991; Das, 2002 and ASTM, 2014) about the method of field data collection. During the field investigation, data collection was made through observation, interview, measuring (geometry and discontinuity data), and field test (Schmidt rebound hammer test). A collection of representative soil and rock sample for laboratory tests also performed in the field survey. To obtain index and strength parameters of soil and rock laboratory tests were conducted on collected samples.

Using data collected from different sources stability analysis and performance evaluation of geometric profiles were made using LEM and FEM. The detailed procedures followed during the modeling of the critical slope sections are discussed in chapter-5. The modeling and analysis software was validated using previous case studies. Finally, discussions were made on the stability condition of the critical slope section and the performance of geometric profiles. Comparison between profiles also made from a different point of view (i.e. construction difficulty, drainage control, aesthetic value, and accesses to side slopes). Figure 3.5 shows the general workflow of the study followed to attain the objectives of the study.

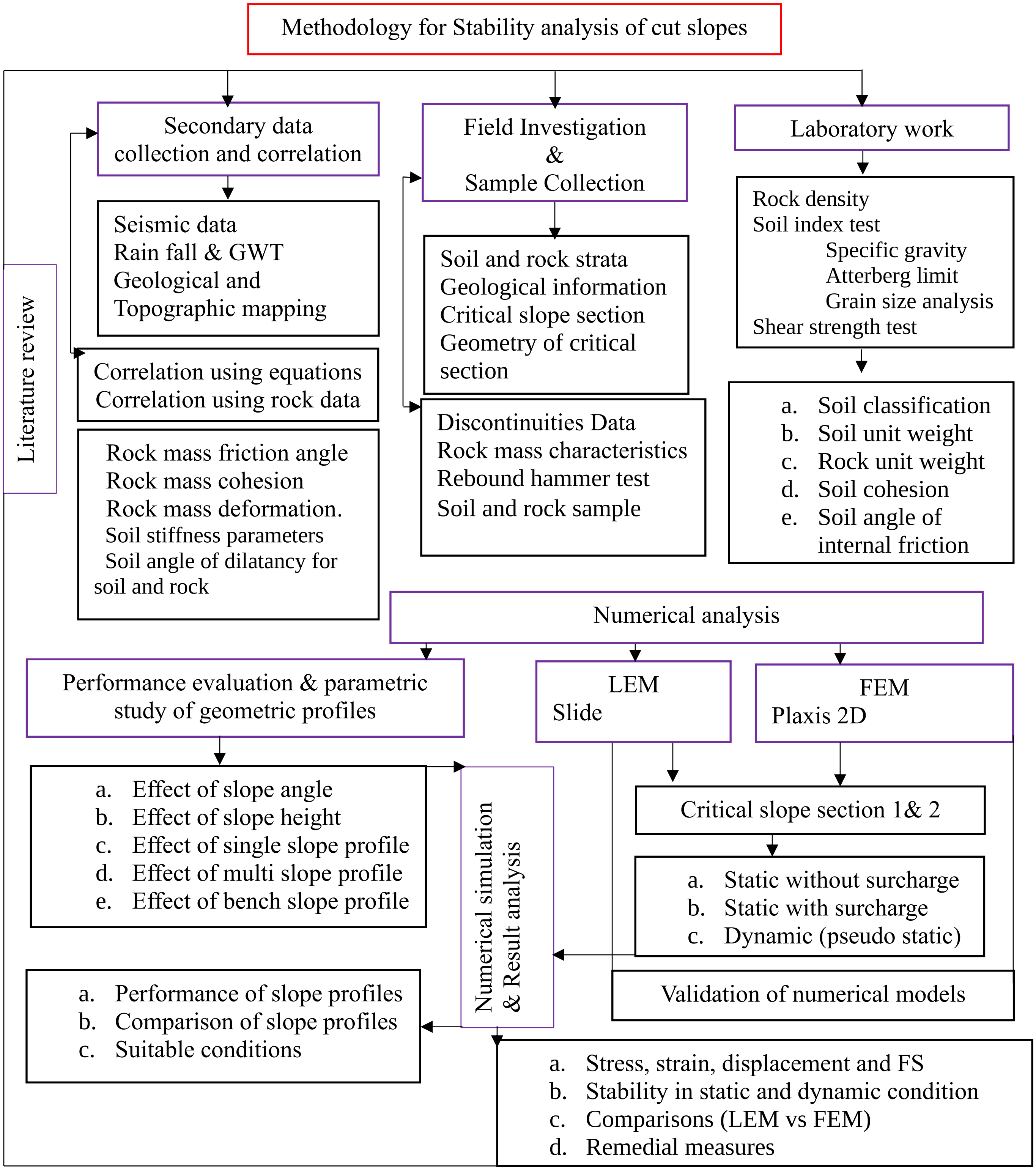

Figure 3-5: General flow chart of the methodology

CHAPTER 4: FIELD AND LABORATORY INVESTIGATION

4.1 Introduction

Slope stability analysis is a complex geotechnical problem that requires a detailed investigation of the hydrological, geological, geometric, and shear strength parameters. Hence in this study attention is given for the collection and processing of appropriate site-specific data used for stability analysis. Generally, data used for numerical modeling is obtained from field surveys, laboratory work, and correlation of field and laboratory data.

4.2 Filed Investigation

After a reconnaissance survey and thorough literature review were done about various causes and mechanisms of slope failure, a detailed field investigation was made to characterize the instability condition of cut slope and to collect data for further stability analysis. During the field survey, information on geological structures, discontinuity characteristics, rock mass characteristics, and drainage condition were identified. The data was collected on critical slope sections identified based on the field failure manifestation. During this investigation, efforts were made to identify possible failure manifestations like tension crack, the inclination of slope face, drainage condition, types of slope material, and weathering conditions. Based on this survey erosion and debris falls from the topsoil layers are identified as potential failure manifestation in the area. It is also seen that rock layers are highly weathered and disintegrated indicating rock mass failure is the potential failure mode in the area.

According to Hoek and Bray (1981) and Wyllie and Mah (2004), surface mapping using the information on rock exposure and discontinuity characteristics gives more reliable data than mapping using information from core data. This is because it provides orientations of discontinuities that are not easily accessible from core data and accessibility of large-scale features compared to small scale drill core. Hence, classification and characterization of rock mass in this study were made using the measured and observed structural, weathering, and discontinuity conditions.

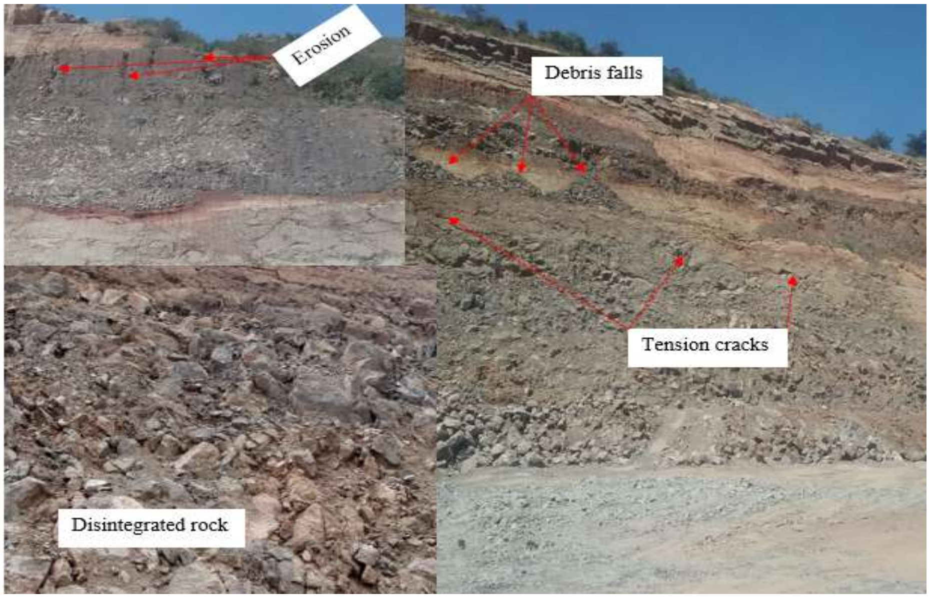

Figure 4.1: Failure manifestations in the road cut slope

From measuring and visual inspection, the discontinuity conditions of rock such as joint orientation, joint spacing, joint filling and aperture, joint roughness, structural and weathering condition were identified in the critical slope section. It has seen that rock sections are highly disintegrated and failure along the discontinuities will seldom occur. As a result, the investigation is focused on the determination of rock mass properties. Using the data collected from field various parameters such as textural classification, geological strength index (GSI), intact rock coefficient (m_i) and disturbance factor (D) were determined. Classification of rock was made based on physical properties like color, texture, origin, and degrees of weathering. The degree of weathering in the critical slope section is determined from the rebound number. The results are summarized in the appendix section.

During the field investigation, soil and rock samples were collected for index and strength tests based on the vertical and horizontal lithological/material variation of the critical slope section. Rock samples having different degrees of weathering were taken from six different locations for density determination in the laboratory. Similarly, four soil samples based on the variation of strata were taken for laboratory determination of index and strength parameters. The sampling of soils was taken 1m horizontally from the face of the slope. The amount, as well as sample location, is decided based on the standards (ASTM, 2014 and EBCS, 2015). Moreover, the compressive strength of intact rock was determined using a rebound hammer test in the field as discussed in the following paragraph.

4.2.1 Determination of uniaxial compressive strength in the field

Compressive strength of the intact rock can be determined from core samples (Hoek and Bray, 1981) or Schmidt hammer strength tests on the field (Barton & Choubey, 1977). For this study, the uniaxial compressive strength (UCS) of intact rock is determined from the Schmidt hammer strength test. Even if the results obtained are based on a local point, the rebound hammer test provides simpler, inexpensive, and likely reliable data due to practically unlimited sample sizes (ASTM, 2014). The test was conducted based on ASTM D5873-14 standard as shown in Figure 4.3. The hammer was applied in horizontal and inclined orientations provided that plunger strikes perpendicular to the surface tested. The test was carried for three trials (each trial has 10 readings) at each sample location. The average value of the rebound number was corrected using correction curves supplied by the manufacturer to the negative vertical direction.

Figure 4.2: Schmidt hammer rebound strength test: A, clean the surface with corundum stone, B, preparing equally spaced square box, C, conduct test and record rebound number, D, convert rebound number to UCS

The value of UCS was obtained from the rebound number by using curves provided by the manufacturer and from equation 4.1 proposed by Barton and Choubey (1977). Where UCS is in Mpa, γ is the dry rock densities in kN/m^3 and R average Schmidt hammer rebound value. Table xxx shows sample results of the test and the other was summarized in appendix B

$$\log10\,(UCS) = 0.00088*\gamma*R + 1.01 \tag{4.1}$$

Table 4.1: Sample result of Schmidt rebound hammer test

Sample code	Trial	Rebound number (R)	R_{avg}	UCS (curve)	avg	UCS (Eqn.)	avg
RSC-11	1	23,26,22,27,24,26,23,21,26,28	25	35	38.33	27.87	34.49
	2	34,30,29,29,31,30,34,33,29,28	31	39		35.73	
	3	35,33,34,32,31,34,35,36,33,31	33	41		39.88	

4.3 Laboratory test

Laboratory tests were carried on soil and rock samples to determine index and strength properties. Grain size analysis, Atterberg limit, specific gravity, optimum moisture content, compaction test, and the direct shear test was conducted on representative soil samples and density test was carried on rock samples.

4.3.1 Determination of rock density

As the unit weight of the rock is one of the input parameters used in stability analyses its determination is necessary for a complete definition of material properties. In this study, the density of rock was determined by buoyancy techniques for irregular rock samples. The test is conducted in the laboratory by taking a minimum of three irregular rock samples from each critical section using the standard suggested by ISRM IS 13030: 1991. Finally, the unit weight of rock was determined from the result ($\gamma = \rho d*g$). The test result and determination of unit weight are summarized in Appendix A.

Table 4.2: Rock unit weight

Sample code	Description	Dry unit weight (kN/m^3)
RSC-11 & RSC-21	Moderately weathered rock	20.1
RSC-12	Highly weathered rock	18.7
RSC-13	Slightly weathered rock	21.7

4.3.2 Index properties of soil

Index properties of soil such as Atterberg limit test, grain size analysis, and specific gravity are used for the correlation, classification, and characterization of the soil in the cut slope section. The test was conducted in soil samples as described in the following paragraph.

4.3.2.1 Specific gravity and Natural water content

The specific gravity of soil is a measure of the density of soil with respect to the same volume of freshwater. The specific gravity for different soils was determined by a pycnometer using ASTM D 854-00 as a standard reference. The results of the test are summarized in table 4.2 and the appendix section. Natural water content(w) is the in-situ water content of soils conducted on afresh excavated soil samples without exposing it for air. The test was conducted on fresh soil samples collected from six different locations based on ASTM D 2216 - Standard test procedure. The results are summarized in Table 4.2 and appendix G.

Table 4.3: Specific gravity and optimum moisture content

Sample code	SSC-11	SSC-12	SSC-21	SSC-22
Specific gravity	2.65	2.64	2.64	2.65
Water content (%)	22.54	13.22	15.35	21.39

4.3.2.2 Particle size distribution

Classification of soil for engineering purposes needs the size and distribution of soil particles throughout the soil mass. As a result, both wet and dry mechanical sieve analysis was made on soil samples collected from the critical section to determine the grain size distribution. The test was conducted based on ASTM D 421 – 85 standard procedure. The results of the test are summarized in Figure 4.3 and appendix G.

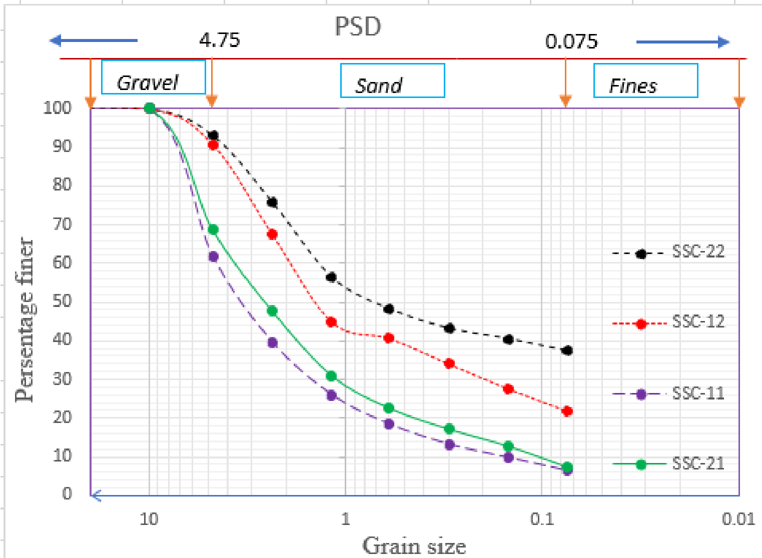

Figure 4.3: Particle size distribution curve

4.3.2.3 Atterberg limit test

Atterberg limit test is used to determine the plastic and liquid limits of a fine-grained soil. The liquid limit (LL) and plastic limit (PL) are the moisture content that defines the point of soil phase changes from liquid to plastic state and plastic to semi-solid state respectively. Atterberg limit is used for soil classification and the correlation of various engineering properties. The test was conducted on soil samples from critical slope sections using ASTM D 4318 standard procedure. The results of the test are summarized in Table 4.4 and the appendix section.

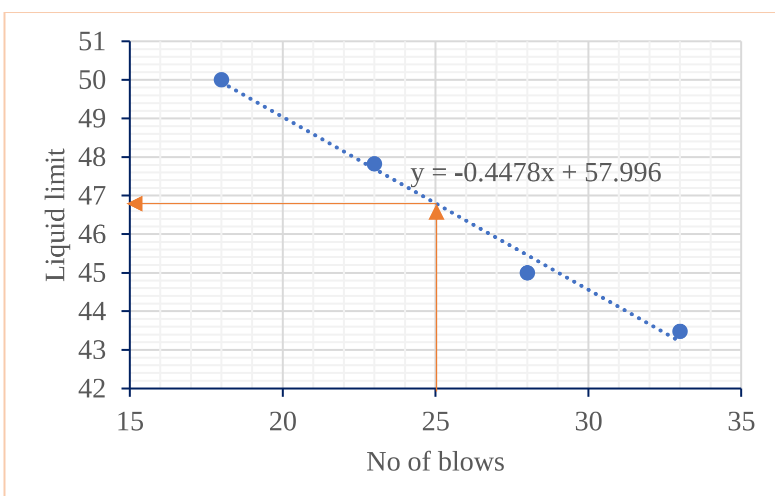

Figure 4.4: Sample liquid limit graph for SSC-22

Table 4.4: Atterberg limit and plastic index

Sample Code	Liquid limit (%)	Plastic limit (%)	Plasticity index
SSC-11	39	26	13
SSC-12	34	26	8
SSC-21	37	24	13
SSC-22	47	28	19

4.3.3 Soil classification

Soils are widely varied in their grain-size distribution, type and quantity of clay minerals present, and its plastic properties. Hence, for various civil engineering works soil classification is necessary to characterize the soils in a specific group. The American Association of State Highway and Transportation Officials (AASHTO) and the Unified Classification System are the two common soil classification systems. In this study classifications of soil were made using the Unified Classification System and it is summarized in Table 4.4.

Table 4.5: Summary of unified soil classification

Sample code	Grain size analysis			Atterberg limit			UCS soil classification
	% Gravel	% Sand	% Fine	LL	PL	PI	
SSC-11	38.2	55.2	6.4	39	26	13	Sand with silt & gravel (SW-SM)
SSC-12	9.2	69	21.8	34	26	8	Silty sand (SM)
SSC-21	31.4	61.2	7.4	37	24	13	Sand with clay & gravel (SW-SC)
SSC-22	6.8	55.9	37.3	47	27	20	Clayey sand (SC)

4.3.4 Compaction test

Compaction is the prosses of decreasing the compressibility of the soil by a mechanical means. It is used to determine the maximum dry density and optimum moisture content of the soil used to remolded the soil in the shear strength test. In this work, the test is conducted using a standard proctor test, on two soil samples. During the test, the mold is filled with three equal layers of soil, and each layer is subjected to 25 drops of the hammer. The results of the test are given in Table 4.5.

Table 4.6: MDD and OMC from compaction test

Sample code	SSC 22	SSC-21
Soil classification	Clayey sand (SC)	Sand with clay & gravel (SW-SC)
MDD (g/cm3)	1.63	1.623
OMC (%)	25.25	19.12

4.3.5 Direct shear test

Shear strength is the maximum soil resistance to shear stresses just before failure as described in the Mohr-Coulomb criterion in Eqn. 2.1. To define the Mohr-Coulomb failure criteria shear strength parameter cohesion(c) and internal angle of friction (φ) were determined from the direct shear test. It is one of the shear strength tests used to determine the strength parameters of cohesionless soils. Taking consideration of unified soil classification, the test was carried out on two remolded soil samples in a predefined failure surface using ASTM D 3080 reference. For the test readings of shear load, shear displacement and normal displacement are recorded for each normal load applied. Then from the Mohr-Coulomb envelope the strength parameters c and φ were determined. The sample test result is summarized in the following graph and the remaining is in appendix G.

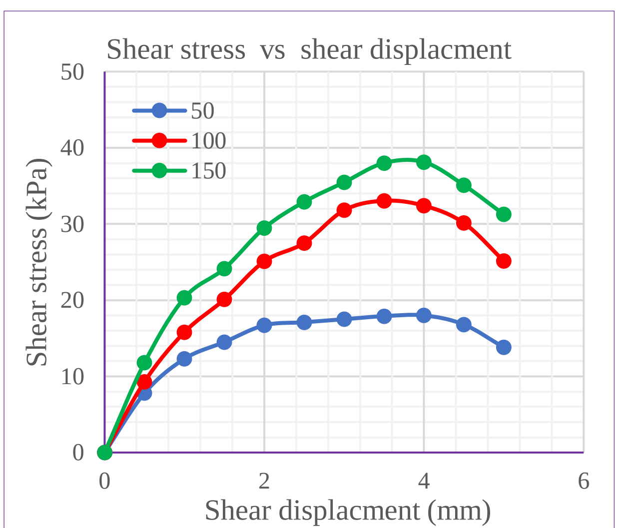

A

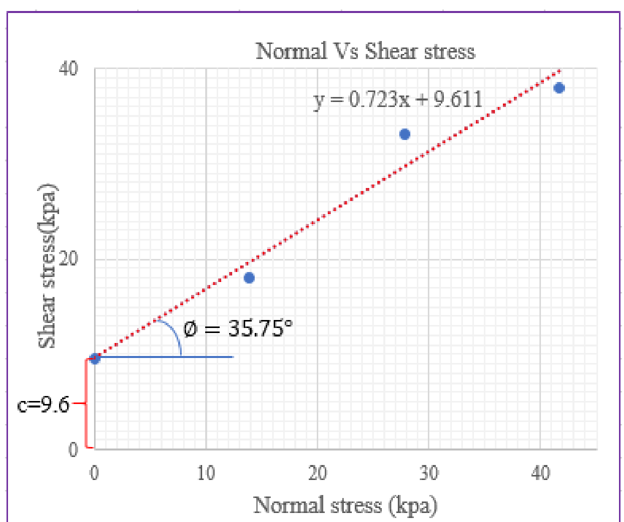

B

Figure 4.5: (A) Shear stress vs shear displacement curve, (B) Shear stress vs normal stress curve

Table 4.7: Summary of shear strength parameters of soils from direct shear test

Sample code	UCS soil classification	γ_{satu}(kN/m^3)	γ_{dry} (kN/m^3)	c (kN/m^2)	$\emptyset^{\circ}$
SSC-21	Sand with clay and gravel	20.1	16.6	9.7	35.75
SSC-22	Clayey sand	20.1	16.4	14.57	27.89

4.4 Correlation and Data processing

4.4.1 Determination of rock mass properties

Based on the scale effects and geological conditions rock slope failures can be formed either along discontinuity surfaces or through the rock mass as discussed in section 2.4 (Wyllie & Mah, 2004). Therefore, the selection of an appropriate rock shear strength and type of stability analysis is governed by the structural geology and discontinuity conditions of the rock mass. If the discontinuity of joints has higher persistence approximately equal to the height of slope the use of discontinuity shear strength is reasonable. In such a slope kinematic analysis is preferable. Whereas if the rock mass is highly fractured and blocky with very short persistency the use of rock mass shear strength provides a good and reliable analysis result (Wyllie & Mah, 2004) and (Hoek & Bray, 1981). In this study, the structural condition of the rock mass is very blocky with very short persistence of discontinuity which favors the use of rock mass strength as discussed in the field survey.

4.4.1.1 Determination of rock mass shear strength

The shear strength of rock mass is determined from the generalized hoke brown strength criterion in terms of the major and minor principal stresses as discussed in chapter 2. As the slope stability analysis involves an examination of the shear strength of the rock mass on the sliding surface which is expressed in terms of the Mohr-Coulomb failure criterion (c and φ). The equivalent Mohr-Coulomb shear strength parameter (c and φ) was determined using Rocdata software (Rocdata 3.0 Rocscience, 2004) based on the Hoek–Brown failure criterion as shown in Figure 4.6. The software uses uniaxial compressive strength (UCS), the geological strength index (GSI), intact rock coefficient (m_i), disturbance factor(D), slope height, and unit weight as discussed below.

1. The uniaxial compressive strength of intact rock (σ_{ci}) was determined from the Schmidt rebound test as discussed in section 4.2 (Appendix B).
2. Intact rock coefficient value (m_i) was taken from the tabulated data of Hoek, Kaiser, and Bawden (1995) for different types of rock. The tabulated data is already built in the rock data software (Appendix E)
3. Geological strength index (GSI)- was obtained by considering weathering conditions of discontinuity surface, rock mass structure, and interlocking of rock blocks as proposed by Wyllie and Mah, (2004) (Appendix C).
4. Disturbance factor (D) – was obtained from Wyllie and Mah, (2004) guideline based on the degree of disturbance of rock mass subjected to mechanical excavation (Appendix C).

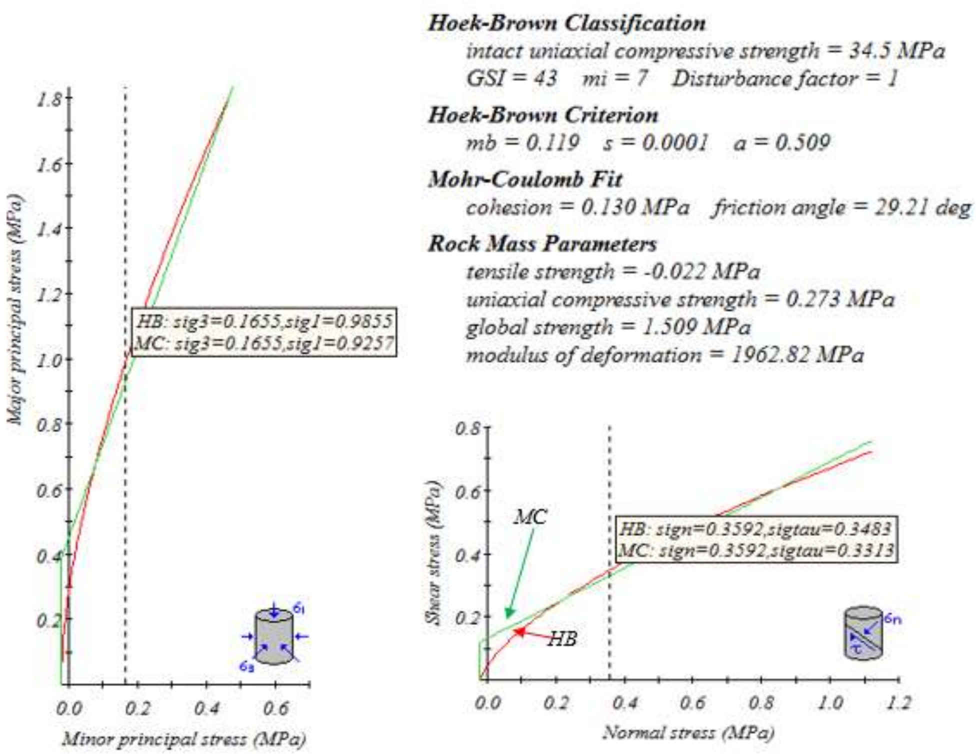

Figure 4.6: Equivalent rock mass properties as calculated from MC and HB criterion

4.4.1.2 Rock mass deformation parameters

Hoek–Brown failure criterion can also allow determination of rock mass modulus of deformation used for numerical analysis of slope stability using equation 4.2 and 4.3 (Sjoberg, 1997 and Hoek & Brown, 1997).

For $\sigma_{ci} \leq 100$Mpa $\quad E_m\,(Gpa) = (1 - \frac{D}{2})\sqrt{\frac{\sigma_{ci}}{100}}\,10^{(\frac{GSI-10}{40})}$ (4.2)

For $\sigma_{ci} > 100$Mpa $\quad E_m(Gpa) = (1 - \frac{D}{2})\,10^{(\frac{GSI-10}{40})}$ (4.3)

The Poisson's ratio of the rock mass is one of the most important rock parameters used for calculating the deformation of rock slopes. The value of poisons ratio for rock mass is estimated by correlating it with internal friction angle as shown in Eqn. 4.4 (Balazs, 2009). On the other hand, due to the relationship between the internal friction angle and the rock mass index (GSI) Balazs (2009) determine the relationship between the Poisson's ratio and the GSI as given in Eqn. 4.5. The deformation modulus and poisons ratio of rock mass obtained from these empirical relations and summarized in Table 3.3 and Appendix F.

$\frac{v}{1-v} = 1 \sin \varphi$ (4.4)

$\nu = -0.002GSI - 0.003mi + 0.457$ (4.5)

Table 4.8: Summary of equivalent rock mass parameters

Sample code	Unit weight (kN/m3)	Cohesion (MPa)	Friction angle (∅˚)	Modulus of Deformation (MPa)	Poisons ratio
RSC-11	20.1	0.013	29.21	1962.8	0.35
RSC-12	18.7	0.060	20.32	686.9	0.381
RSC-21	20.1	0.212	35.68	3293.8	0.34
RSC-22	18.7	0.044	16.82	487.6	0.42

4.4.1.3 Soil stiffness parameters

The stiffness parameters for soil (E and v) are used for deformation analysis in numerical modeling. Hence, suitable values of these parameters were obtained from numerical correlations and Literature. The drained poisons ratio of granular soils is obtained from equation 4.6 as suggested by Kulhawy and Mayne (1990) and Bowles's (1996) recommendation. The long-term modulus of elasticity of the soil is correlated with SPT N value as proposed by Begemann (1974), (J.Ameratunga et al., 2016), and Das (1995) recommendation. The results are summarized in appendix G.

$v_d = 0.1 + 0.3\,\frac{\emptyset' - 25}{20} \quad for\ \emptyset' < 45°$ (4.6)

$\frac{E_s}{p_a} = \alpha N_{60}$ (4.7)

CHAPTER 5: NUMERICAL MODELING AND VALIDATION

5.1 Introduction

Numerical models allow geotechnical engineers to simulate the real and actual situations of the geotechnical problem such as construction stages, various loading conditions, excavation conditions, and boundary conditions. The result allows to get a better understanding of the mechanisms of failure, deformation, and safety of structures. The finite element method is a common and power full advanced numerical modeling tool in geotechnical engineering. For the same reason, the method was selected for this work to predict the stability of the road cut slope and to investigate the performance of slope profiles. Plaxis-2D was used to determine the deformation and safety factor under static and dynamic loading conditions. The limit equilibrium method also included in this evaluation using a LE based slide software.

In this section, the procedures required to model and analysis of slopes in FEM (plaxis) and LEM (slide) are included. The numerical evaluation in the performance of slope profiles also addressed in this chapter. Finally, validation of the model was carried out using previous case studies obtained from the literature.

5.2 Formulation of finite element method

Finite element modeling is a method of discretizing a continuum into small pieces or elements to describe the behavior or actions of individual pieces and reconnecting them to represent the behavior of the continuum as a whole (Plaxis, 2013). Each element has some nodes and each node have some degrees of freedom corresponding to displacement components in deformation analysis.

Defining the problem domain is the 1st step in FEM which includes defining the geometrical model, material model, and applying boundary conditions. The domain can be later discretized into a series of continuum elements to form a mesh that connects with nodes to transfer forces and displacements between them. Triangular areal elements were used to discretize soils in plaxis 2D software. Once the problem domain is defined and discretized into finite elements the element stiffness functions are formed (Plaxis, 2013). Equation 5.1 shows the relationship of element stiffness matrix (K), a vector of an unknown degree of freedom or nodal displacement (d), and a resultant vector of element nodal forces (*f*). The elastic element stiffness matrix is also expressed as a function of strain interpolation matrix (B) and an elastic material matrix (D^e) as shown in Eqn 5.2.

$$[K]\{d\} = \{f\} \tag{5.1}$$

$$K = \int B^T D^e \, B dV \tag{4.2}$$

The element stiffness matrix is gathered and assembled to form a global continuum equation containing the material and geometric data. The unknown nodal displacements are solved from the global equations by applying known boundary conditions and the values between nodes are obtained from interpolated shape functions. The remaining parameter forces, stresses, and strains are obtained by post-processing using determined nodal displacements in the element and global equations (Plaxis, 2013). In numerical modeling proper selection of parameters such as element type, mesh size, boundary conditions, constitutive models increase the accuracy of results. Hence, emphasis was given in the selection of these parameters. The selection and modeling of these parameters are discussed in the following paragraphs.

5.3 Modeling with plaxis 2D

5.3.1 Geometric modeling

Two critical sections of the cut slope were used for plaxis modeling as shown in figure 5.1. During FE geometric modeling the selection of model extent influences the accuracy of the result. To minimize this effect the selection of domain extent was made by performing sensitivity analysis for vertical and lateral boundaries under constant loading condition. From the result, the boundary with a negligible effect on deformation (displacement) was selected as shown in Figure 5.2. Then the selected domain of slope geometry was modeled using both plaxis 2D. As the slope have a constant cross-section with a larger thickness plane strain model was used during modeling.

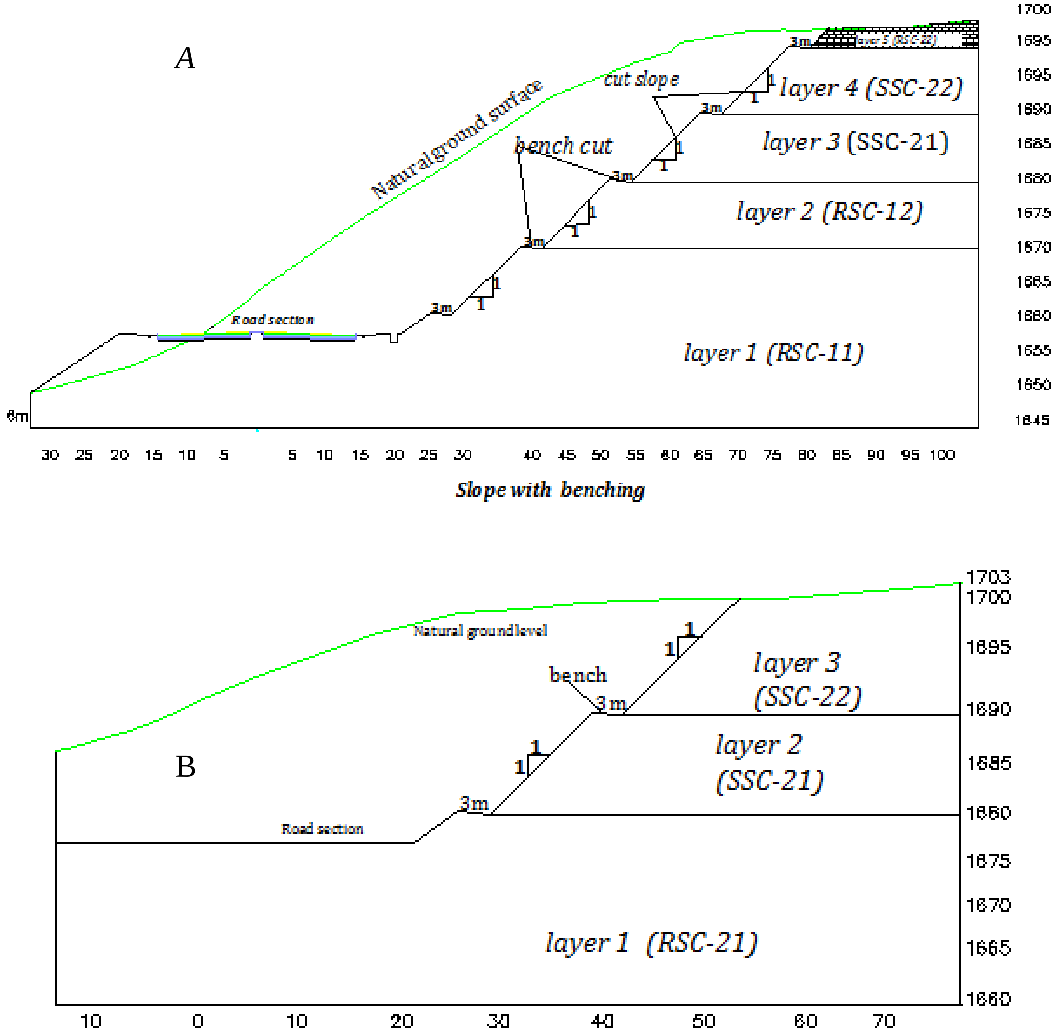

Figure 5.1: Geometry of cut slope for (A), critical section-1 (B), critical section-2

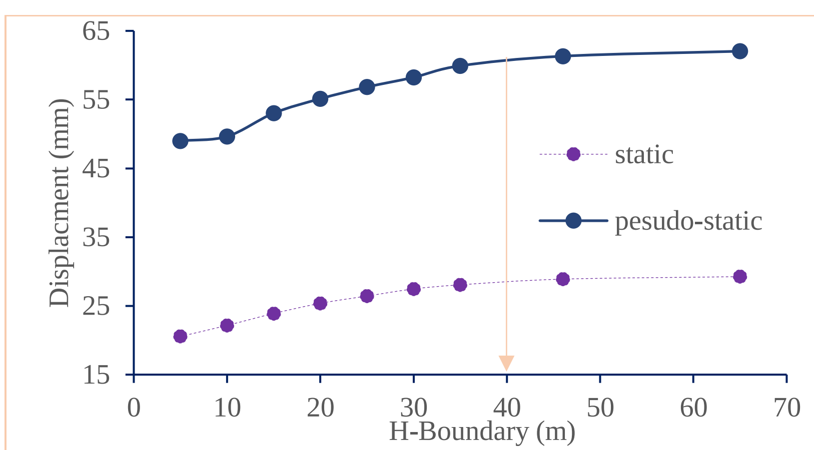

Figure 5.2: Sensitivity analysis for the selection of model boundary

5.3.2 Material modeling

The mechanical behavior of soils and rocks can be modeled with various digress of accuracy. For this study, the elastic perfectly plastic Mohr-Coulomb model was used. Rock layers were modeled using Hoek's -Brown equivalent Mohr-Coulomb model. The model uses E and v as soil elasticity, φ, and c as soil plasticity and ψ as angle of dilatancy. The model does not include stiffness varying with stress and strain. The effective soil and rock parameters determined in chapter 3 and summarized in Table 5.1 were used for this modeling.

Table 5.1: Soil and rock parameters used in numerical modeling

Sample code	Description of soil and rocks	γ_{stu} (kN/m^3)	γ_{dry} (kN/m^3)	c (kN/m^2)	$\emptyset^\circ$	ψ°	E (MPa)	v
SSC-22	Clayey sand	20.1	16.4	14.57	27.89	0	25	0.215
SSC-21	Sand with clay and gravel	20.1	16.6	9.7	35.75	5.75	35	0.261
RSC-11	Slightly to moderately weathered rock	21.3	20.1	130	29.21	0	1962.8	0.35
RSC-12	Highly weathered rock	19.8	18.7	600	20.32	0	686.9	0.38
RSC-21	Slightly to moderately weathered rock	21.3	20.1	212	35.68	5.68	3293.8	0.34

5.3.3 Boundary conditions

During FE modeling appropriate boundary conditions (i.e. both essential and natural) must be assigned to represent the actual problem accurately. This includes providing fixities, assigning flow boundaries, surcharge loads, and prescribed displacements. During static deformation analysis the model boundaries of the soil and rock were constrained in the vertical and lateral directions where the displacement due to applied load is negligible i.e. lateral boundaries was fixed against horizontal movement (ux = 0) and the vertical boundaries were fixed for both vertical and horizontal movement (ux =uy = 0) as shown in Figure 5.3.

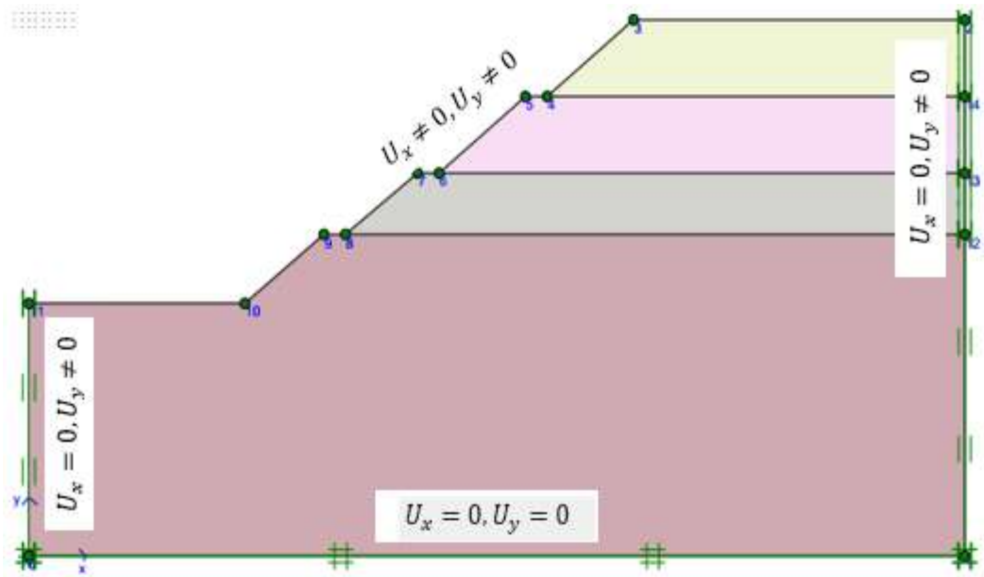

Figure 5.3: Boundary conditions for Plaxis 2D modeling

5.3.4 Mesh generation

The finite element numerical method is based on the discretization of a continuum into finite elements, describing the behavior or actions of each element and reconnecting them to represent the continuum. Different types of elements like a beam, shell, solid and different types of shapes like triangular, quadrilateral, tetrahedral with various order of equations can be used in FE discretization based on the nature of the project. In this work, the 4th order 15-node triangular element was used. Generally, the accuracy of the solution is increased with decreasing element size and increasing the order of interpolation (i.e. quadratic is more accurate than linear). But the computation time increases with decreasing element size and increasing order of interpolation (Plaxis 2013). To avoid such disadvantages optimal mesh size was selected by conducting sensitivity analysis. It was carried by evaluating the effect of different mesh sizes on total and horizontal displacement with constant loading conditions as shown in Figure 5.4.

From Figure 5.4 reducing element, size increases horizontal displacement and its effect becomes negligible beyond element number 324 (fine mush size). Accordingly, fine mesh sizes were used for this modeling. Finally, mesh generation was made using automatic unstructured mesh as shown in Figure 5.5.

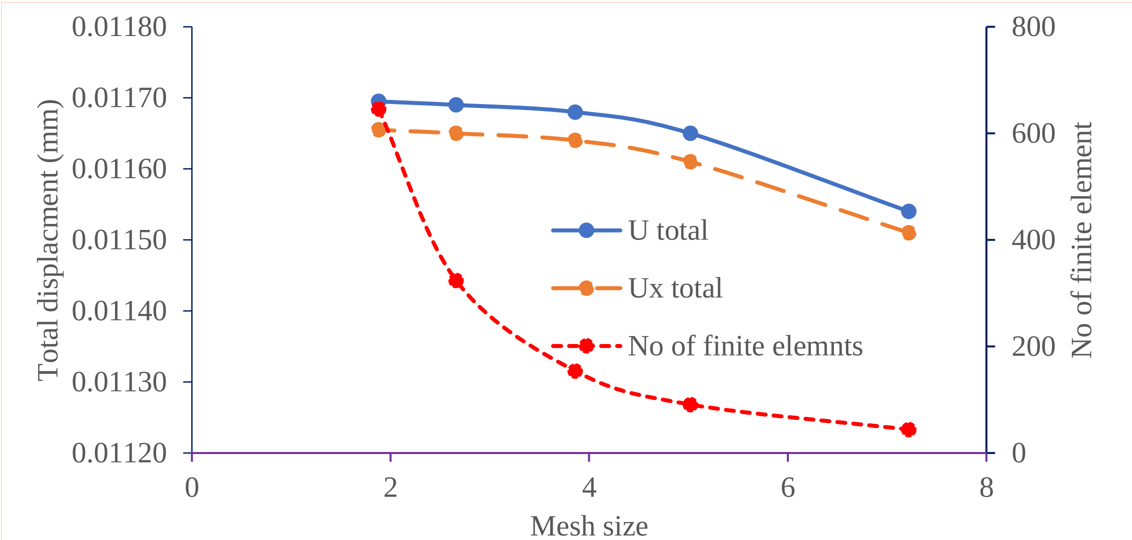

Figure 5.4: Sensitivity analysis for mesh size

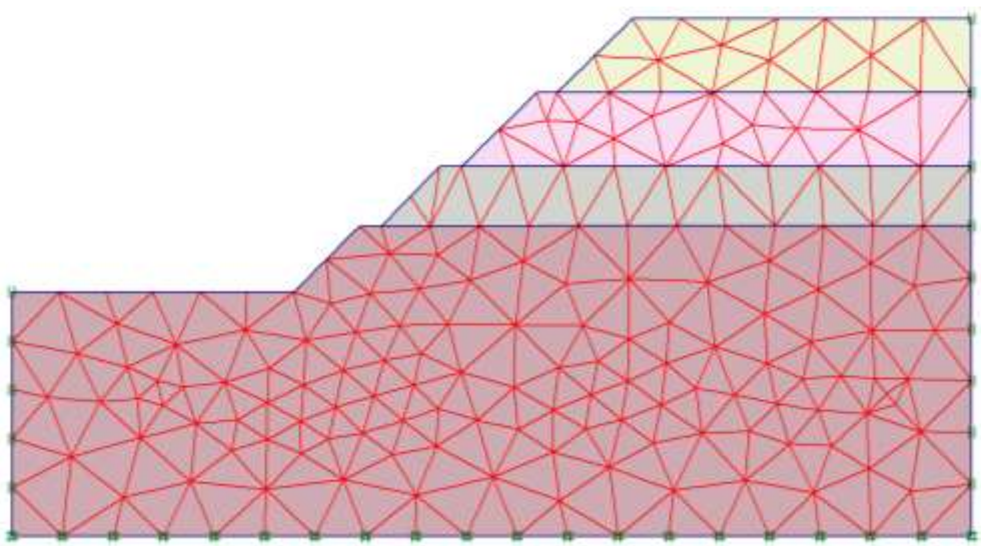

Figure 5.5: Meshing/ discretization of the model

5.3.5 Calculations with plaxis

Plaxis allows various calculation options (i.e. plastic calculation, safety analysis, dynamic analysis, and fully coupled flow-deformation analysis) depending on loading and/or boundary conditions. The execution of these calculation needs a generation of initial stress and pore water pressure distribution. Hence, the initial stress distribution was generated by k_0 procedure in terms of σ'_{v_0} *and* σ'_{x_0}. The horizontal initial stress values are related to the vertical one using $K_{0,x}$ as shown in figure Eqn. 5.3. On the other hand, the initial pore water condition was generated using phreatic level from the global water level.

$$\sigma'_{x0} = K_{0,x} * \sigma'_{v0} \tag{5.3}$$

Moreover, as the non-linear numerical analysis is an approximate method there is always some drift of result from the exact solution. To bound this error within safe and working limits plaxis allows the use of tolerated error. In this modeling, a tolerated error 0.01 or 1% was used in all calculations by varying iterations from 100 to 1000 depending on the loading and type of calculation.

5.3.5.1 Deformation analysis

The deformation analysis was carried with plastic calculation i.e. used for an elastic-plastic deformation analysis using constant stiffness. The method is suitable when the change of pore water pressure with time is not necessary (i.e. the case). Two critical slope sections were analyzed in this method using static and dynamic loading conditions. In the static condition, the evaluation was made for its material weight using $\sum M_{weight}$ as a multiplier. The hard rock at the top of the slope is represented as a surcharge load ($q = \gamma * h$). Whereas the dynamic condition was carried by introducing the earthquake forces in terms of horizontal acceleration coefficient (α=0.12 and 0.15) which uses multiplier (ΣMaccel) in the calculation routine. In this analysis additional horizontal driving force (α *$\sum M_{weight}$) was applied from the previous step as discussed in chapter 2. Table 5.2 shows the calculation phases and corresponding loading types.

5.3.5.2 Safety analysis

To evaluate the stability of the slope factor of safety was determined for each critical section using plaxis 2D. In plaxis safety analysis was carried using a phi-c reduction method i.e. a method where the shear strength parameters (c & tan∅) are successively reduced until the failure occurs. During the prosses the strength reduction factor ($\sum Msf$) is increased start from 1. The global safety factor is equal to the total multipliers $\sum Msf$ at the point of failure which is expressed as the ratio of initial and reduced strength parameters as shown in Eqn. 5.4.

$$\mathrm{FS} = \sum \mathrm{Msf} = \frac{\tan\emptyset_{input}}{\tan\emptyset_{\mathrm{reduced}}} = \frac{\mathrm{C_{input}}}{\mathrm{C_{reduced}}} = \frac{\mathrm{Su_{\,input}}}{\mathrm{Su_{reduced}}} \tag{5.4}$$

Table 5.2: Loading conditions and its calculation phase in plaxis software

Phase No	Lording Conditions	Start from	Calculation type	Loading input
Initial	Initial stress distribution	0	Initial stress	Ko procedure
Phase 1	Static with M_{weight}	0	Plastic/deformation	Staged construction
Phase 2	Static with surcharge	1	Plastic/ deformation	Stage construction
Phase 3	Pseudo static with Maccel	2	Plastic/ deformation	Total multiplayer
Phase 4	Static with M_{weight}	1	Phi/c reduction	Incremental multiplayer
Phase 5	Static with surcharge	2	Phi/c reduction	Incremental multiplayer
Phase 6	Pseudo static with Maccel	3	Phi/c reduction	Incremental multiplayer

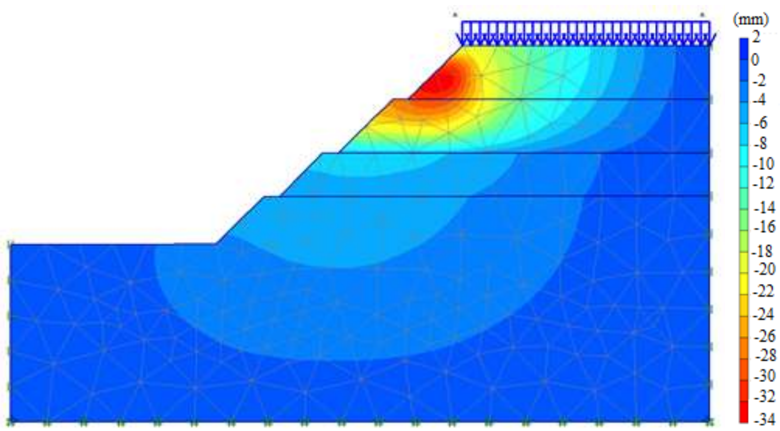

Figure 5.6: Deformation of slope section 1 for phase 2 in plaxis 2D

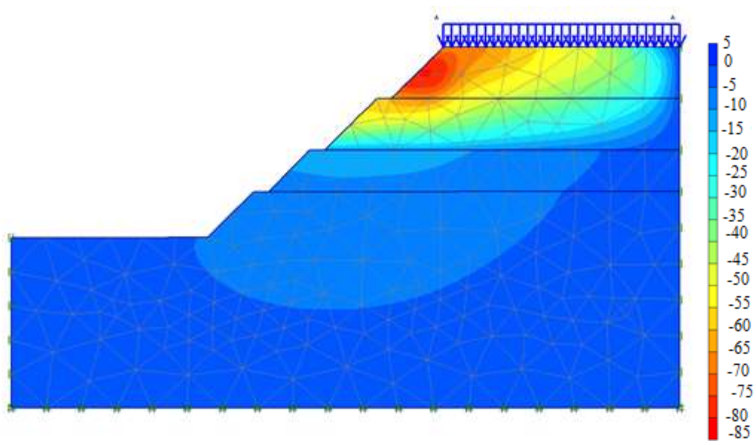

Figure 5.7: Deformation of slope section 1 for phase 3 in plaxis 2D

5.4 Modeling with slide

Modeling was also made in slide software to evaluate the FS of the slope using LEM to compare the result with FEM. The first step in slide modeling is the project setting where various important modeling and analysis options of the problem i.e. failure direction, units, analysis methods, and groundwater conditions are set. Two critical sections of the cut slope were modeled with similar geometric boundaries used in plaxis software. Mohr-Coulomb strength criterion was used to define the material properties of the slope. The criterion uses unit weight, cohesion, and angle of internal friction as the input parameter. In the analysis factor of safety and slip surface were evaluated for both static and dynamic loading conditions using bishop, Jambu, and GLE method. During modeling, most slope failures occur in a circular slip surface with little inaccuracy unless there are geological layers that favor the failure in a non-circular slip surface. Hence, a circular failure surface was used to define the type of slip surface and grid search is used to locate the critical slip surface (slip surface with the lowest safety factor). Figure 4.8 shows the slice, depth of slip surface, and grid search for FS using the GLE method.

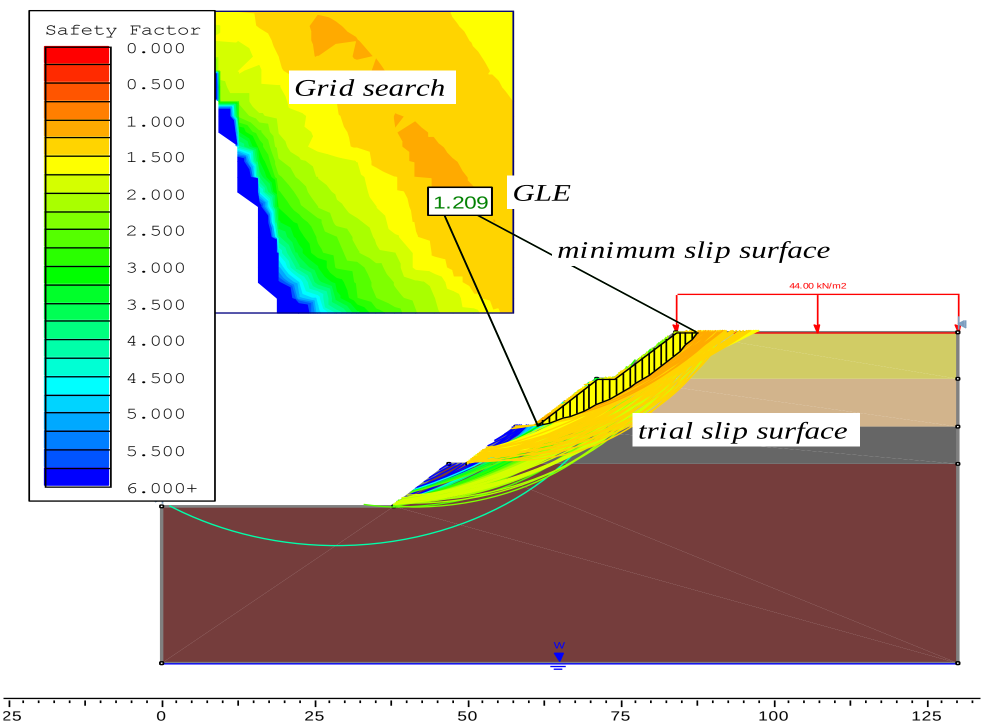

Figure 5.8: FS evaluation using slide software (slope section-1)

5.5 Performance evaluation of the slope profiles

Generally, the design of the slope is depending on the type of slope material, geological, and hydrological condition. Similarly, the selection of appropriate geometry also plays a key role in the stability of slope. The knowledge of performance and behavior of geometric parameters (i.e. slope height, slope angle, and slope profiles) in different soil and loading condition is used for selection as well as the economical design of slopes. Hence, the performance of different slope profiles and their geometric parameters was investigated in this study numerically using PLAXIS software. A selected slope section on the case study area was used for the evaluation and the modeling is according to the procedures discussed in section 5.3. The evaluation was made based on the following points.

1. The slope section in Figure 5.9A was modeled in a single slope profile and the effect of slope angle and slope height is evaluated.
2. The slope section in Figure 5.9B is modeled for different combinations of multi slope profiles and its performance is evaluated from the result in comparison with single slope profiles.
3. The slope section in Figure 5.9A is modeled for different bench slope, bench height, and bench width to evaluate the performance of bench with different values of these parameters and in comparison, with a single slope profile.
4. The cut slope given in critical slope section-1 of Figure 5.1A is modeled with three slope profiles and their performance was compared based on the result.

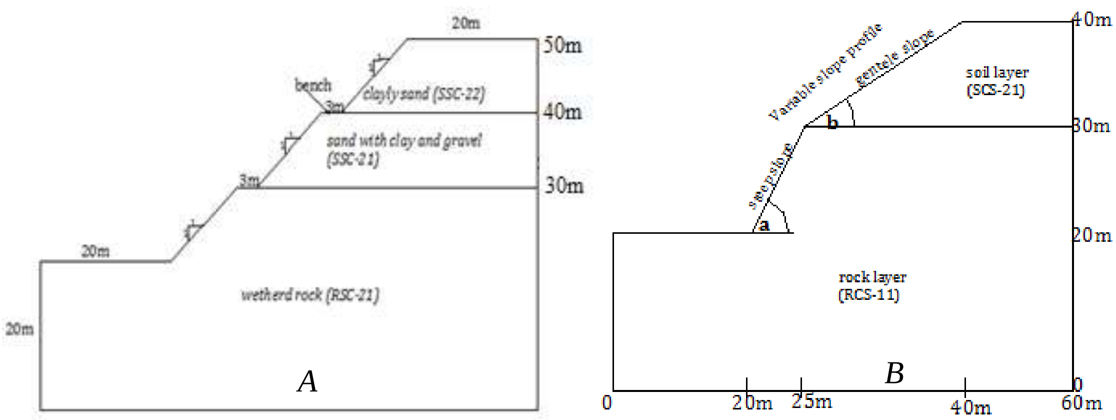

Figure 5.9: Typical cross-section of the road cut slope in the Goro to Abagada road project

5.6 Numerical validation

The software and procedures used to model critical slope sections in this study should be validated before the results of the analysis are accepted. As it is difficult to measure or/and monitor the deformation and FS in the field, existing literature of previous case studies and hand calculations were used to validate this numerical modeling.

5.6.1 Validation with previous case studies

To validate the study with the previous case studies two slope sections first introduced by Zhang (1988) and Cheng et al., (2007) were used. The slope sections were later used by numerous investigators (i.e. Ferdlund and Krahn, 1977; Chen et al., 2003; Griffiths and Marquez, 2007; Phase2, 2011; Nian et al., 2012; Zhang et al., 2013; Chaowei et al., 2019) to validate their 2D and 3D slope stability evaluations. Hence, these slope sections were modeled using a slide, Plaxis -2D, and Plaxis-3D software with the same material and boundary condition. The details of the evaluation were included in appendix H and the summary of the result as shown in Figure 5.10 and Table 5.3. Accordingly, the results obtained from the present evaluation show a good agreement with previous results of different investigators with adrift of less than 5%.

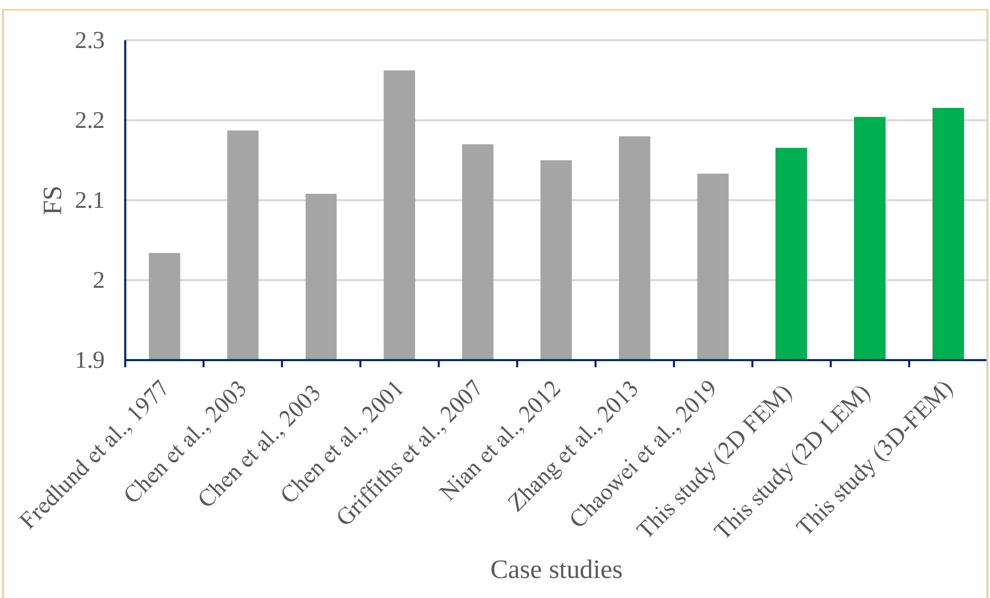

Figure 5.10: FS from different researchers and this study on Zhang (1988) slope section.

Table 5.3: FS from Cheng et al., (2007) and this study

Method	Previous studies		This study		
	LEM (avg)	Phase (FEM)	Plaxis 2D	Slide (bishop)	Slide (GLE)
FS	1.383	1.38	1.376	1.39	1.384

5.6.2 Validation with hand Calculation

To validate the numerical modeling with hand calculation the critical slope section 1 was evaluated using the ordinary method of a slice (Fellenius method) as shown in Figure 5.11. FS were determined for circular trial slip surface AC by considering the location of slip surface on LE based slide software.

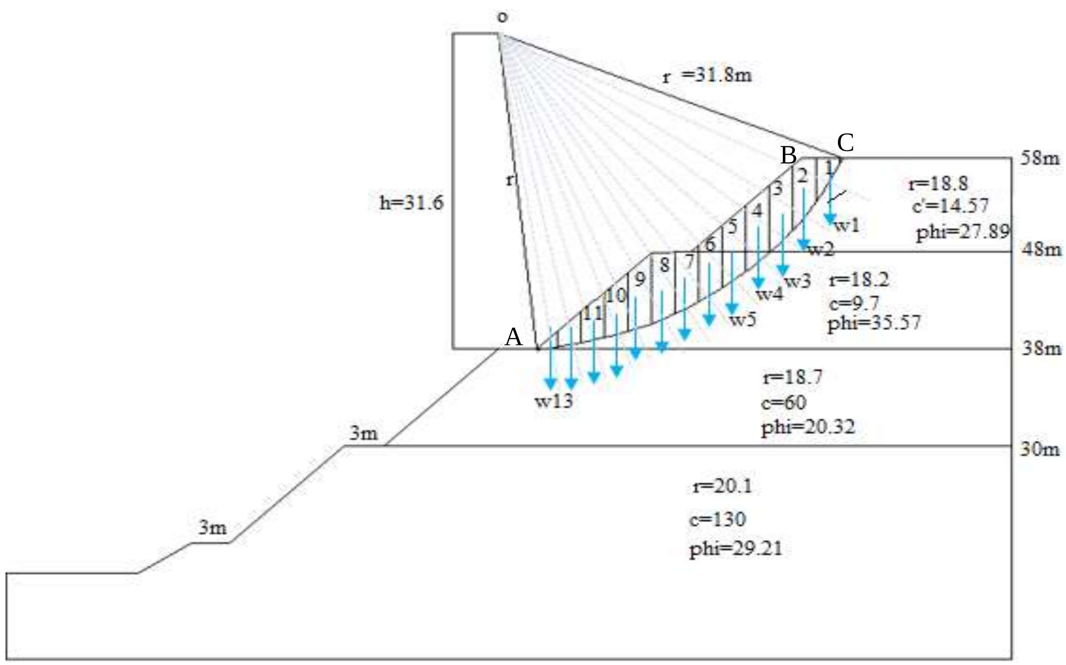

Figure 5.11: Slip surface for hand calculation on slope section 1

For equilibrium of trial wedge ABC, the moment of driving force about "o" equals the moment of resisting force about "o".

$$\sum_{n=1}^{n=p} W_n * r * sin\alpha_n = \sum_{n=1}^{n=p} \frac{1}{FS}\left(C' + \frac{W_n \cos\alpha_n}{l_n} tan\emptyset'\right) l_n * r \quad 5.5$$

$$FS = \sum_{n=1}^{n=p} \frac{(c' l_n + W_n \cos\alpha_n \tan\emptyset')}{\sum_{n=1}^{n=p} W_n sin\alpha_n} \qquad \text{where } l_n = \frac{b_n}{cos\alpha_n} \quad 5.6$$

Table 5.4: Calculation of resisting and driving forces for each slice

Slice no	W	α_n	c'	∅	l_n	$cos\alpha_n$	$sin\alpha_n$	$Wcos\alpha_n$	$Wsin\alpha_n$
1	89.5	62	14.57	27.89	4.26	0.47	0.88	42.0	79.0
2	200.8	56	14.57	27.89	3.58	0.56	0.83	112.3	166.5
3	246.1	49	14.57	27.89	3.05	0.66	0.75	161.5	185.7
Summation for layer 1					10.885			315.7	431.2
4	250.7	44	9.7	35.57	2.78	0.72	0.69	180.3	174.1
5	239.3	39	9.7	35.57	2.57	0.78	0.63	186.0	150.6
6	216.9	35	9.7	35.57	2.44	0.82	0.57	177.7	124.4
7	214.2	30	9.7	35.57	2.31	0.87	0.50	185.5	107.1
8	255.5	26	9.7	35.57	2.23	0.90	0.44	229.7	112.0
9	251.7	22	9.7	35.57	2.16	0.93	0.37	233.4	94.3
10	190.6	18	9.7	35.57	2.10	0.95	0.31	181.2	58.9
11	154.0	15	9.7	35.57	2.07	0.97	0.26	148.7	39.9
12	97.9	11	9.7	35.57	2.04	0.98	0.19	96.1	18.7
13	23.8	8	9.7	35.57	2.02	0.99	0.14	23.6	3.3
Summation for layer 2					22.718			1642.2	883.3

Then the FS of the slope is evaluated using equation 5.6.

$$FS = \sum_{n=1}^{n=p} \frac{((14.57*10.885+9.7*22.718)+(315.7*\tan 27.89+1642.2\ tan 35.57))}{\sum_{n=1}^{n=p}(431.2+883.3)} = 1.308$$

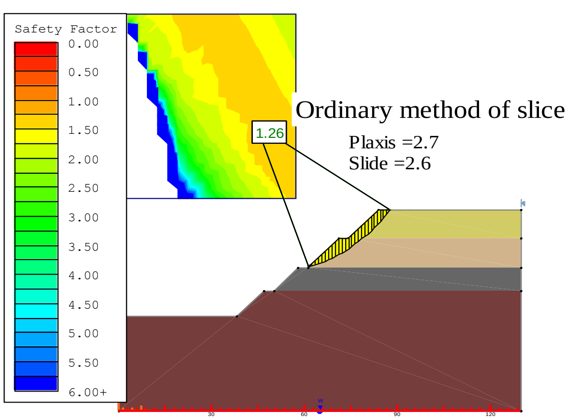

- The result obtained from hand calculation agrees with the result obtained from software's (i.e. only 2.99% drift from plaxis and 3.8% from slide software). This drift is due to approximation on hand calculation solution.
- Since all the validation shows a good agreement with previous case studies it is reasonable to accept the results.

Figure 5.12: comparison of CSS-1 with hand calculation

CHAPTER 6: RESULT AND DISCUSSION

6.1 Introduction

As discussed in section 5 different modeling was made to evaluate the stability conditions of the slope and performance of slope profiles on critical slope sections. In this section, a discussion was made on the analysis result and stability condition of the slope section for static and dynamic loading. A comparison of results also included between FEM & LEM. Furthermore, performance evaluation results of slope profiles also presented (i.e. discussion was made on the performance, suitable condition, and advantages of one over another for a different point of view).

6.2 Discussion on the analysis results of the critical slope section

6.2.1 Deformation analysis result

The deformation of two critical sections was evaluated for its initial condition (i.e. with and without surcharge) and pseudo-static force. Figures 6.1 A shows the total horizontal deformation result from plaxis 2D in its initial condition. The total displacements of the slope are 32.83. The maximum deformation of slope occurs on the top two layers of the slope material indicating that slope instability problems will occur in this section. Some sections of the slope have a rock layer at the hill extending up to 2.1m. To represent the effect of this layer the slope is analyzed using a surcharge load of 44 kN at the top of the slope as shown in Figure 6.1 B. Accordingly, the maximum deformation is increased to 52.84 from its initial condition. From this, it is understood that the probability of failure is higher in the slope section with the rock layer at the top.

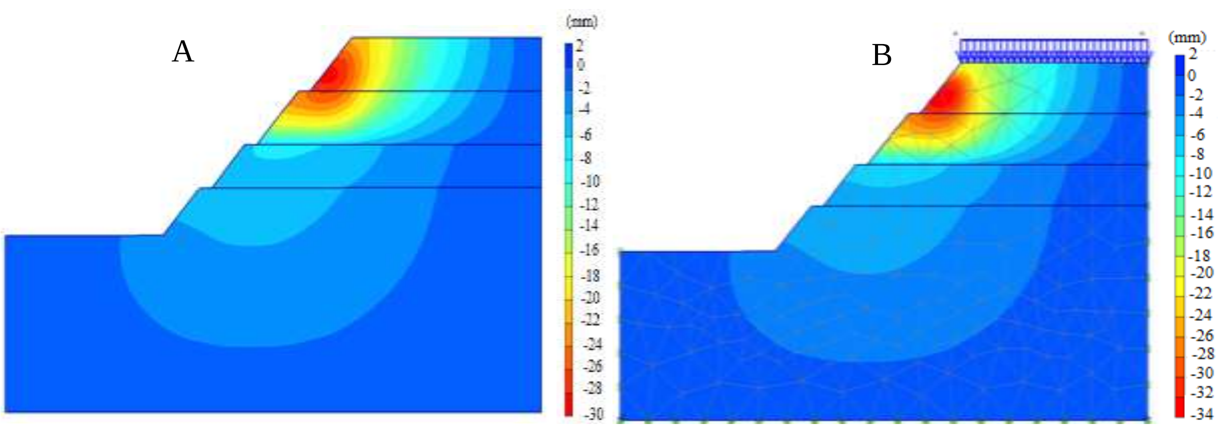

Figure 6.1: Total horizontal displacement for a static condition with and without surcharge

Further analysis of this slope section was made to evaluate the effect of an earthquake. The analysis was carried in a pseudo-static method by representing the earthquake in the horizontal acceleration coefficient $\alpha = 0.12$ *and* $\alpha = 0.15$. Figure 6.3 shows the deformation of the slope section for both surcharge and earthquake load and Figure 6.2 indicates the increase in deformation of the slope section in three loading conditions (i.e. static without surcharge, static with surcharge, and pseudo-static). It has been seen that during pseudo-static analysis the maximum load ∑Marcel is less than 1 indicating that failure occurs during this loading. From the result, deformation is increased by 93.78 mm in earthquake loading (PGA=0.15). But it must be recognized that the deformation is only static (i.e. not resulted from dynamic vibration) in this loading condition.

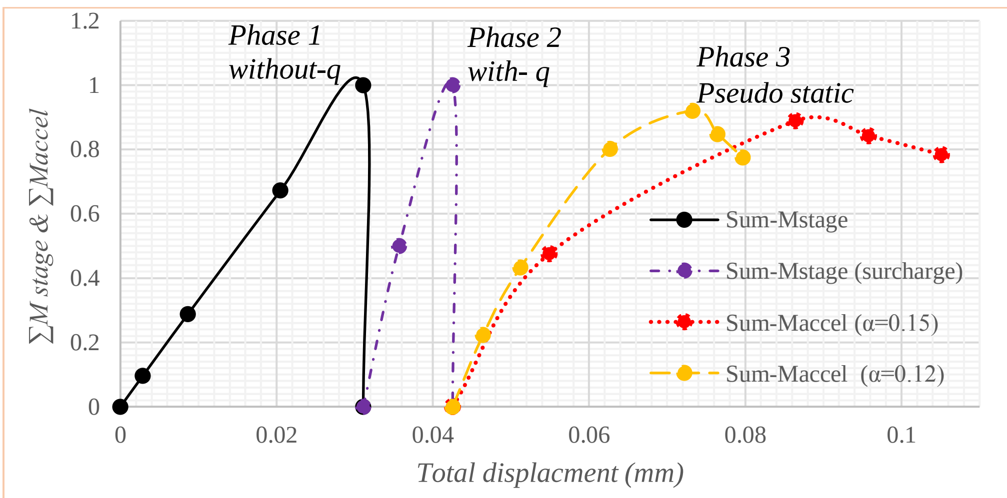

Figure 6.2: Sample result of deformation (load-displacement curve) from plaxis 2D at point A

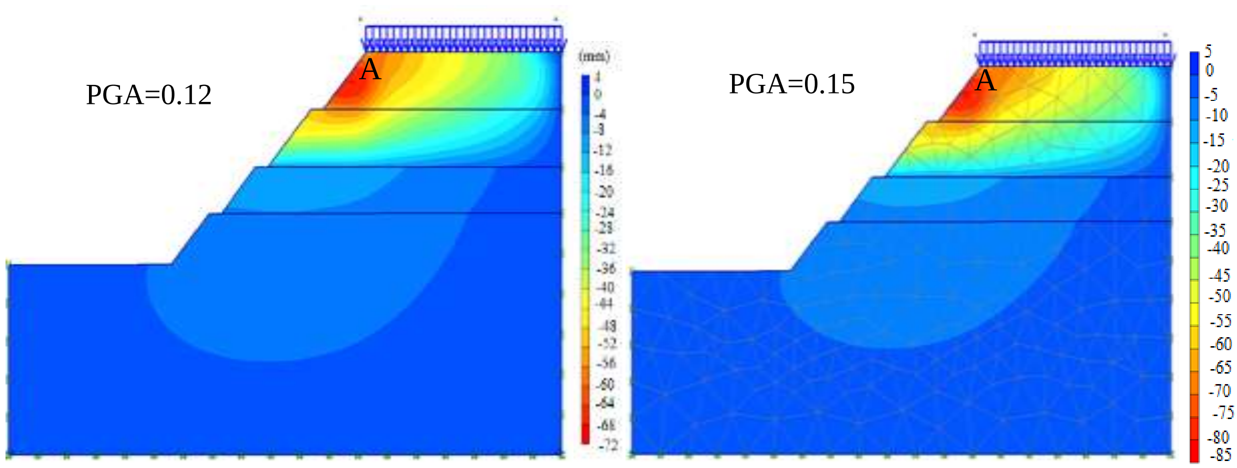

Figure 6.3: Deformation of slope section 1 from pseudo-static and surcharge loading

From all the above analysis results the maximum deformation (maximum strain) occurs at the top two soil layers. This validates the result of a field survey and laboratory investigation, as this section shows weaker material properties and different failure manifestations. Hence it is concluded that this clayey sand layer is the potentially unstable layer of the slope section. Similarly, the failure occurs at the shallow depth of the slope section, which indicates that no deep-seated failure will be expected in this section.

6.2.2 Results of Safety analysis

To identify the level of stability the factor of safety was evaluated for critical slope sections using LEM (slide software) and FEM (plaxis 2D). The evaluation was made for three loading conditions in a dry state. Underneath the results of FS and stability of the slope for static and dynamic loading conditions are discussed.

6.2.2.1 FS result from plaxis 2D

The safety factor of both critical sections was evaluated in plaxis 2D using the phi-c reduction method as discussed in chapter four. The evaluation was made for static and dynamic loading with and without a surcharge load. Figure 6.4 and Table 6.1 shows the evaluation of FS using phi-c reduction method and FS results for different loading condition respectively. Accordingly, the stability of slope decreases in the order of static without surcharge, static with surcharge, and pseudo-static. The maximum FS is 1.27 occurs when the slope is model without any additional load in its dry condition. The value is reduced by 23% and 26% due to the introduction of horizontal pseudo-static acceleration coefficient α=0.12 & α=0.15 respectively as given in Table 6.1.

Similarly, deformation and FS are evaluated at critical slope section-2 for static and dynamic conditions. Since as no rock layer is in this section there is no need to uses surcharges in the evaluation of FS. From the result, the maximum FS in SSC-2 is 1.302 in static condition and it is reduced into 0.981 when a horizontal acceleration coefficient of 0.15 is applied. From this, it is recognized that slope section 2 is relatively stable than slope section 1. But as FS from the pseudo-static analysis is less than 1 the slope is unstable in dynamic condition.

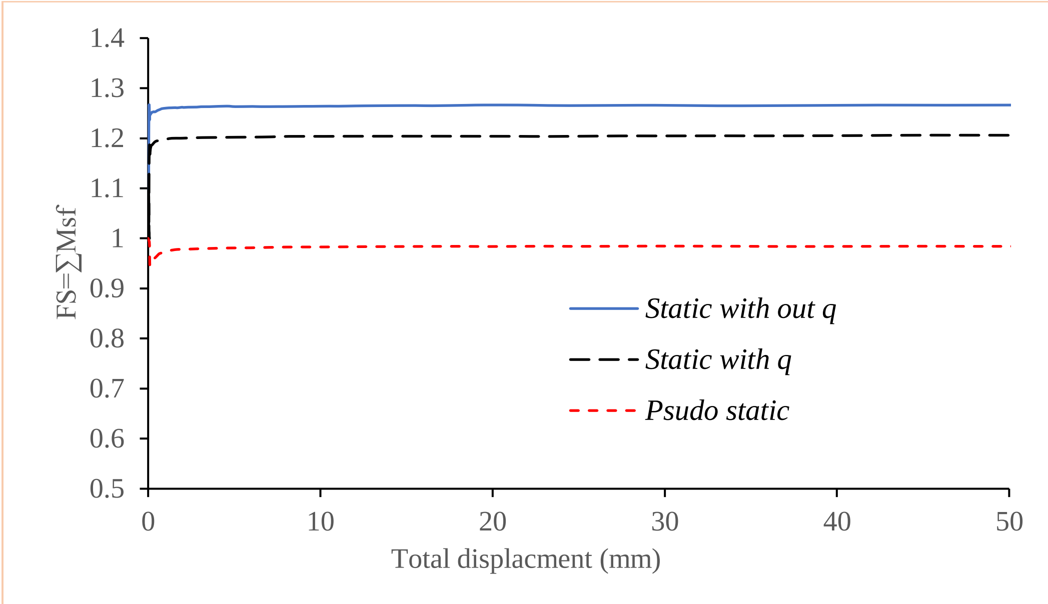

Figure 6.4: FS for slope section-1 from Plaxis 2D using the strength reduction method

Table 6.1: FS from Plaxis software for CSS-1 and CSS-2

Software	Method	CSS-1				CSS-2		
		Dry static w-out q	Dry static w- q	Pseudo-static		Dry static	Pseudo-static	
				0.12	0.15		α =0.12	α =0.15
Plaxis	2D	1.27	1.207	0.985	0.942	1.302	1.037	0.981

6.2.2.2 FS from slide

The stability of slope also evaluated using LEM (i.e. GLE, bishop, and Jambu corrected method) using slide software. Both critical sections of the slope were evaluated for the same loading conditions as plaxis software. As the slide is a LE based software it only evaluates the depth of slip surface and FS using the method of a slice as shown in figure 6.5. Table 6.2 shows FS results for both critical sections using the same loading condition. The minimum FS in the static condition is 2.85, 2.89, and 2.88 in Bishop, Janbu, and GLE method respectively. From the result, it is seen that FS shows a slight variation between different analysis methods. Like the strength reduction method, the FS is reduced by 24% and 26% from its initial condition due to the introduction of a horizontal pseudo-static acceleration coefficient 0.12 and 0.15. From figure 6.5 it is shown that the slip surface for minimum FS occurs in the topsoil layers like the deformation analysis. Moreover, the slip surface shows a shallow translational type of slope failure indicating that deep sated failure is seldom to occur.

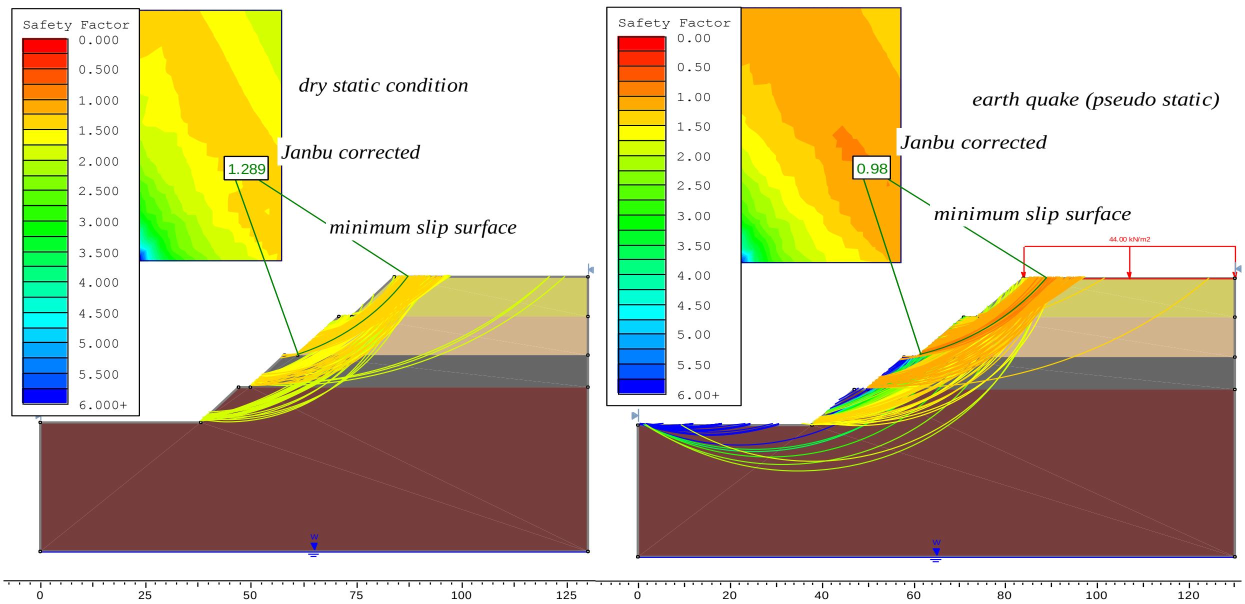

Figure 6.5: FS evaluation using slide software (slope section-1)

Table 6.2: FS from Slide software for CSS-1 and CSS-2

Software	Method	CSS-1				CSS-2		
		Dry static w-out q	Dry static w- q	Pseudo-static		Dry static	Pseudo-static	
				0.12	0.15		α =0.12	α =0.15
Slide	Bishop	1.285	1.194	0.991	0.947	1.301	1.061	1.009
	Janbu	1.289	1.18	0.975	0.932	1.302	1.056	1.004
	GLE	1.288	1.209	1.01	0.965	1.313	1.073	1.022

6.2.3 Stability condition of the slope

Theoretically, all slopes with a factor of safety greater than unity are safe. However, many design standards recommend the use of FS greater than one. The reason behind it is that uncertainties from the material investigation, the use of boundary conditions, the method of analysis, and numerical approximation can influence the analysis result. Hence as this work also passes through all these stages considering a safe FS greater than one is reasonable. As shown from the analysis result presented above the FS for critical section varies from 1.2 to 1.3 in dry static condition. From this, the stability of the slope can be taken as marginally safe. While FS is reduced up to 0.932 in pseudo-static analysis indicating that the slope will not be longer stable during earthquake loading.

From the numerical analysis the potential failure surface, maximum deformation, and minimum FS have occurred in the upper two soil layers (SSC-21 and SSC-22) of the slope section. The result is more likely as filed manifestations like erosion, tension cracks, debris flows, and weaker material characteristics are detected in this section during field survey. Therefore, these two layers are grouped as a potentially unstable layer of the slope section. It is also seen that the rock sections of the slope are disintegrated with closely spaced joints and the possible mode of slope failure occurs through its rock mass. But as a general, the rock layers are relatively stable sections of the slope. Generally, the FS result indicates the stability of slope is marginally safe in static conditions and unstable in dynamic conditions.

6.2.4 Remedial measures

To recommend suitable remedial measures for a potentially unstable section of the slope, assessment of the probability of failure is needed as focused in this work. Based on the actual stability condition of the slope obtained from numerical evaluation and field investigation suitable remedial measures were recommended in this study. Generally, remedial measures of slope failure are categorized into four groups (i.e. modification of slope geometry, drainage control, retaining structure, and internal soil reinforcement). For this case, drainage control and internal soil reinforcements are recommended to maintain the stability of the critical slope sections.

Soils in the potential failure section are highly erodible as recognized from the detailed field survey and erosion is identified as a failure manifestation. According to Abera (2007), the groundwater recharge from rainfall is negligible in the area and many of the rainfall are changed in to run off. Therefore, the slope section needs appropriate surface drainage to prevents the section from erosion and infiltration. This includes a combination of: -

1. Cutoff drain at the top of the slope to prevent the flood from entering into the slope section from the adjacent area.

2. Herringbone drains (shallow slope drains) at the surface of the slope.
3. Lateral drainage (bench drain) to collect rainwater from each bench slope and drain it laterally to spillways.
4. Open channel spillways to drain floods from cutoff and bench drains safely to toe drains.
5. Covering of slope face with vegetable to prevent surface erosion and rainwater infiltration It is noted that covering the slope face with grass or/and vegetation provides additional strength and aesthetic value for the slope.

On the other hand, the quality of the rock layers in SSC-1 ranges from poor to good, and closely spaced joints were observed on it. This layer is relatively stable as the numerical analysis shows shallow slope failure, but to increase its stability in earthquake conditions structural supports are needed. Therefore, one or combination of reinforcing remedial measures such as; shotcrete, wire mesh, rock bolts, grouting, or anchoring should be applied to maintain its stability.

6.2.5 Comparison of LEM and FEM

The LEM and FEM are compered using results from the slide and plaxis software. Outputs show that a slightly higher FS is obtained in LEM than FEM. It has been seen that results from FEM (plaxis software) give more information about the failure surface i.e. the stress, strain, deformation, and displacements at any point in the slope section. Whereas the LEM (slide) gives only uniform FS along the failure surface. The deformation in FEM (plaxis) indicates that failure can occur in any shape and the movement can vary at each point of the slope section as shown in Figure 6.6. This disproves the assumptions of uniform FS along the slip surface and rigid movement above the failure surface in LEM**.** Besides, the strength reduction method provides a more realistic estimation of FS and slope failure (i.e. non-convergence of algorism in a specified iteration indicates failure as shown in Figure 6.4) compared with the LEM (i.e. searching of the minimum FS in the predefined shape of failure surface). Figures 6.6 and 6.7 show the total displacements at each finite element node and the relative shear stress (i.e. the proximity of the stress points to the Mohr-Coulomb failure envelop) from FEM which is not accessible in LEM. On the other hand, Figure 6.8 shows the FS and slip surface in LEM using different approaches. The result shows that the value of FS also varies within LEM depending on the method used.

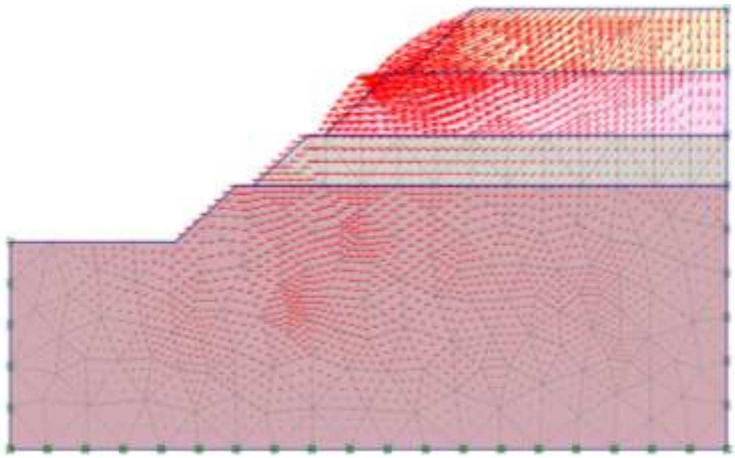

Figure 6.6: Total displacements at each node of finite element (plaxis 2D**)**

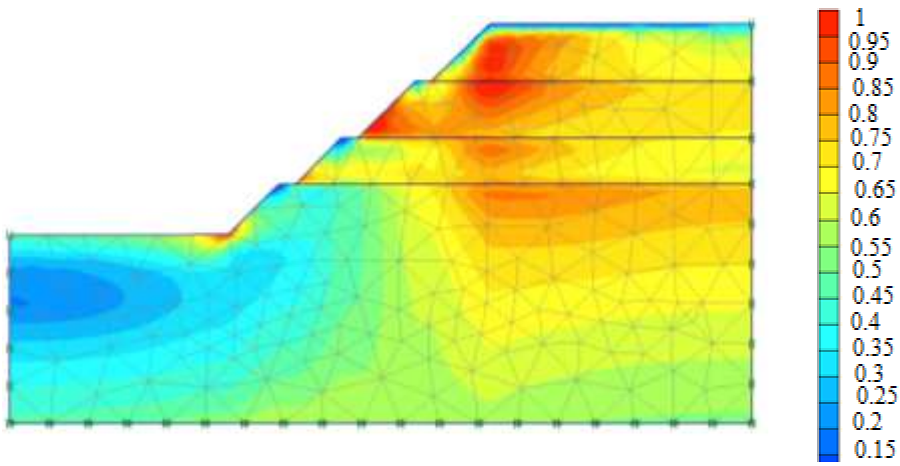

Figure 6.7: Relative shear stress of slope section 1 (plaxis 2D)

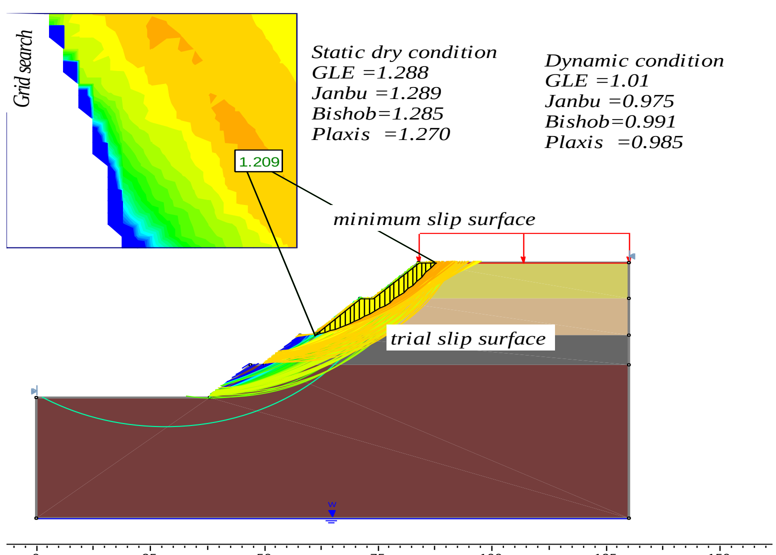

Figure 6.8: FS and slip surface using LEM (Slide).

6.3 Parametric study on performance of Geometric profiles

Geometry of slope is among the most critical factors controlling the stability of the slope. Hence investigation was made on the performance or /and effect of geometric parameters including slope angle, slope height, and slope profile (i.e. single slope, multi slope, and bench slope). The evaluation was made numerically on selected critical slope sections interims deformation and FS using plaxis software. In this section, the effect of slope height, slope angle, bench width, no of bench, and bench angle was evaluated as a parametric study. Finally, a comparison of slope profiles was also made based on FS, the difficulty of construction, appearance or beauty, drainage control, and accessibility for maintenance.

6.3.1 Effect of slope height and slope angle

Slope angle and height affect the stability of slopes as the increase of these parameters increases the shear stress while decreasing shear strength on the potential rupture plane. To examine the effect of these parameters numerical models were made for different slope height and different slope angles. The slope section given in Figure 5.9 A was modeled for 27˚, 34˚, 45˚, 63˚, and 73˚ to evaluate the effect of slope angle on the FS of the slope. The result in Figure 6.9 clearly shows that the increasing slope angle significantly reduces the FS.

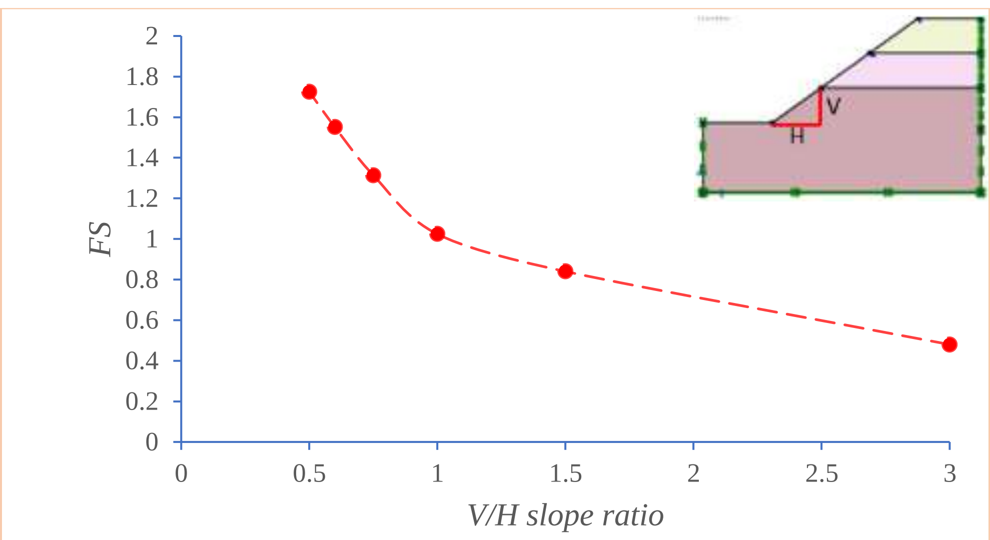

Figure 6.9: Effect of slope angle on the FS of the slope

Similarly, the effect of slope height was examined by analyzing the ideally sandy lean clay slope for different slope heights. The evaluation result in Figure 6.10 shows increasing slope height increases the deformation and decrease the factor of safety of the slope. It is recognized that both slope height and slope angle reduce the FS of slope in the same principle i.e. increasing self-weight (driving force) above the failure surface and decreasing the normal force (resisting force) on the failure surface. Hence designing safe slopes with a single slope profile needs a very gentle slope when the height of the slope is higher which makes it uneconomical.

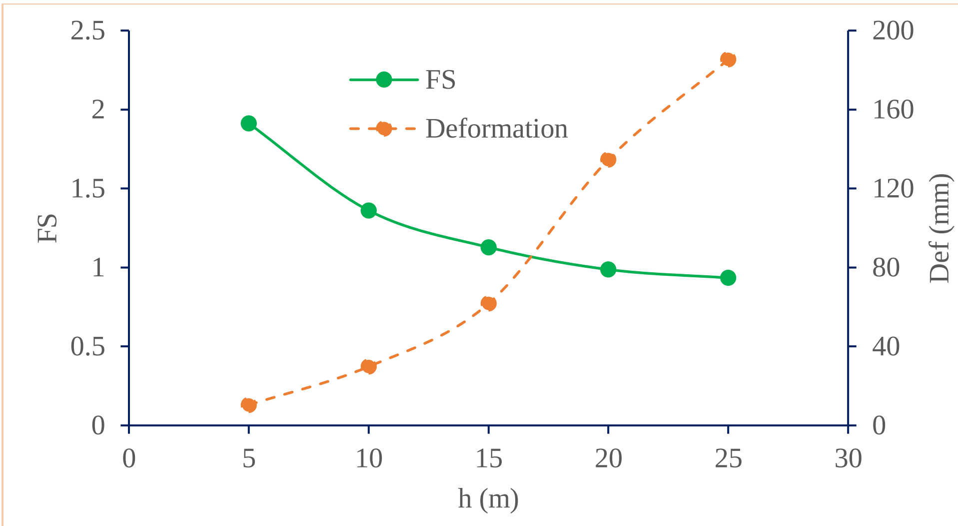

Figure 6.10: Effect of slope height on the FS and deformation of slope

6.3.2 Performance of bench on the slope stability

The benched slope profile is a technique in which the overall slope is divided into multiple small slopes. The technique is used to avoid the design of very high and gentle slopes on a single slope profile. To examine the performance of benching on the stability of slopes a typical slope section given in Figure 5.9 was used. Different parameters i.e. bench width cut angle and no bench was varied simultaneously to evaluate their effect on the deformation and factor of safety of slope.

The effect of slope bench on the factor of safety was determined by evaluating the given slope section for five bench widths with a constant 10m bench height. Figure 6.11 shows the 2D plaxis results of the analysis. Generally, the use of bench improves the FS of the slope compared with single slope profiles. But its effectiveness depends on bench width, bench height, and bench slope. As the figure indicates slope stability increases with increasing bench width, (i.e. The FS increases in 3.5%, 7.7%, and 12% from single slope profile in 1:1 slope ratio when we use 1m, 2m and 3m bench widths respectively). Similarly, the deformation of the slope is also decreased with increased bench width. The reason is that increase in bench width reduces the weight or driving force above the failure surface.

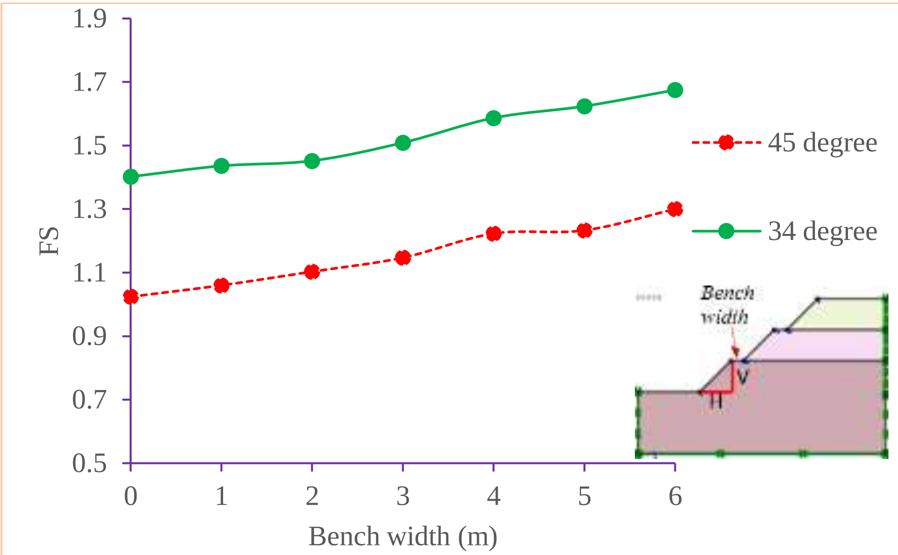

Figure 6.11: Effect of bench, and bench width on the FS from plaxis 2D

The effect of the bench with various slope angle also examined by varying the cut slope for constant bench width. Figure 6.12 shows the percentage change of factor of safety from equivalent single slope profile for different slope ratio i.e. FS changes in 1.7%, 3.6%, 7.7% and 17.4% from single slope profile for slope angle 27˚, 34˚,45˚ and 63˚ respectively in 2m bench width. The result indicates that the use of benching is more effective in areas of steep cut slopes. This is because gentle slopes give higher FS in a single slope which decreases with increasing slope angle and needs the use of bench.

On the other hand, no of bench (i.e. height of bench) in a slope profile also affects the stability of slopes. Its effect was evaluated using uniform clayey sand soil in two cases (i.e. case 1, when the overall cut varies with constant slope within bench. Case 2, when overall cut is constant with varied slope within bench). The modeling was made with 7, 10, and 15m bench height with 3m constant bench width. Figure 6.13 shows the plot of FS and No of bench that indicates increasing stability slope with decreasing bench height for case 1. However, in case 2 decreasing bench height provides only a slight change in FS. In this case, FS is improved when slope height is reduced up to 10m. The result indicates that reduction of bench height is effective up to optimum bench slope is reached in case 2. The reason behind it is that decreasing slope height beyond this point will change the slope to a very steep angle

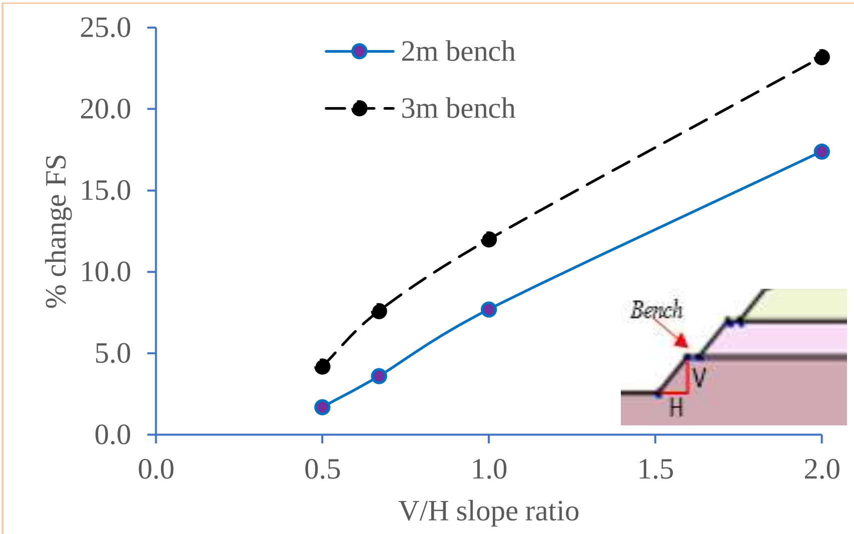

Figure 6.12: Effect of bench on different slope angle

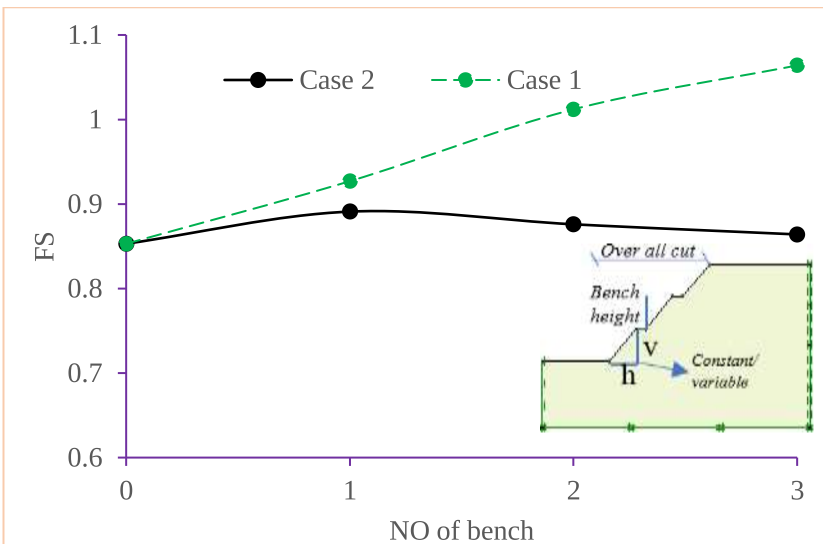

Figure 6.13: The effect of bench height on FS with constant and varied slope within bench.

In all the above cases benching provides good stability for slopes. To demonstrate it the critical slope section-1 used for stability analysis in section 6.2 is evaluated for both single and bench slope profiles. The actual slope cut was made by using 3m bench width every 10m bench height. Accordingly, the use of bench in this slope provides a 13% increase in FS when compared to its single slope profile. Generally, benches improve stability of slope in the opposite principle of slope height and slope angle by decreasing the driving force of the slope. The method is effective to avoid the use of gentle and high slopes in the design of cut slope.

6.3.3 Performance of multi slope profile on slope stability

Multi-slope profiles are another type of slope geometry where the slope angle varies within a section. It allows the use of steep and gentle slope in stiff and loses materials respectively when a single slope comprises stratified soil. In this section, the performance of multi slope profile in comparison with a single slope was evaluated numerically. The slope section in Figure 6.14 consists of both soil and rock were used for this examination. The FS was evaluated for different combinations of bottom (a) and upper (b) slope.

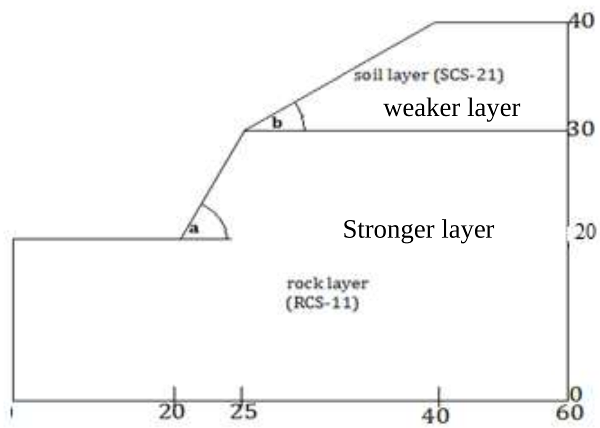

Figure 6.14: Idealized slope section and its plaxis 2D model

The analysis result is presented in Table 6.3 and Figure 6.15 for a different combination of a and b. Accordingly, the use of multi slope profile improves FS when the strength of the material comprises the slope is varied. In this case, FS is improved up to 30 % from a single slope profile when the slope of weaker section is decreased and that of stiffer section is increased. The principle is that multi slope profiles reduce the driving force from the weaker section and increases it in the stiffer section of the slope. The amount of change in FS depends on the strength characteristics of the slope section, but there is no doubt in the performance of multi slope profile in stratified slopes.

Table 6.3: FS for different multi slope profiles (a= bottom /stronger slope and b= top/weaker slope)

Slope								
Slope	a (stronger layer)	45	48	51.3	55	59	63.4	68
	b (weaker layer)	45	42.3	39.8	37.5	35.5	33.69	32
FS		1.202	1.251	1.325	1.414	1.432	1.503	1.569

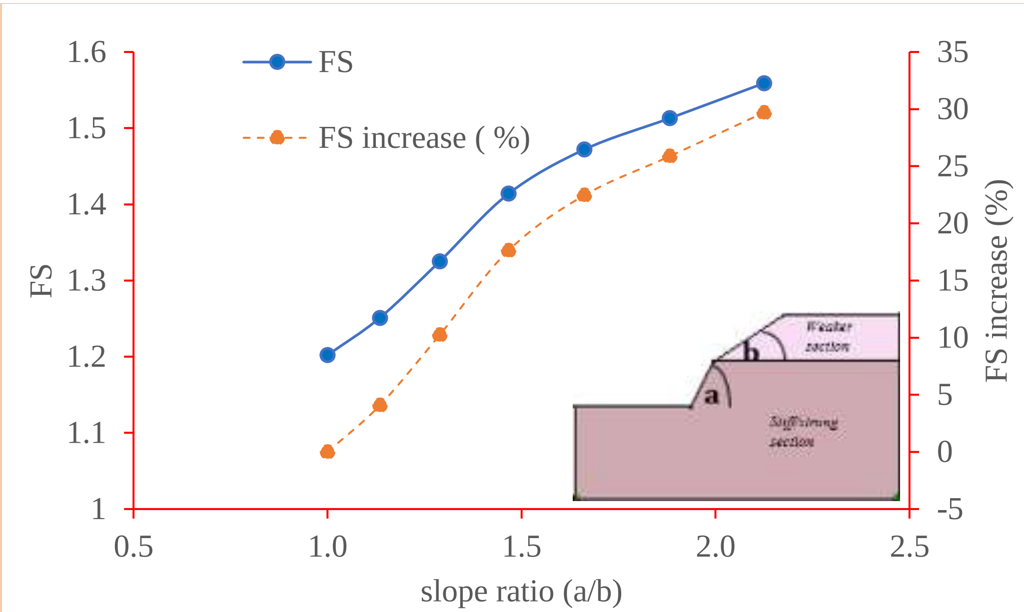

Figure 6.15: FS and its change from single slope in % for different combination of slope profiles

Moreover, to support the above result the critical slope section-1 in section 6.2 was evaluated for three different combinations of multi slope profiles. The adjustment of a multi slope profile is made without changing overall slope geometry (adjustment is made only within the slope having various strength). The result shows the use of multi slope profile can improve the FS of the slope section up to 22.7% from the actual profile. Figure 6.16 shows the effect of benching and multi slope profile on the stability of critical slope section-1. Accordingly, FS changes in 13%, 22.7%, and 37.5% from single slope profile in bench, multi-slope, and the combinations of both methods respectively. As the slope section is a stratified material comprising both soil and rocks the use of bench and multi slope profile provides a significant improvement of FS. Moreover, its ability to provide improvement without extra excavation makes multi slope profile more economical remedial measures in stratified soils.

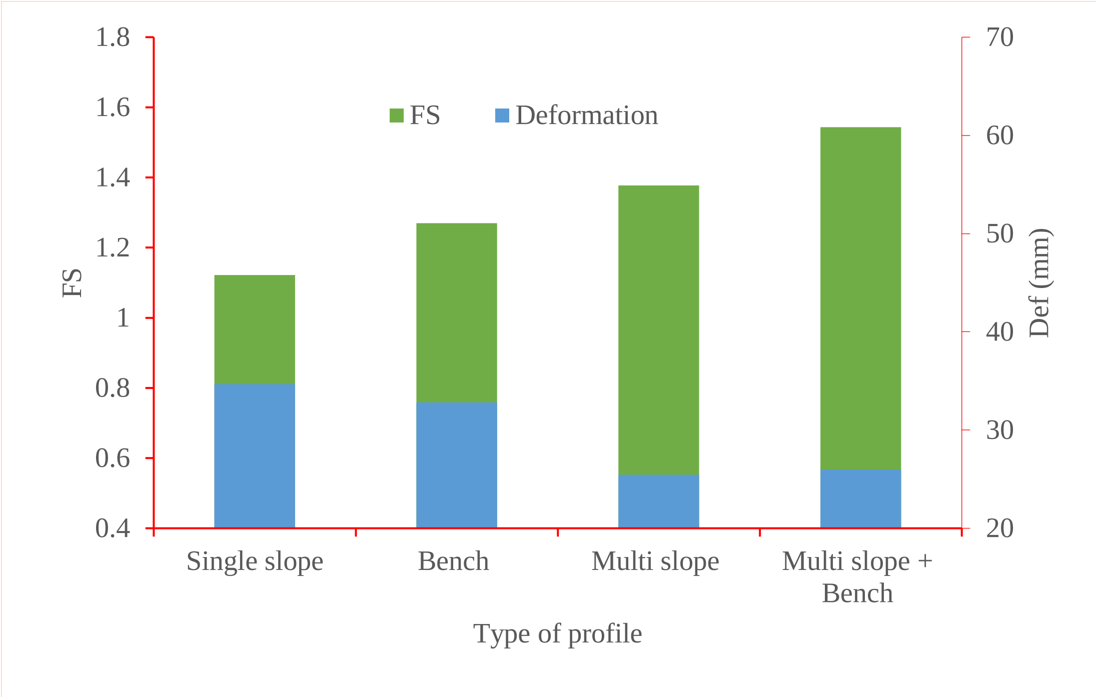

Figure 6.16: FS of critical slope section 1 for different slope profiles

6.4 Comparison of slope profiles

From the above evaluation, it is recognized that modification of slope geometry is one and the very first economical alternative of slope stability improvement. Although this investigation is made in a specific type of slope material there is no doubt in the role of geometric modification in slope stability. However, the selection of these slope geometry should depend on site-specific parameters i.e. susceptibility of the slope to erosion and infiltration, the variability of slope material, the height of slope, and adjacent area of the slope.

According to the evaluation result, the use of a single slope profile is effective in homogenous stiff slope material when the height of the slope is low. Otherwise, the method may not be safe and economical choice as weak and high slope sections need very gentle slopes. Multi slope profiles are suitable in slopes where there is material strength variability. It provides a very economical slope design without extra excavation by adjusting only within the slope section. Especially the method is ideal in slopes comprise both rock and soil. The use of bench is an effective geometric measure instability improvement when the height of the slope is large. It increases FS by reducing the driving force above the failure surface. In addition to its direct impact on FS of the slope, these slope profiles have advantages and limitations. Therefore, the selection of slope profiles should be based on site-specific considerations of drainage, need for maintenance, aesthetic value, and need for extra excavation. For example, benches provide various advantages such as, (1) it reduces the area of the slope exposed to rainfall infiltration as it allows the use of steep slope between every benching. (2), It provides effective drainage control by collecting the rainwater from each slope profile and draining it laterally to ditches. (3), it provides access to side slopes for maintenance, plantation of vegetation, and decoration. (4), it uses for collection of debris falls above it. (5), it provides aesthetic value and better appearance for slopes especially when it located around towns. On the other hand, the need for extra excavation in adjacent areas and installations of lateral drainage can be taken as a limitation in bench slopes. The selection of slope profiles should be based on site-specific advantages and disadvantages. Figure 6.17 shows the summary of advantages and disadvantages for a bench, multi, and single slope profiles.

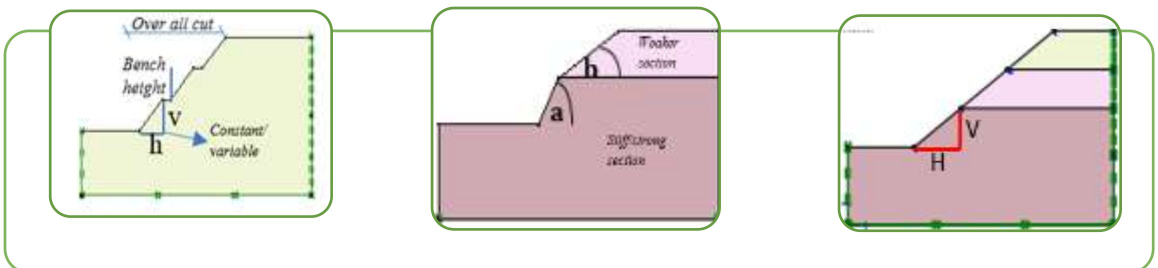

-Suitable in high slopes.

-Provide better drainage control.

-Provide access to slopes for maintainace

-Provide better appearance.

-Need extra cut or excavation.

- Suitable in stratified slopes.

-Less perform in drainage control.

-Difficult to acsses slopes for maintainance

-Provides a good appearance for slope.

- No need of extra excavation (economical)

-Suitable in short and stiff slopes

-Poor performance in drainage control

-Difficult to acsses slopes for maintainance

-Provides Poor apperiance

Figure 6.17: Summary of slope profiles on different point of view

CHAPTER 7: CONCLUSION AND RECOMMENDATION

7.1 Conclusion

This study was carried out on a newly constructed highway road cut slope from Goro to Abagada in Adama city. The area is in the rift valley region (high earthquake risk zone). The cut slope extends up to 40m height and a considerable sign of failures such as tension cracks, debris flows, and erosion are observed on it from field manifestations. Hence, this study emphasizes on the stability analysis and performance evaluation of geometric profiles on the stability of slopes.

Stability analysis was done for the objective of identifying the geomechanical parameters and evaluating the stability condition of a slope. The soil and rock parameters for this evaluation were obtained from the field survey, laboratory work, and correlation or/and processing of field and laboratory data. During field survey identification of failure manifestations and critical slope section, observation, interview, measurement, and sample collection for laboratory test was made. From this survey, it has seen that rock sections are highly disintegrated and rock mass failure is the potential failure mode on the slope. A laboratory test was also carried on soil and rock samples to determine index and strength properties. Then the stability evaluation was done in a dry state for static and dynamic (pseudo-static) loading conditions using the limit equilibrium method (slide software) and finite element method (plaxis 2D). The elastoplastic Mohr-Coulomb material model was used in all finite element analysis. From stability analysis, the following conclusions were made.

1. The analysis results in the critical slope section show that the slope is marginally stable with FS varying from 1.2 to 1.3 in static condition and unstable in earthquake loading with FS below 1.
2. Comparison of FE and LEM using results from slide and plaxis software show that a slightly higher FS is obtained in LEM. It is also seen that finite element slope stability analysis gives more valuable information about the failure surface including stress, strain, deformation, and displacement at any point in the slope section.

The performance evaluation of slope profiles was made for the objective of creating awareness on the effect and its suitable condition of different geometric profiles on slope stability. The effect of geometric parameters like slope height, slope angle, bench width, no of bench and bench angle on slope stability were evaluated under this section using plaxis software. The evaluation was made interims of FS and deformation on selected critical slope sections in the study area. Comparison also made between slope profiles on their performance and other advantages like drainage control, access to maintenance, and aesthetic value. From the result, it has seen that geometric modification will improve the stability of slopes better and economically compared to other structural remedies. The following conclusions are drawn from the performance evaluation of slope profiles.

1. The stability of slope decreases with an increase in slope height and slope angle. This leads to an uneconomical design of high slopes in a single slope profile.
2. Benching provides important stability for cut slope (i.e. the uses of 1m, 2m, and 3m bench every 10m increase FS by 3.5%, 7.5%, and 12% respectively from single slope profile). It is more effective in steep slopes (i.e. FS changes in 1.7%, 3.6%, 7.7%, and 17.4% from single slope profile for slope angle 27, 34, 45 and 63 respectively in 2m bench). Moreover, the performance of the bench slope is affected by bench height, the effect is more significant when the slope angle within the bench keeps constant.
3. Multi-slope profile provides an effective performance on slope stability in a stratified soil of varied strength. It allows economical slope design without extra excavation by adjusting only within the slope section. The method is more effective in combination with benches.
4. In addition to its geometric effect on the FS, slope profiles have different performance on drainage control, access to maintenance, and aesthetic value. Therefore, the selection of slope profiles during design should be based on site-specific considerations

7.2 Recommendations

The study was mainly focused on stability analysis of road cut slope and performance evaluation of slope profiles using different approaches. Therefore, based on analysis results, analysis methods, and performance evaluations the following recommendations were made.

1. It is strongly recommended to install an appropriate drainage system and one or a combination of slope reinforcement to maintain the stability of the cut slope.

2. Even if FEM provides better information about failure mechanisms, still LEM is commonly used in the evaluation of slopes. Therefore, it is better to use deformation-based FEM for safe and economical designs of slopes.

On the other hand, as the slope stability and performance evaluation were conducted within a limited scope, further research can be carried on following.

1. The analysis of earthquake force with the pseudo-static method provides only the static FS for the slope. To better understand about the failure mechanism of slope dynamic analysis is recommended for future work.
2. The performance evaluation of slope profiles was made interims of slope stability on the selected slope sections on the study area. But slope profiles also have different performance in drainage control. Hence, it is recommended to conduct the evaluation under rainfall infiltration.

SPECIAL ACKNOWLEDGEMENT

This research project is funded by Adama Science and Technology University under the grant number

ASTU/SM-R/044/19

Adama, Ethiopa

REFERENCES

Abera, T. (2007). Hydrogeological and Hydrogeomechanical Assessment in the Adama (Nazareth)- Dera Area Central Ethiopia. *A Thesis Submitted to the School of Graduate Studies Addis Abeba University.*

Ahemed, S., Chala, E. T., & Rao, K. (2016). Rock Mass Slope Stability Analysis Under Static and Dynamic Conditions in Mumbai, India. *Soil Dynamics and Earthquake Geotechnical, Engineering. Springer, Singapore*, 189-198.

Anand, H., Dumesa G., & Woyesa A. (2019). Numerical Analysis of Slope Stability- A Parametric Study. *International Journal for Research in Applied Science & Engineering Technology (IJRASET) ISSN: 2321-9653,* IC Value: 45.98.

Arai, K., & Tagyo, K. (2004). Application of the Finite Element Method to Slope Stability Soils; *Soils and Foundations. 25(1), 43-51.*

Aryal, K. P. (2006). Slope Stability Evaluations by Limit Equilibrium and Finite Element Methods. Norwegian University of Science and Technology.

ASTM. (2014). Annual Book of ASTM Standards for Soil and Rock (I)*: D420-D5876 Volume 04.08 and soil and rock (II): D5877 Volume 04.09*.

Balazs, V. (2009). A Possible Method for Estimating the Poisson's Rate Values of the Rock Masses. *Acta Geod. Geoph. Hung., Vol. 44(3)*, pp. 313–322.

Barton, N. (1973). Review of A New Shear Strength Criterion for Rock Joints. *Engng Geol. 7, 287 332*.

Barton, N., & Choubey, V. (1977). The Shear Strength of Rock Joints in Theory and Practice. *Rock Mech. 10(1-2), 1-54.*

Burman, A., Acharya, S. P., Sahay, R. R., & Maity, D. (2015). A Comparative Study of Slope Stability Analysis Using Traditional Limit Equilibrium Method and Finite Element Method. *Asian Journal of Civil Engineering.*

Chaowei, S., Junrui, C., Bin, M., Tao, L., Ying, G., & Huanfeng, Q. (2019). Stability Charts for Pseudo-Static Stability Analysis of 3D Homogeneous Soil Slopes using Strength Reduction Finite Element Method.

Chaudhary, K.B., Domingos, V.H., Gitirana J., Fredlund M., & Lu, H. (2016). Three-Dimensional Slope Stability. Geometric Effects. *Tailings and Mine Waste Conference'16. Keystone, Colorado, USA.*

Chen, B. (2018). Finite Element Strength Reduction Analysis on Slope Stability Based on ANSYS. *Environmental and Earth Sciences Research Journal*, 4(3), 60-65.

Chien-Yuan C., & Wei-Cheng W. (2019). Combined Effect of Rainfall Seepage and Seismic Shaking on Slope Stability by Using a Three-Dimensional Stability Analysis. *International Journal of Engineering and Technology, Vol. 11, No. 1*.

Christofer, K., Harianto, R., & Alfrendo, S. (2017). Effect of Variations In Rainfall Intensity on Slope Stability in Singapore. *International Soil and Water Conservation Research; Singapore 639811*.

Chung, M. Y., & Yong, V. H. (2019). The Effect of Rainfall Variability on Slope Stability in Canada Hill, Miri. IOP Conference Series: *Materials Science and Engineering, Curtin University Malaysia.*

D. G. Fredlund, & J. Krahn. (1977). Comparison of Slope Stability Methods of Analysis. *Canadian Geotechnical Journal, vol. 14, no. 3,* pp. 429–439.

Dagnachew, D. (2011). Investigation on Some of the Engineering Characteristics of Soils in Adama Town *(Master's Thesis Addis Ababa University).* A.A.

Das, B. (2002). Soil Mechanics Laboratory Manual. *Sixth Edition Oxford University Press.New York.*

Das, B. (2010). Principles of Geotechnical Engineering; *Seventh Edition. Stamford, CT 06902, USA.*

Demissie, S. (2018). Landslide Hazard Evaluation and Zonation in Dilbe and Its Surrounding Area Northwestern Central Ethiopia; an Integrated GIS-Based Grid Overlay and Statistical Approach *(Master's thesis, Addis Ababa University).* A.A.

Egeli, H., & Firat, P. (2011). Mechanism and Modelling of Shallow Soil Slope Stability During High Intensity and Short Duration Rainfall. *Izmir Institute of Technology, Department of Civil Engineering, Urla, Izmir, 35430, Turkey*.

Eleyas, A., Li Jian Lin, Costas I. Sachpazis, Deng Hua Feng, Sun Xu Shu, & Anthimos S. Anastasiadis. (2016). Probabilistic Slope Stability Evaluation for the New Railway Embankment in Ethiopia. *Electronic Journal of Geotechnical Engineering (21.11)*, pp 4247-4272.

Eleyas, A., Li Jian Lin, Costas I. Sachpaz, Deng Hua Feng, Sun Xu Shu, & Anthimos Anastasiadis (2016). Discussion on the Analysis, Prevention, and Mitigation Measures of Slope Instability Problems: A case of Ethiopian Railways. *Electronic Journal of Geotechnical Engineering, (21.12)*, pp 4101-4119.

Eleyas, A., Li Jian Lin, Costas I. Sachpazis, Deng Hua Feng, Sun Xu Shu, & Xiaoliang Xu. (2017). Slope Stability Evaluation for the New Railway Embankment using Stochastic and Finite Element Method. *Electronic Journal of Geotechnical Engineering; (22.01)*, pp 33-49.

Endalu, C. T., K. Seshagiri Rao, Swapnil Mishra, & Ankesh Kumar. (2016). Geomechanical Properties of Volcanic Rocks from Deccan Traps, India. *ISRM VII Brazilian Symposium on Rock Mechanics-SBMR. International Society for Rock Mechanics and Rock Engineering*.

Endalu, C. T., Rao, T., & Akx, M. (2016). Estimating Engineering Properties of Weathered Rocks from Deccan Trap. *6th Indian rock Mechanics Conference, IIT Bombay*, 17-18.

Endalu, T., & Seshagiri K. R. (2017). Influence of Weathering on the Engineering Behavior of Rocks under Triaxial Confining Conditions. *Geotechnical Frontiers*, 570-578.

ERA. (2013). *G*eotechnical Design Manual; Ethiopian Roads Authority series of Road and Bridge Design documents. Addis Ababa, Ethiopia.

Ermias, B., Raghuvanshi, T. K., & Abebe, B. (2017). Landslide Hazard Zonation (LHZ) around Alemketema Town, North Showa Zone, Central Ethiopia-A GIS-based Expert Evaluation Approach. *International Jornal of Earth science*, P.P.33-44.

Fathiyah, H., & Early, B. (2017). Parametric Study on the Effect of Rainfall Pattern to Slope Stability; Department of Civil Engineering, University of Indonesia.

Gadaawin, L. (2019). Slope Stability Analyses Along Selected Road Section from Gutane Migiru Town to Finca'a Sugar Factory, Oromia, Western Ethiopia: *Addis Ababa Science and Technology University*.

Gebremicheal, S. (2017). Landslide Hazard Evaluation and Zonation in and Around Hagereselam Town, *A Thesis Submitted to School of Earth sciences Addis Ababa University, Ethiopia.*

Griffiths, D., & Marquez, R. (2007). Three-Dimensional Slope Stability Analysis by Elasto-Plastic Finite Elements. *Geotechnique. 57 (6)*, 537-546.

H. Zebarjadi, D., R. Khaloo, K., R. Rafiee, Yarahmadi, B., & A.R. Yarahmadi, B. (2018). Effects of Geometrical and Geomechanical Properties on Slope Stability of Open-Pit Mines using 2D And 3D Finite Difference Methods. *Journal of Mining & Environment, Vol. 9, No. 4*, 941-957.

Halder, S., Imam, M. O., & Basir, M. S. (2017). A Detailed Analysis of Slope Stability Using Finite Element Method (FEM). *Chittagong University of Engineering & Technology; Bangladesh*.

Hoek, E., & Bray, J. (1981). Rock Slope Engineering (Revised Third Edition). *Institution of Mining and Metallurgy, London, p.358.*

Hoek, E., & Brown, E. (1997). Practical Estimates of Rock Mass Strength. *International journal of rock mechanics and mining sciences, 34(8)*, 1165-1186.

IS. (1991). Indian Standard Method for Determination of Rock Characteristics. *In Bureau of Indian Standards Manak Bhavan 9 Bahadur Shah Zafar Marg; New Delhi*.

J. Ameratunga, Nagaratnam, S., & Braja M. D. (2016). Correlations of Soil and Rock Properties in Geotechnical Engineering.

J. Chen, J.H. Yin, & C. F. Lee. (2003). Upper Bound Limit Analysis of Slope Stability using Rigid Finite Elements and Nonlinear Programming. *Canadian Geotechnical Journal, vol. 40, no.4*, pp. 742–752.

Kedir, M., & Zhuping, S. (2018). Cut Soil Slope Stability Analysis Along National Highway at Wozeka–Gidole Road, Ethiopia.

Kramer, S. (1996). Geotechnical Earthquake Engineering. University of Washington, USA: *Prentice-Hall International Series in Civil Engineering and Soil Mechanics*.

Li, A.-J. (2009). Two and Three Dimensional Stability Analysis of Soil and Rock Slopes. *University of Western Australia, School of Civil and Water Resources Engineering.*

Lian, H., Xiao, C., Yingbin, Z., Liang, L., & De-Jian, L. (2015). Stability Analysis of Seismic Slopes with Cracks. *Central South University, Changsha, Hunan 410075, China.*

Navya, B., & Hymavathi, J. (2017). Stability Analysis of Slope with Different Soil Types and Its Stabilization Techniques; *Department of Civil Engineering, Institute of Aeronautical Engineering Dundigal.*

Nurly, G., Lee M. L., & Marwan, A. (2006). Transient Seepage and Slope Stability Analysis for Rainfall Induced Landslide: A Case Study.

Phase2. (2011). 2D Elasto-Plastic Finite Element Program for Slope and Excavation Stability Analyses*; Slope Stability Verification Manual.* Rocscience Inc.

Plaxis. (2013). Finite Element Program Developed for the Analysis of Deformation, Stability, and Ground Water Flow in Geotechnical Engineerin*g. Ground Water Flow in Geotechnical Engineering Bv, Netherlands.*

Plaxis-2D. (2002). Finite Element Program Developed for the Analysis of Deformation, Stability, and Ground Water Flow in Geotechnical Engineering*: Delft University of Technology and Plaxis Bv, Netherlands.*

Popescu, M. (2001). A Suggested Method for Reporting Landslide Remedial Measures International Union of Geological Sciences Working Group on Landslides, Commission on Landslide Remediation.

Prasad, N. (2017). Landslides - Causes and Mitigation Technical Report Centre for Water Resources Development and Management, India.

Raghuvanshi, T. K. (2017). Plane Failure in Rock Slopes–A Review on Stability Analysis Techniques. *Journal of King Saud University-Science.*

Rocdata. (2004). Strength Analysis of Rock and Soil Masses Using the Generalized Hoek-Brown Mohr-Coulomb, Barton-Bandis, and Power Curve failure criteria*; Rocscience Inc.*

S. Alfat, L.M. Zulmasri, S. Asfar, & M. S. Rianse. (2019). Slope Stability Analysis Through Variational Slope Geometry Using Fellenius Method. *Journal of Physics: Conf. Series 1242*.

Samuel, A. (2017). Slope Stability Analysis of Rainfall Induced Landslides. A Case Study on Gohatsion - Dejen Road Abay Gorge. *Master's Thesis in Addis Ababa Science and Technology University*. A.A.

Samuel, K., Samson, E., Asnake, K., & Eyob, T. (2012). Technical Notes and Proposed Guidelines on Updated Seismic Codes in Ethiopia Implication for Large-Scale Infrastructure.

Searom, G. (2017). *L*andslide Hazard Evaluation and Zonation in and Around Hagereselam Town. *A Thesis Submitted to School of Earth sciences Addis Ababa University, Ethiopia.*

Seifu, K. (2013). Groundwater in Ethiopia; Features, Numbers, and Opportunities. *Department of Earth Sciences Addis Ababa University, Addis Ababa.*

Sharma, A. K. (2008). Landslide and Its Mitigation for Disaster Management Using Remote Sensing and GIS Technique-A Case Study of the Gangtok Area, East Sikkim*; Doctoral dissertation, Sikkim Manipal University of Health, Medical and Technological Sciences.*

Sjoberg, J. (1997). *E*stimating Rock Mass Strength Using the Hooks Brown Failure Criterion and Rook Mass Classification, a Review, and Application to the Aznalkollar Open Pit. *Internal Report Division of Rock Mechanics.*

Slide. (2002). 2D Limit Equilibrium Slope Stability for Soil and Rock Slopes; Rocscience Inc.

Varnes, D. (1978). Slope Movements Types and Processes, Schuster RL & Krizek RJ Ed.-Landslide, Analysis, and Control. *Transportation Research Board Sp. Rep, (176)*.

Woldearegay, K. (2013). Review of the Occurrences and Influencing Factors of Landslides in the Highlands of Ethiopia With Implications For Infrastructural Development. *Momona Ethiopian Journal of Science*, 5(1), 3-31.

Wyllie, D., & Mah, C. (2004). Rock Slope Engineering Civil and Mining, 4th Edition. *Spon Press, New York.*

X. Zhang. (1988). Three-Dimensional Stability Analysis of Concave Slopes in Plan View. *Journal of Geotechnical Engineering, vol. 114, no. 6,* pp. 658–671.

Yifru, B. A., & Ayehu, F. M. (2017). Prediction of Groundwater Level Fluctuation towards Rainfall Induced Landslide: Case of Blue Nile Gorge, Central Ethiopia. *Open Journal of Modern Hydrology*.

Z. Chen, X. Wang, C. Haberfield, J.-H. Yin, & Y. Wang. (2001). A Three-Dimensional Slope Stability Analysis Method Using the Upper Bound Theorem. *International Journal of Rock Mechanics and Mining Sciences, vol. 38, no. 3*, pp. 369–378.

Zetseat, G. (2018). *A*n Investigation into the Ground Motion Amplification Potential of Selected Sites of Addis Ababa City. *School of Graduate Studies of Addis Ababa University; Addis Ababa.*

Zhang, Y., Chen, G., Zheng, L., Li, Y. , & Zhuang. (2013). Effects of Geometries on Three-Dimensional Slope Stability. *Canadian Geotechnical Journal. 50 (3),* 233-249.

APPENDIX

Appendix A Rock density in the laboratory

Table A.1: Determination of rock unit weight from buoyancy test (Standard IS 13030: 1991)

Rock type	Sample No	Oven dry mass (kg)	V1 (l)	V2 (l)	V3 (l)	Density (kg/m3)	Unit weight (kN/m^3)
Bottom layer (RSC-11 & RSC-21)	1	0.139	0.70	0.77	0.07	2138.5	21.0
	2	0.136		0.77	0.07	2000.0	19.6
	3	0.16		0.78	0.08	2000.0	19.6
	4	0.126		0.76	0.06	2048.8	20.1
	average						20.1
2nd layer (RSC-12 & RSC-22)	1	0.055	0.50	0.53	0.03	1833.3	18.0
	2	0.101		0.55	0.05	2020.0	19.8
	3	0.13		0.57	0.06	2000.0	19.6
	4	0.065		0.54	0.04	1710.5	16.8
	5	0.05		0.53	0.03	1785.7	17.5
	6	0.057		0.53	0.03	2111.1	20.7
	average						18.7
Top layer (RSC-13 & RSC-23)	1	0.085	0.50	0.54	0.04	2266.7	22.2
	2	0.087		0.54	0.04	2175.0	21.3
	3	0.097		0.54	0.04	2365.9	23.2
	4	0.097		0.55	0.05	2108.7	20.7
	5	0.043		0.52	0.02	2150.0	21.1
	average						21.7

Appendix B Determination of Schmidt Hammer Rebound value in the field

The test is conducted according to ASTM D5873-14 Standard reference using the following procedures.

1. The surface to be measured is identified (smooth, clean, and dry).
2. Wipe it to clean the dust and grime using corundum stone to smooth the surface.
3. Then equally spaced square box is prepared on the smooth surface away from the edges.

4. Then ten readings of rebound number are taken at each point of testing by applying the hammer in a perpendicular direction. Here the average of ten readings is taken as a representative rebound number and conversion or correlation is made using it.

5. For tests conducted at 45-degree correction is made to the negative vertical direction by using B-PROCEQ curve provided in the Schmidt hammer reding.

Table A.2: Schmidt hammer test for UCS (three tests @ 10 reputations are conducted for 6 sample location) (Standard ASTM 5873-14)

ID	RSC-11			RSC-12			RSC-13			RSC-21			RSC-22		RSC-23	
Trial	1	2	3	1	2	3	1	2	3	1	2	3	1	2	1	2
Rebound Number R	23	34	35	26	18	27	58	62	62	37	48	36	21	21	60	54
	26	30	33	25	23	26	62	58	63	41	54	34	25	17	54	59
	22	29	34	23	25	25	58	61	59	38	56	37	23	21	55	58
	27	29	32	22	26	24	57	59	58	41	47	39	26	20	56	59
	24	31	31	26	27	20	61	57	59	40	57	41	21	18	59	58
	26	30	34	12	24	22	60	56	60	37	52	40	21	22	60	57
	23	34	35	19	24	19	63	57	57	35	54	35	20	19	61	60
	21	33	36	21	23	18	61	59	59	38	49	37	19	20	57	56
	26	29	33	25	22	20	58	58	62	41	55	39	20	17	59	54
	28	28	31	27	26	23	57	59	63	42	51	40	21	21	55	54
Ravg	25	31	33	24	24	22	60	59	60	39	52	38	22	20	58	57
Ravg	29.6			23.3			59.4			43.0			20.7		56.9	

Table A.3: Summary of UCS from curves and equations Barton and Choubey (1977).

Slope Section	Sample ID	Orientation (°)	Avg rebound No	Unit weight (kN/m^3)	UCS from Eqn. (Mpa)	UCS from curves (MPa)
CS-1	RSC-11	45	29.6	20.1	34.5	38
	RSC-12	45	23.3	18.7	24.8	30
	RSC-13	0	59.4	21.7	139.7	135
CS-2	RSC-21	45	43.0	20.1	61.3	55
	RSC-22	45	20.7	18.7	22.4	28
	RSC-23	0	56.9	21.7	126.9	125

NB: - For this analysis UCS obtained from the equation is used

Appendix C Geological strength index (GSI) and disturbance factor(D)

Geological strength index (GSI)- an estimate of reduction in rock mass strength for different geological conditions. Its value was obtained by considering weathering condition of discontinuity surface, rock mass structure and interlocking of rock blocks in successive site visit as proposed by Wyllie and Mah, (2004). Similarly, disturbance factor (D) was obtained by considering the degree of disturbance due to excavation based on the guidelines proposed by Wyllie and Mah, (2004)

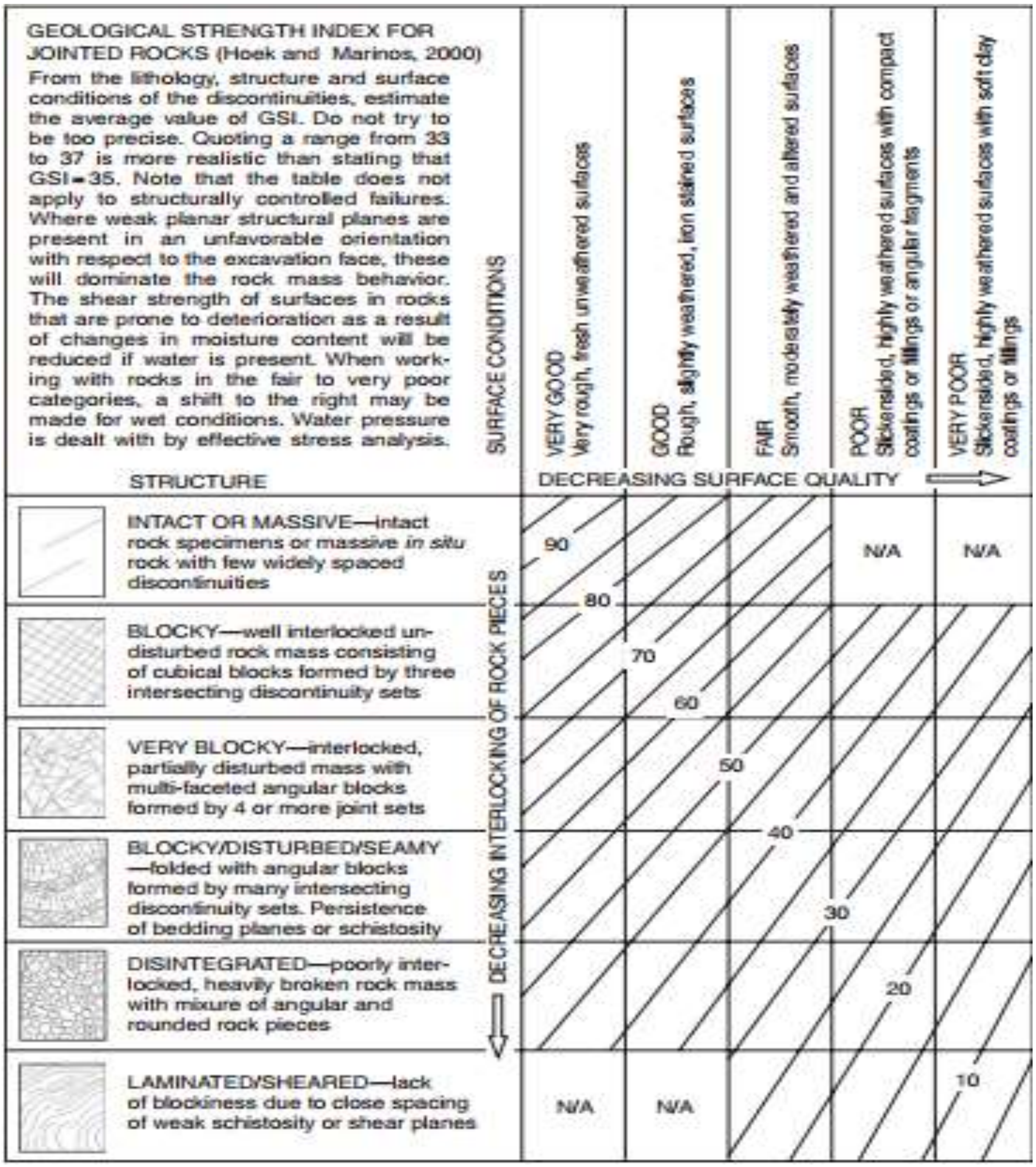

Figure A.1: GSI values characterizing blocky rock masses based on particle interlocking and discontinuity condition (Wyllie and Mah, 2004).

Table A.4: Geological strength index (GSI) and Disturbance factor (D) (Wyllie and Mah, 2004)

Section	Location	Geological structure	Surface condition	GSI	Exec condition	D
Critical section 1	RSC-11	Blocky/Disturbed	Fair	40 to 45	Poor	1
	RSC-12	Disintegrated	Very poor	20 to 25	good	0.7
	RSC-13	Intact/Massive	Very good	80 to 85	good	0.7
Critical section 2	RSC-21	Very blocky	Fair	45 to 48	poor	1
	RSC-22	Disintegrated	Very poor	15 to 20	good	0.7
	RSC-23	Intact/Massive	Very good	78 to 83	good	0.7

Appendix E Intact rock coefficient

Intact rock coefficient was determined based on the texture and type of rock obtained from field survey as recommended by Wyllie & Mah, 2004, and incorporated in rock data software. From Schmidt rebound number many of the sections of rock layers show weaker strength. Hence conservative values of mi were adopted in this work as given in Table A.6.

Table A.5: Intact rock coefficient and basic friction angle based on

Section	Location	Texture of rock	Mi
Critical section 1	RSC-11	Obsidian (very fine)	19 ± 3
	RSC-12	Tuff (fine)	13 ± 5
	RSC-13	Obsidian (very fine)	19 ± 3
Critical section 2	RSC-21	Tuff (fine)	19 ± 3
	RSC-22	Obsidian (very fine)	13 ± 5
	RSC-23	Obsidian (very fine)	19 ± 3

Appendix F Determination of rock shear strength and deformation properties using rock data software.

The strength and stiffness parameters of rock mass were determined by correlating the rock characteristics data measured and observed during field investigation. The correlation was made using rock data software for different rock shear strength criteria discussed in chapter two. Rocdata software is a program used for determining soil and rock mass strength parameters through laboratory or field investigation data. The program is used to fit the linear Mohr-Coulomb strength criterion with non-linear generalized Hoek-Brown (Rocdata, 2004).

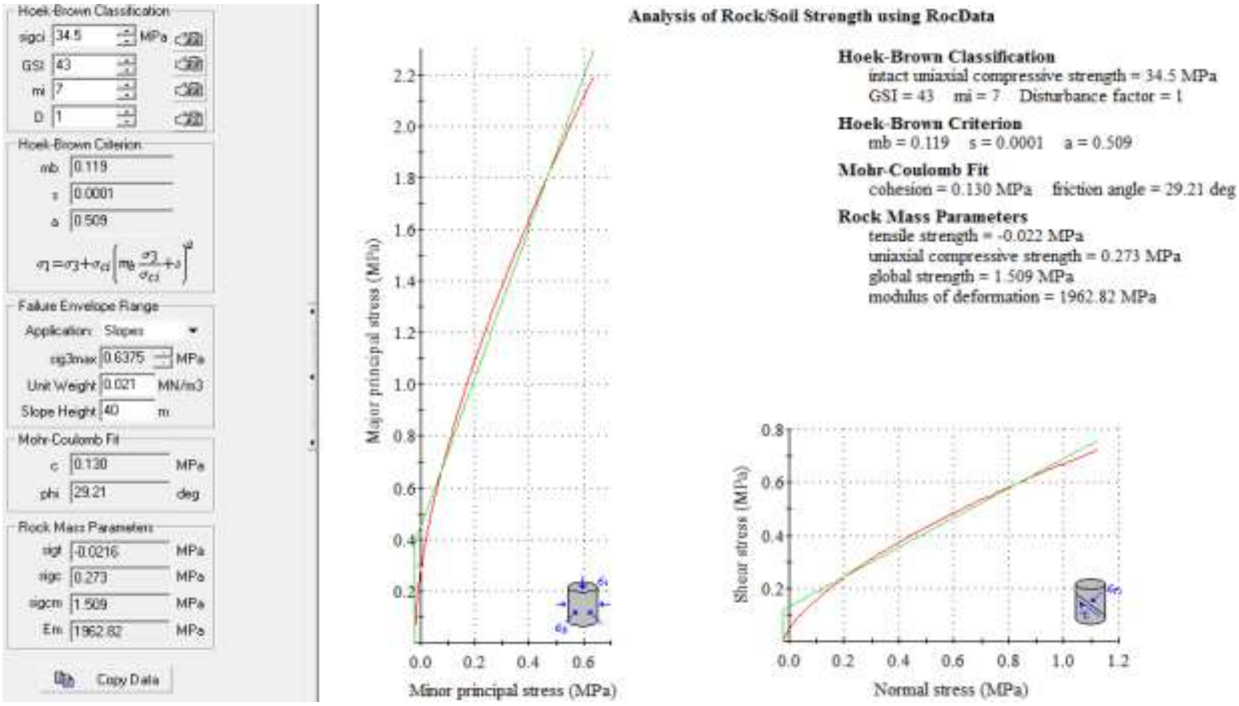

Figure A.2: Determination of rock mass strength using rock data software

Table A.5: Deformation modulus and poisons ratio of the rock mass

Sample code	UCS (Mpa)	D	mi	GSI	E (Mpa)	v
RSC-11	34.5	1	7	43	1962.8	0.35
RSC-12	24.8	0.7	4	23	686.9	0.41
RSC-13	139.7	0.7	9	83	43442.4	0.26
RSC-21	61.3	1	7	47	3293.8	0.34
RSC-22	22.4	0.7	4	18	487.6	0.42
RSC-23	126.9	0.7	9	80	36552.2	0.27

Table A.6: Mohr coulomb equivalent shear strength parameters from Hoke's-brown generalized criterion for rock mass structure (Rocdata 3.0 Rocscience, 2004).

Sample code	Dry unit weight	GSI	mi	Slope height	D	Mohr-Coulomb (Rock data)		Hoeks-Brown (Rock Data)		
						C (Mpa)	Ø°	Mb	s	a
RSC-11	20.1	43	7	40	1	0.013	29.23	0.12	1.0E-04	0.51
RSC-12	18.7	23	4	40	0.7	0.06	20.32	0.06	1.4E-05	0.54
RSC-13	21.7	83	9	40	0.7	6.638	54.23	3.54	8.5E-02	0.50
RSC-21	20.1	47	7	40	1	0.212	35.68	0.16	1.0E-04	0.51
RSC-22	18.7	18	4	40	0.7	0.044	16.82	0.04	6.9E-06	0.55
RSC-23	21.7	80	9	40	0.7	4.715	54.37	2.33	5.5E-02	0.50

Appendix G Index and strength properties of soil in the laboratory

1. *Grain size analysis*

Grain size analysis was conducted in collected soil samples using both wet and dry sieving. Only one sample is presented and all the others are summarized using particle size distribution curve.

Sample code- SSC-22

Type of sieve- Wet sieving

Table A.7: Grain size distribution test

Sieve no	Sieve size	M sieve	M sieve + soil	M soil retained	M soil retained %	Commutative retained	% finer	Classification	
4	4.75	0.445	0.479	0.034	6.80	6.80	93.20	6.80	Gravel
8	2.36	0.405	0.492	0.087	17.40	24.20	75.80		
16	1.18	0.359	0.456	0.097	19.40	43.60	56.40		
30	0.6	0.33	0.371	0.041	8.20	51.80	48.20		
50	0.3	0.296	0.321	0.025	5.00	56.80	43.20		
100	0.15	0.278	0.2915	0.0135	2.70	59.50	40.50		
200	0.075	0.271	0.287	0.016	3.20	62.70	37.30	55.90	sand
Pan	Pan	0.252	0.4385	0.1865	37.30	100.00	0.00	37.30	Fine soil
Sum				0.5	100.00	100.00			

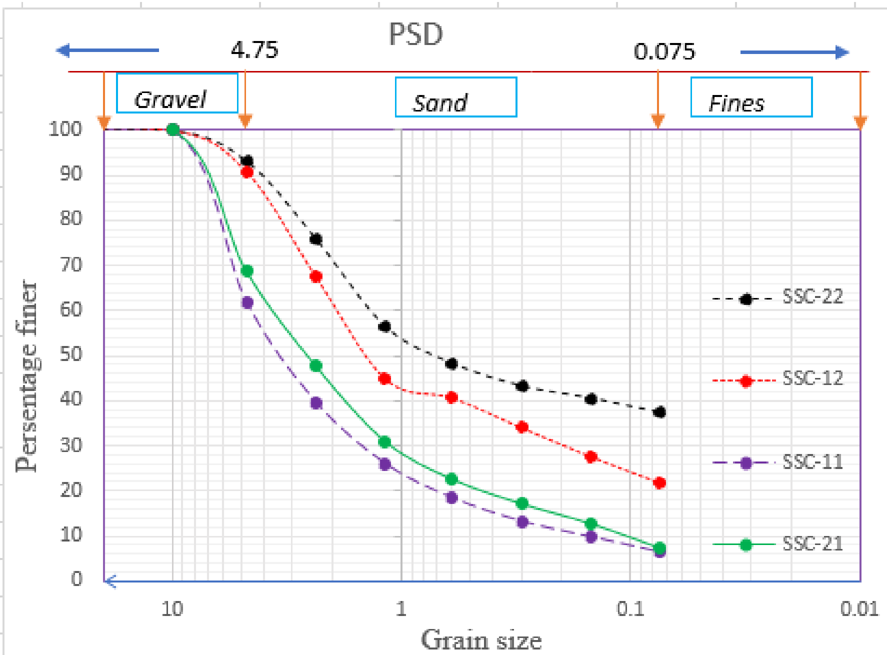

Figure A.3: Particle size distribution curve

2. *Atterberg limit*

Atterberg limit (Liquid limit and Plastic limit) of the soil was determined using the Casagrande method (ASTM D 4318). Similarly, the optimum moisture content of the soil was determined from fresh samples using ASTM D 2216. Sample determinations of Atterberg limit test for SSC-22 are presented in Table A.8 and others are summarized in Table A.9.

Table A.8: Sample Atterberg limit and water content test of soil (SSC-22)

Test Type	Liquid limit					Plastic limit		Optimum water content		
Can No.	LL1	LL2	LL3	LL4		PL-1	PL-2	1	2	3
Can weight	0.03	0.03	0.029	0.03		0.03	0.029	0.03	0.03	0.03
Can+ wet soil	0.063	0.059	0.063	0.066		0.039	0.048	0.082	0.091	0.097
Can + dry soil	0.053	0.05	0.052	0.054		0.037	0.044	0.072	0.08	0.085
Wt. of dry soil	0.023	0.02	0.023	0.024		0.007	0.015	0.042	0.05	0.055
Wt. of water	0.01	0.009	0.011	0.012		0.002	0.004	0.01	0.011	0.012
Water content	43.48	45.00	47.83	50.00		28.57	25.67	23.81	22.00	21.82
No. Of drop	33	28	23	18	Avg	27		22.54		

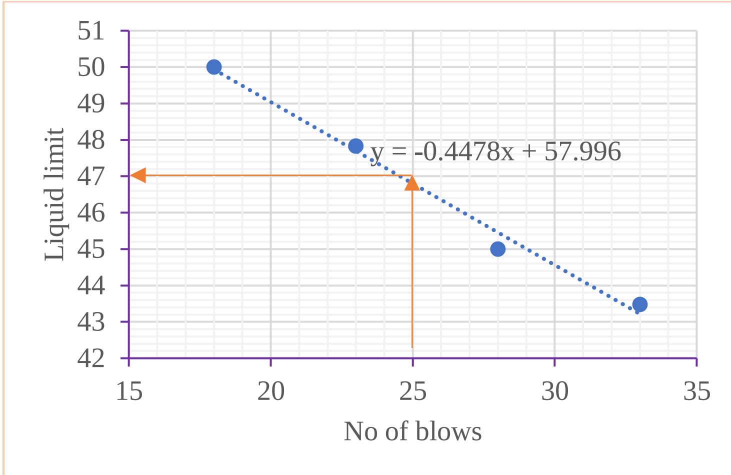

Figure A.4: Liquid limit determination

Table A.9: Summary of Atterberg limit and plasticity index

Code	LL %	PL %	w %	PI
SSC-11	39	26	15.35	13
SSC-12	34	26	13.22	8
SSC-21	37	24	21.39	13
SSC-22	47	27	22.54	20

3. *Specific gravity of soil*

The specific gravity of soil sample was determined using ASTM D 854-00 – Standard Test for Specific Gravity of Soil Solids by Pycnometer. The sample determination of specific gravity is presented in Table A.10 and others are summarized in Table A.11.

Table A.10: Specific gravity test for soil sample SSC-22

Trial No.	SG1	SG2	SG4
Weight of Pycnometer, M1	0.464	0.464	0.464
Weight of Pycnometer dry Soil, M2	0.584	0.584	0.584
Wt. Pycnometer + Soil + Water, M3	1.580	1.579	1.581
Wt. of Water + Pycnometer, M4	1.503	1.503	1.503
Specific gravity of the Soil, Gs	2.661	2.615	2.703
Average Gs	2.65		

Table A.11: Summery of specific gravity test

Sample code	SSC-11	SSC-12	SSC-21	SSC-22
SG	2.65	2.64	2.64	2.65

4. *Shear strength test*

Shear strength of the soil is the principal engineering property that controls the stability of soil slopes. Shear failure in soil occurs when induced stress exceeds the shear strength of soils. This relationship is defined interims of cohesion, internal angle of friction, and normal stress by Mohr coulomb criteria as discussed in chapter 2. There are different shear strength tests used to determine these parameters. In this study, a direct shear test on the remolded soil sample was conducted using ASTM D3080-98 as a reference. The following table and figures show the result of the direct shear test.

Sample code SSC-22

Soil classification Clayey sand

Table A.12: Records of reading and shear stress calculation

Gage displacement	Shear displacement	Proving shear			Shear load			Shear stress		
		50	100	150	50	100	150	50	100	150
0	0	0	0	0	0.000	0.000	0.000	0	0	0
50	0.5	6	7	9	0.047	0.056	0.071	8	9	12
100	1.0	9	12	15	0.074	0.095	0.122	12	16	20
150	1.5	11	16	18	0.087	0.121	0.145	15	20	24
200	2.0	13	19	22	0.100	0.151	0.177	17	25	29
250	2.5	14	21	25	0.103	0.165	0.197	17	28	33
300	3.0	14	24	27	0.105	0.191	0.213	18	32	35
350	3.5	14	25	29	0.107	0.198	0.228	18	33	38
400	4.0	14	25	29	0.108	0.194	0.229	18	32	38
450	4.5	12	23	27	0.101	0.181	0.211	17	30	35
500	5.0	10	19	23	0.083	0.151	0.188	14	25	31
Max Shear Stress								18	33	38

Table A.13: Normal stress vs shear stress curve

Test	Normal load	Normal stress	Shear stress
Trial-1	50	14	18
Trial-2	100	28	33
Trial-3	150	42	38

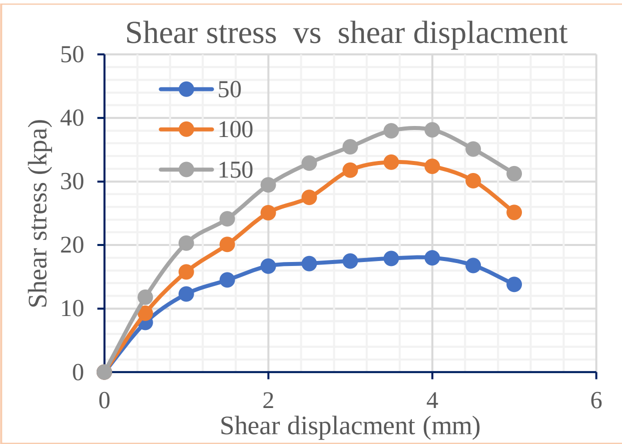

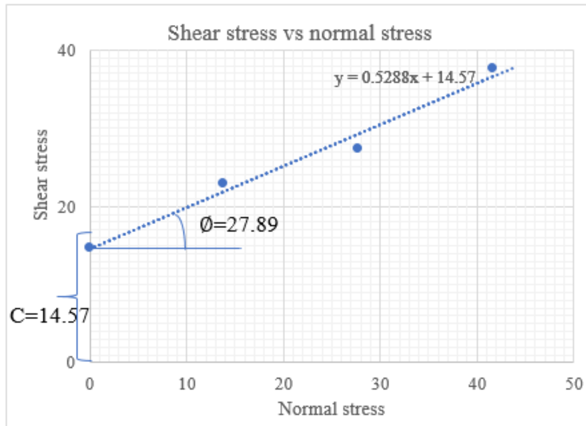

Figure A.5: (A) Shear stress vs shear displacement curve, (B) Normal stress vs shear stress curve

Sample code SSC-21

Soil classification Sand with clay and gravel

Table A.14: Records of reading and shear stress calculation

Gage displacement	Shear displacement	Proving shear			Shear load			Shear stress		
		50	100	150	50	100	150	50	100	150
0	0	0	0	0	0.000	0.000	0.000	0	0	0
50	1	4	6	9	0.035	0.050	0.071	6	8	12
100	1	8	10	12	0.068	0.079	0.099	11	13	17
150	2	10	13	17	0.083	0.109	0.131	14	18	22
200	2	13	16	21	0.100	0.125	0.165	17	21	28
250	3	14	17	22	0.111	0.139	0.179	19	23	30
300	3	15	20	25	0.117	0.157	0.201	19	26	34
350	4	16	21	27	0.128	0.164	0.217	21	27	36
400	4	17	20	28	0.137	0.163	0.225	23	27	38
450	5	16	19	27	0.125	0.155	0.217	21	26	36
500	5	14	17	26	0.112	0.139	0.205	19	23	34
Max Shear stress								23	27	38

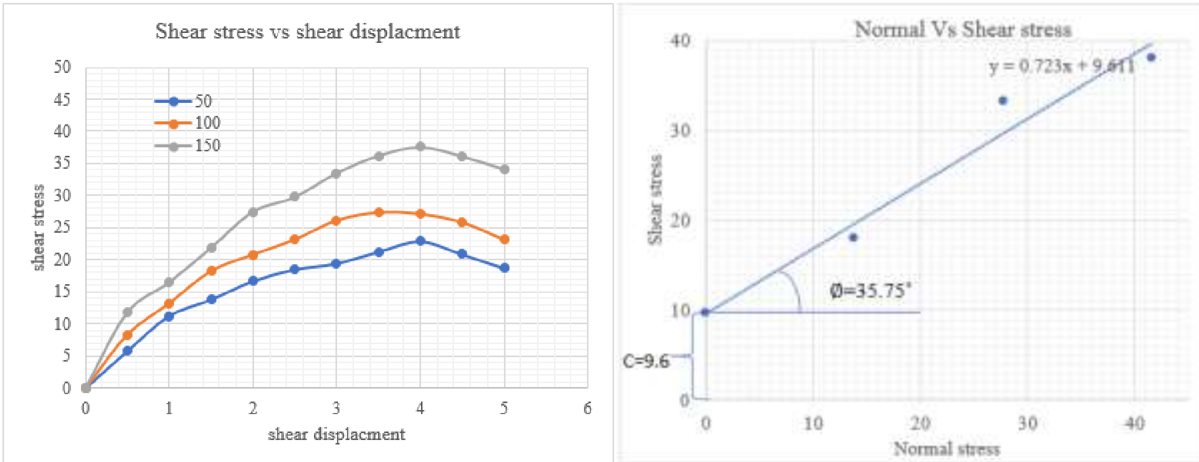

Figure A.6: (A) Shear stress vs shear displacement curve, (B) Normal stress vs shear stress curve

5. *Soil stiffness parameters*

The stiffness parameters for soil (E and v) used for numerical modeling were obtained from correlations and recommendations. Das (1995) and Bowles's (1996) recommendation are considered and peck, Hanson, and thornburn (1974) and Kulhawy and Mayne (1990) correlation were used to select representative data as sited from (J Ameratunga et al., 2016).

Kulhawy and Mayne (1990); $v_d = 0.1 + 0.3\frac{\emptyset' - 25}{20} \quad for\ \emptyset' < 45°$

Peck, Hanson and thornburn (1974) (Jay Ameratunga et al., 2016);

$$\emptyset(deg) = 27.1 + 0.3N_{60} - 0.00054[N_{60}]^2$$

Kulhawy and Mayne (1990); $\frac{E_s}{p_a} = \alpha N_{60}$

Table A.15: Summery of stiffness parameters of soil (NB; v* and E* are used for modeling)

Sample code	USCS Classification	v*	v (Bowels 1996)	v (Das 1995)	E*	E (Das 1995)
SSC-21	Sand w clay & gravel	0.261	0.2-0.4	0.25-0.4	35000	34400-69000
SSC-22	Clayey sand	0.215	0.2-0.3	0.2-0.4	25000	10350-27600
v* = Correlation (Kulhawy and Mayne (1990), E*= Correlation Begemann (1974) and Jay Ameratunga (2016).						

Appendix H Numerical validation

To validate the software and procedures used to model critical slope sections in this study existing literature of previous case studies was used. Hence, the typical slope section introduced by Zhang (1988) was analyzed in this study. The cross-section and its material parameters of this slope are shown in Figure A.7 and Table A.15 respectively. Zhang originally used an extended Spencer's method to analyze this example. Then, numerous investigators (i.e. Ferdlund and Krahn, 1977; Chen et al., 2003; Griffiths and Marquez, 2007; Nian et al., 2012; Zhang et al., 2013; Chaowei et al., 2019) have used this model to validate their 2D and 3D slope stability evaluations.

Table A. 16: Material properties slope section used for the validation (Zhang, 1988)

Material	E (MPa)	v	γ (kN/m^3)	$\emptyset^\circ$	c(kPa)	ψ°
Soil	10	0.25	18.8	20	29	0

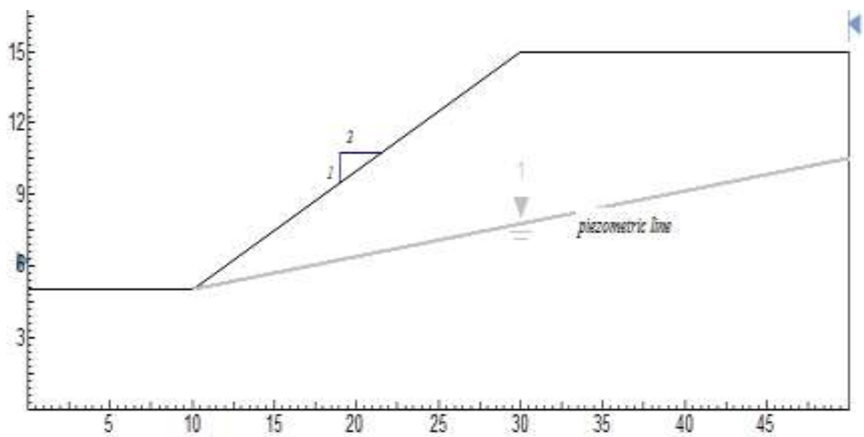

Figure A.7: Geometry of slope used for validation (Zhang, 1988)

The slope section given in Figure A.7 was modeled using a slide, Plaxis -2D, and Plaxis-3D software as shown in figure A.8. The FS obtained from the analysis and the previous case studies on this slope section are summarized in Table A.17. Accordingly, the results obtained from this evaluation show a good agreement with the previous results of different investigators.

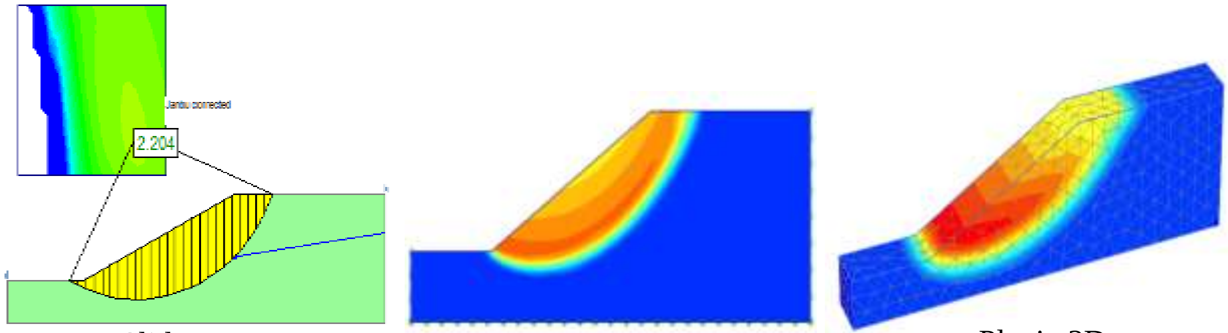

Slide Plaxis-2D Plaxis-3D

Figure A.8: Modeling of slope section used for validation in slide, Plaxis-2D, and Plaxis-3D

Table A.17: FS result of different researchers and this evaluation

Method	Software	Material model	FS	Reference
2D LEM	USSP*		2.034**	Fredlund and Krahn, 1977
3D-LEM	-	-	2.187	Chen et al., 2003
2D-LEM			2.108	
3D UB-LAM	EMU-3D	-	2.262	Chen et al., 2001
3D-FEM	-	MC	2.17	Griffiths and Marquez, 2007
3D-FEM	-	MC	2.15	Nian et al., 2012
3D -FDM	FLAC-3D	-	2.18	Zhang et al., 2013
3D-FEM	ABACUS	MC	2.133	Chaowei et al., 2019
2D-FEM	Plaxis	MC	2.165	This evaluation
2D-LEM (JC)	Slide	MC	2.204	This evaluation
3D-FEM	Plaxis	MC	2.215	This evaluation

* University of Saskatchewan SLOPE program. ** Average of six different LEM

Further validation was made for plaxis 2D and slide using the slope section provided by Cheng et al., (2007) as sited from Phase2 (2011). The geometry and material properties are shown in Figure A.9 and Table A.18. Modeling was made using plaxis and slide as shown in Figure A.10. From the results given in Table A.19, both plaxis and slide software agree well to the previous case studies. Since all the validation shows a good agreement with previous case studies it is reasonable to accept the results.

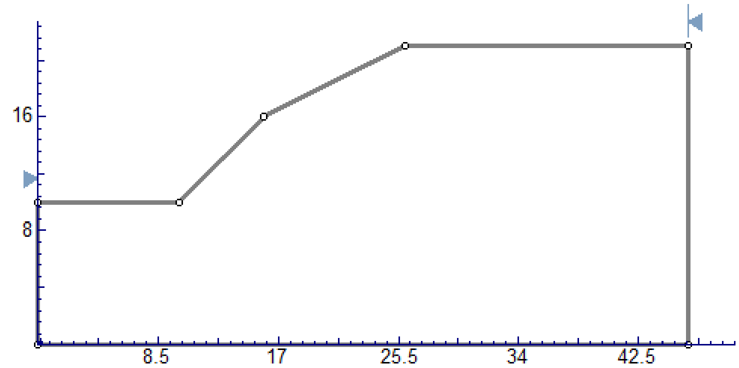

Figure A.9: Slope section used for validation (Phase2, 2011).

Table A.18: Material properties used for validation (Phase2, 2011).

Material	E (Mpa)	v	γ (KN/m3)	φ°	c(Kpa)	ψ°
Soil	14	0.3	20	30	10	0

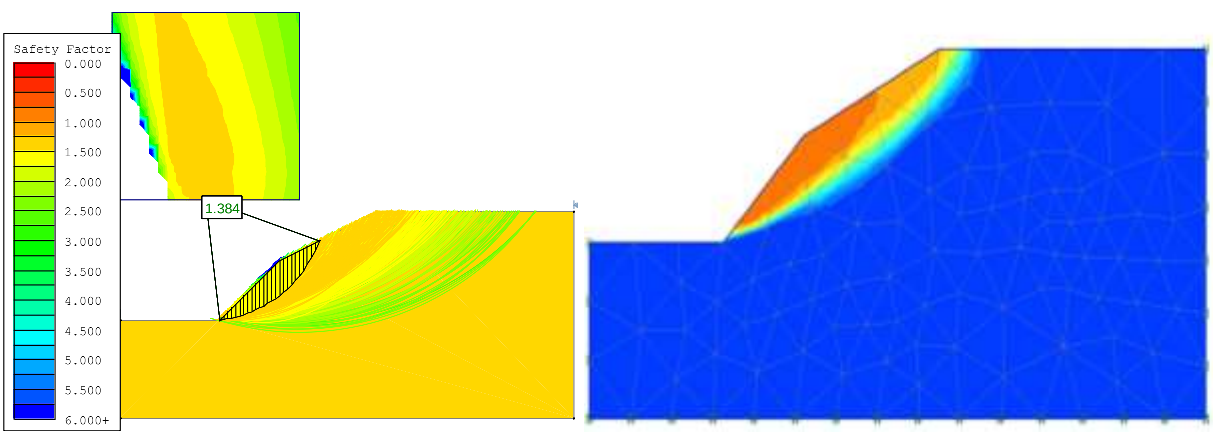

Figure A. 20: Plaxis and slide modeling for validation

Table A.19: FS of analysis result and previous works

Method	Previous studies		This analysis		
	LEM (avg)	Phase (FEM)	Plaxis 2D	Slide (bishop)	Slide (GLE)
FS	1.383	1.38	1.376	1.39	1.384